Project Report
ATC-428

Airspace Flow Rate Forecast Algorithms, Validation, and Implementation

M. Matthews
R. DeLaura
M. Veillette
J. Venuti
J. Kuchar

15 December 2015

Lincoln Laboratory
MASSACHUSETTS INSTITUTE OF TECHNOLOGY
LEXINGTON, MASSACHUSETTS

Prepared for the Federal Aviation Administration,
Washington, DC 20591

This document is disseminated under the sponsorship of the Department of Transportation, Federal Aviation Administration (FAA), in the interest of information exchange. The United States Government assumes no liability for its contents or use thereof.

This material is based upon work supported under Air Force Contract No. FA8721-05-C-0002 and FA8702-15-D-0001. Any opinions, findings, conclusions or recommendations expressed in this material are those of the author(s) and do not necessarily reflect the views of the FAA.

TECHNICAL REPORT STANDARD TITLE PAGE

1. Report No.	2. Government Accession No.	3. Recipient's Catalog No.
ATC-428		

4. Title and Subtitle	5. Report Date
Airspace Flow Rate Forecast Algorithms, Validation and Implementation	15 December 2015
	6. Performing Organization Code

7. Author(s)	8. Performing Organization Report No.
Michael Matthews, Richard DeLaura, Mark Veillette, Joseph Venuti, and James Kuchar	ATC-428

9. Performing Organization Name and Address	10. Work Unit No. (TRAIS)
MIT Lincoln Laboratory 244 Wood Street Lexington, MA 02420-9108	11. Contract or Grant No. FA8721-05-C-0002 and/or FA8702-15-D-0001

12. Sponsoring Agency Name and Address	13. Type of Report and Period Covered
Department of Transportation Federal Aviation Administration 800 Independence Ave., S.W. Washington, DC 20591	Project Report
	14. Sponsoring Agency Code

15. Supplementary Notes

This report is based on studies performed at Lincoln Laboratory, a federally funded research and development center operated by Massachusetts Institute of Technology, under Air Force Contract FA8721-05-C-0002 and/or FA8702-15-D-0001.

16. Abstract

This report summarizes work performed by MIT Lincoln Laboratory during the period 1 February 2015 – 30 November 2015 focused on developing and improving algorithms to estimate the impact of convective weather on air traffic flows. The core motivation for the work is the need to improve strategic traffic flow management decision-making in the National Airspace System. The algorithms developed as part of this work translate multiple weather forecast products into a discrete airspace impact metric called permeability.

17. Key Words	18. Distribution Statement
	This document is available to the public through the National Technical Information Service, Springfield, VA 22161.

19. Security Classif. (of this report)	20. Security Classif. (of this page)	21. No. of Pages	22. Price
Unclassified	Unclassified	148	

FORM DOT F 1700.7 (8-72) Reproduction of completed page authorized

This page intentionally left blank.

EXECUTIVE SUMMARY

This technical report summarizes work performed by MIT Lincoln Laboratory during the period 1 February 2015 – 30 November 2015 focused on developing and improving algorithms to estimate the impact of convective weather on air traffic flows. The FY15 algorithm development work was funded by the Federal Aviation Administration (FAA) AJV-73 Technical Analysis and Operational Requirements organization. Field evaluations were supported via the FAA AJM-33 Consolidated Storm Prediction for Aviation (CoSPA) program.

The core motivation for the work is the need to improve strategic traffic flow management decision-making in the National Airspace System. Currently, traffic managers must interpret forecasts of traffic demand, weather, airspace constraints, and other information to determine appropriate Traffic Management Initiative (TMI) actions that avoid over-delivery of traffic into impacted airspace. Due to the many stakeholders involved, decisions require close collaboration with other air traffic control facilities and airlines. While often effective, the current process relies heavily on prior user expertise and may impose high mental workload. These challenges can be mitigated through improvements in decision support such as those discussed in this report.

The algorithms developed as part of this work translate multiple weather forecast products into a discrete airspace impact metric called *permeability*. Permeability can be used to support categorical estimates of airspace impact and can also be converted into achievable or sustainable traffic flow rates. This translation provides stakeholders with explicit reference values they can use during the collaborative decision-making process in order to weigh various TMI actions and the likelihoods of different outcomes. As described in this report, in FY15 the algorithms were further matured and improved, implemented in a real-time decision-support system, and evaluated in the field at several targeted facilities.

The work accomplished this year provided the following specific contributions, summarized briefly here and explained in more detail in the body of the report:

1. Airspace permeability was defined as a key metric of translated weather impact. Permeability represents the degree to which traffic flows are constrained by convective weather in a given airspace region. Permeability can also be further translated into a categorical impact metric (e.g., none, moderate, severe) or a quantitative measure of the achievable or sustainable traffic flow rates that the airspace can support.

2. Airspace regions defined when translating weather into permeability can be arbitrarily sized, oriented, and located. Typically, airspace regions in this study were chosen to conform to existing Flow Constrained Area (FCA) boundaries. The orientation of the airspace region affects the permeability metric that is computed. For example, a convective line of weather that

lies across the airspace flow will generally result in a lower permeability measure than weather oriented parallel to the traffic flow.

3. Permeability was computed using the previously-developed and validated Convective Weather Avoidance Model (CWAM) and Weather Avoidance Field (WAF). CWAM and WAF are core components of the Route Availability Planning Tool (RAPT) which is part of the Traffic Flow Management System. For this work, the output of CWAM was processed across a set of routes and assimilated to compute the overall permeability or impact of convective weather on an airspace region.

4. Based on historical analysis of traffic and weather, statistics representing *achievable* and *sustainable* flow rates were derived for 57 different airspace regions. Those flow rates were then mapped against the permeability metrics for the same situations. While *achievable* flow rates may be possible for short time periods, significant effort would typically be required on the part of the sector controllers to manage that volume of aircraft safely. *Sustainable* flow rates represent values more typically observed for the given level of permeability, and so are more likely targets for long-term flow rates.

5. A machine learning capability was developed to forecast permeability and uncertainty from 0 - 12 hr, combining several heterogeneous deterministic and probabilistic forecast products. This represents a first-of-its-kind system to integrate extrapolation, High Resolution Rapid Refresh (HRRR), Short Range Ensemble Forecast (SREF), and Local Aviation Model Output Statistics Program (LAMP) forecasts into a single decision support metric. The machine learning algorithm was trained so as to minimize the size of the uncertainty bounds on the forecasted permeability. The uncertainty bounds provide feedback to the user as to whether the weather forecasts are in general agreement (leading to narrower bounds) or contradictory (leading to wider bounds), which may aid in hedging TMI decisions.

6. A by-product of the machine learning algorithm to forecast permeability is the ability to determine the relative value of each input source toward the output of the algorithm. This enables the algorithm to provide a quantitative mapping of the relative importance of each forecast product (extrapolation, HRRR, SREF, LAMP) across the 0-12 hr forecast horizon. The result is an ability to articulate, for example, when numerical-model-based forecasts such as SREF or LAMP may outperform extrapolation forecasts at longer lead times.

7. The translation of weather into permeability and the forecast of permeability and its uncertainty for 0-12 hr was implemented in a real-time decision support display called the Traffic Flow Impact (TFI) tool. TFI was then evaluated at selected FAA and airline facilities during the convective weather season as part of the FAA's ongoing CoSPA program.

8. A portfolio of future research and development topics were identified during the course of this work, described in more detail in Section 5. These include:

a. Site-specific adaptation for converting permeability into traffic flow rates for specific airspace resources.

b. Translation of permeability into TMI parameters including event onset, duration, and depth of impact. This requires additional information elicitation from users and Subject Matter Experts in order to determine appropriate settings for these parameters as well as methods to convey uncertainties.

c. Extension of TFI to accommodate multiple-FCA and Collaborative Trajectory Options Program (CTOP) operations.

d. Integration of TFI forecast capabilities into Operational Response Development (ORD) concepts.

e. Further investigation of interpretation and use of uncertainty information in airspace impact forecasts.

f. Airspace impact forecasting for progressive decision making and operational bridging.

To summarize, two key recommendations of this report are:

1. Leverage laboratory simulation exercises, operational feedback, and other subject matter experts to refine the understanding of how permeability, achievable/sustainable flow rates, forecast uncertainty, and workload interrelate. This is critical toward developing requirements for future decision support systems that will be effective once fielded.

2. Extend the modeling and analysis work performed to date so as to encompass a range of spatial scales (from single routes to entire Air Route Traffic Control Centers (ARTCCs)) and progressive decision-making timescales. This will be important to determine how concepts such as TFI can be used to support CTOP in the near-term, and as a component of broader Operational Response Development activities in the long-term.

This page intentionally left blank.

ACKNOWLEDGEMENTS

This work was sponsored by the Federal Aviation Administration under Air Force Contract No. FA8721-05-C-0002. Opinions, interpretations, conclusions, and recommendations are those of the authors and are not necessarily endorsed by the United States Government. We are especially appreciative of the support provided by Rob Hunt and Yong Li, FAA AJV-73, for funding work to develop algorithm improvements, and Tom Webster, FAA AJM-33, for the funding and support to conduct the CoSPA field evaluations. We also wish to thank Anthony Tisdall, Lead of System Operations at the ATC Command Center, and the other dedicated staff at the FAA and airline facilities for their time and insights into the strategic decision-making process. Finally, we wish to thank Haig Iskenderian, Kim Calden, Brad Crowe, Peter Erickson, Fulvio Fabrizi, Richard Ferris, Darin Meyer, and Ngaire Underhill of MIT Lincoln Laboratory for their contributions to this work.

This page intentionally left blank.

TABLE OF CONTENTS

TABLE OF CONTENTS
(Continued)

Page

LIST OF ILLUSTRATIONS

LIST OF ILLUSTRATIONS
(Continued)

LIST OF ILLUSTRATIONS
(Continued)

LIST OF ILLUSTRATIONS
(Continued)

LIST OF ILLUSTRATIONS
(Continued)

LIST OF ILLUSTRATIONS
(Continued)

LIST OF ILLUSTRATIONS
(Continued)

LIST OF ILLUSTRATIONS
(Continued)

LIST OF ILLUSTRATIONS
(Continued)

LIST OF ILLUSTRATIONS
(Continued)

LIST OF ILLUSTRATIONS
(Continued)

This page intentionally left blank.

1. INTRODUCTION

Weather accounts for over 70% of the delay in the US National Airspace System (NAS) and convective weather accounts for 60% of these weather delays [1](Figure 1). To mitigate these delays, forecasts of convective weather are used by traffic flow managers to match traffic demand to capacity constraints of specific air traffic resources, such as en route flows or departure fixes, via a strategic management plan. Traffic demand for impacted resources is managed through the application of traffic management initiatives (TMI) that either completely removes demand from an impacted airspace resource or that reduces demand by delaying the departure of flights filed through the impacted airspace.

The desired outcome of strategic planning is to ensure that demand and capacity are sufficiently balanced at the impacted resources to ensure that tactical management and execution can handle flight demand efficiently (e.g., with minimal airborne holding, pilot deviations and tactical reroutes, etc.). The Traffic Flow Impact (TFI) capability, discussed in this report, provides a forecast of airspace impact plus explicit uncertainty bounds to help guide TMI decisions in balancing demand and capacity in the 4- to 12-hour planning horizon. Traffic planners have never had a forecast such as this that provides explicit information about weather impacts directly coupled to specific TMI decisions such as Airspace Flow Programs (AFP), Ground Delay Programs (GDP), and strategic reroutes.

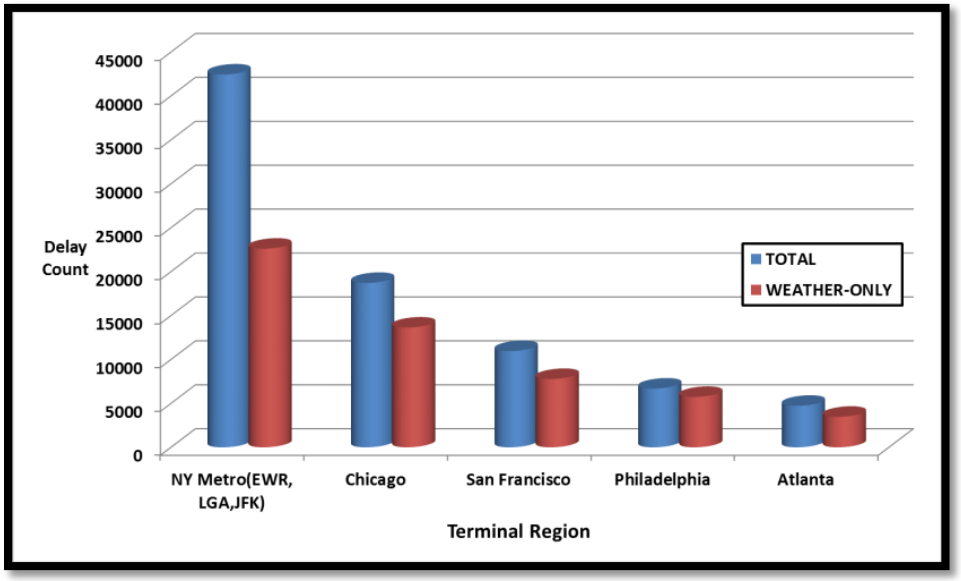

Figure 1. April-September 2014 Delay Statistics (OPSNET/ASPM) showing total delay count versus weather only at seven of the highest delay terminals. Convective weather accounts for more than 60% of the total weather delay.

1.1 BACKGROUND

Typical strategic TMI programs used by the Air Traffic Managers include mandatory playbook reroutes, Ground Delay Programs (GDP), and Airspace Flow Programs (AFP) as shown in Figure 2. Since these TMIs require the pre-departure management of demand, such decisions must be made several hours in advance of the event onset. This longer lead-time also allows airline operators to plan for the schedule and fueling consequences of the TMI.

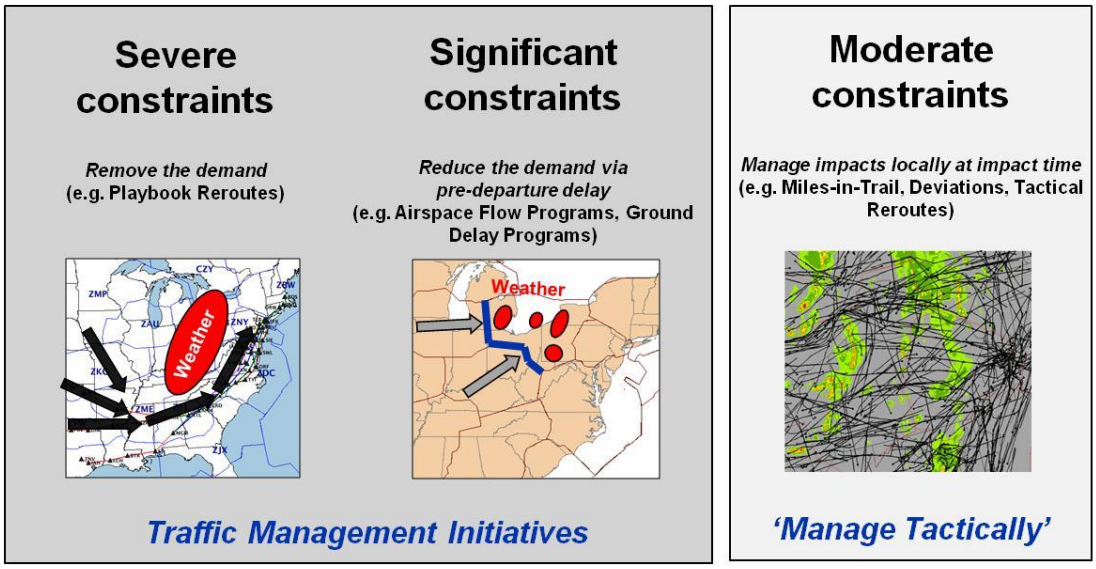

Figure 2. Relationship between weather-related capacity constraints and TMI to manage demand.

To set the critical parameters of the TMI such as start time, duration and maximum flow reduction, decision-makers require weather forecasts of the impacted airspace 4 to 12 hours in advance of the event. Several weather-only convective forecasts are available to the traffic planner in the strategic time domain, such as the Consolidated Storm Prediction for Aviation (CoSPA)[2], Short Range Ensemble Forecast (SREF)[3] and Collaborative Convective Forecast Product (CCFP)[4]. However, these forecasts provide little guidance concerning the level of impact on the air traffic resources and the precise location, severity, scale, and timing of operationally significant storms; and the human response to those storms can be notoriously difficult to predict. Therefore, the decision maker is left to make critical TMI decisions based on a subjective assessment of potentially conflicting weather forecast information (Figure 3).

Convective weather forecast models have improved significantly in the past ten years. The High Resolution Rapid Refresh (HRRR)[5] developed by National Oceanic and Atmospheric Administration (NOAA) at the Earth System Research Laboratory consistently predicts days with high impact on aviation operations. The HRRR enables radar-like forecast images that can be used to aid in translating convective

storms into potential traffic impact. Probabilistic NOAA models such at the SREF[6] and the Localized Aviation MOS Program (LAMP)[7] have also proven to be reliable with some high impact convective events.

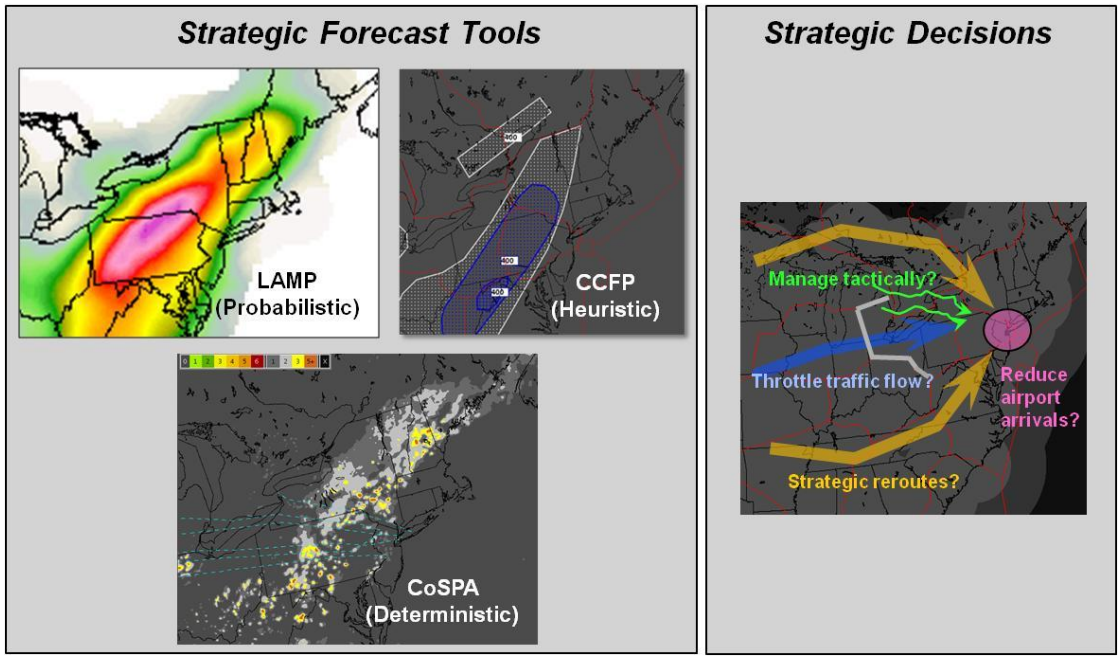

Figure 3. Current convective weather forecast products and the strategic decisions that traffic planners must make.

1.2 PROBLEM STATEMENT

The lack of an explicit translation of weather forecasts into resource constraints is a shortfall in the current weather information available to air traffic managers for strategic traffic flow management. There are several consequences of this shortfall. First, without an explicit translation there is a lack of an operationally relevant methodology to assess weather forecast resource impact and overall forecast performance. Each participant (e.g., Air Traffic Control System Command Center (ATCSCC), Air Route Traffic Control Center (ARTCC) Traffic Manager Unit (TMU), and Airline Operations Centers) comes into the collaborative strategic planning process with their own set of operational objectives, favorite forecast information, risk tolerance, etc. This wide and often divergent range of opinions and goals must somehow be melded into a plan of action. Without shared objective forecasts of weather impacts and estimates of decision risk, there is little common ground upon which to base discussions about the best plan of action that addresses the different legitimate concerns of stakeholders. Second, the utility of convective weather forecasts is directly related to the quality of decisions and NAS performance outcomes that the forecasts can support. The definition of explicit, validated weather translations provides

an objective and operationally relevant measure of truth against which forecasts can be compared. Without translation-based forecast evaluations, it is difficult to determine how much of the operational shortfall in convective weather mitigation is due to poor weather forecasts and how much is the result of poor interpretation and application of forecast information.

1.3 CURRENT FORECAST CAPABILITIES

Previous efforts to estimate convective weather impacts have focused either on individual Air Traffic Control (ATC) sectors[8] or sector-traversing flows[9]. Such resources are important to tactical operations, as traffic managers seek to avoid sector overloads that can result in sector closures and excessive airborne holding. However, sector-level impacts are a poor match for strategic planning. Strategic planners usually focus on key, large-scale traffic flows that traverse often congested en route airspace (e.g. ARTCCs) or that carry traffic to or from transition airspace for busy metroplexes. Furthermore, the precision of convective weather forecast needed to estimate sector capacities is unachievable in the strategic planning time horizon.

As mentioned previously, convective weather model forecasts have improved significantly over the past decade with the aid of faster, more powerful computers able to utilize higher resolution data on smaller and smaller grids. These improved model forecasts are grossly under-utilized in Traffic Flow Management (TFM) decision-making due to several possible reasons. Users are aware that weather forecast models can be incorrect and are therefore often afraid of the consequences of providing a TFM decision based on an inaccurate forecast. Users also suffer from "information overload" resulting from the need to evaluate many weather forecast products that have no true translation to air traffic flow management (ATFM) impact. Only a few experienced traffic managers are able to translate models into actionable information, but even then, they are unable to convince other stakeholders to implement restrictive programs. Even these highly experienced traffic managers can often struggle with how to incorporate forecast uncertainty into go/no-go decisions. Finally, customers and other strategic planning participants consistently challenge demand-reducing TMI programs based on different stakeholders' business models and specific facility operations. The current operational system provides neither translation nor impact assessment to aid stakeholders in formulating the operational plan.

Although current convective model forecasts are highly advanced, they continue to lack an easily interpretable measure of confidence or uncertainty that would allow traffic managers to assess the related risk involved in a specific TMI decision. Examples of four methods, currently used operationally, that attempt to provide forecast confidence are shown in Figure 4. The LAMP (Figure 4A) and CCFP (Figure 4C) provide forecast guidance based on probability. Confidence is therefore inferred from a probability value alone; the forecast is often converted to a go/no-go decision by the users and does not easily translate into TFM decisions. Deterministic forecasts like the Corridor Integrated Weather System (CIWS; Figure 4B) and CoSPA (Figure 4D) infer confidence through prior forecast performance and model agreement. All of these examples cast the confidence or uncertainty in terms of weather and not operational impact; and none of them easily translate into TFM decisions.

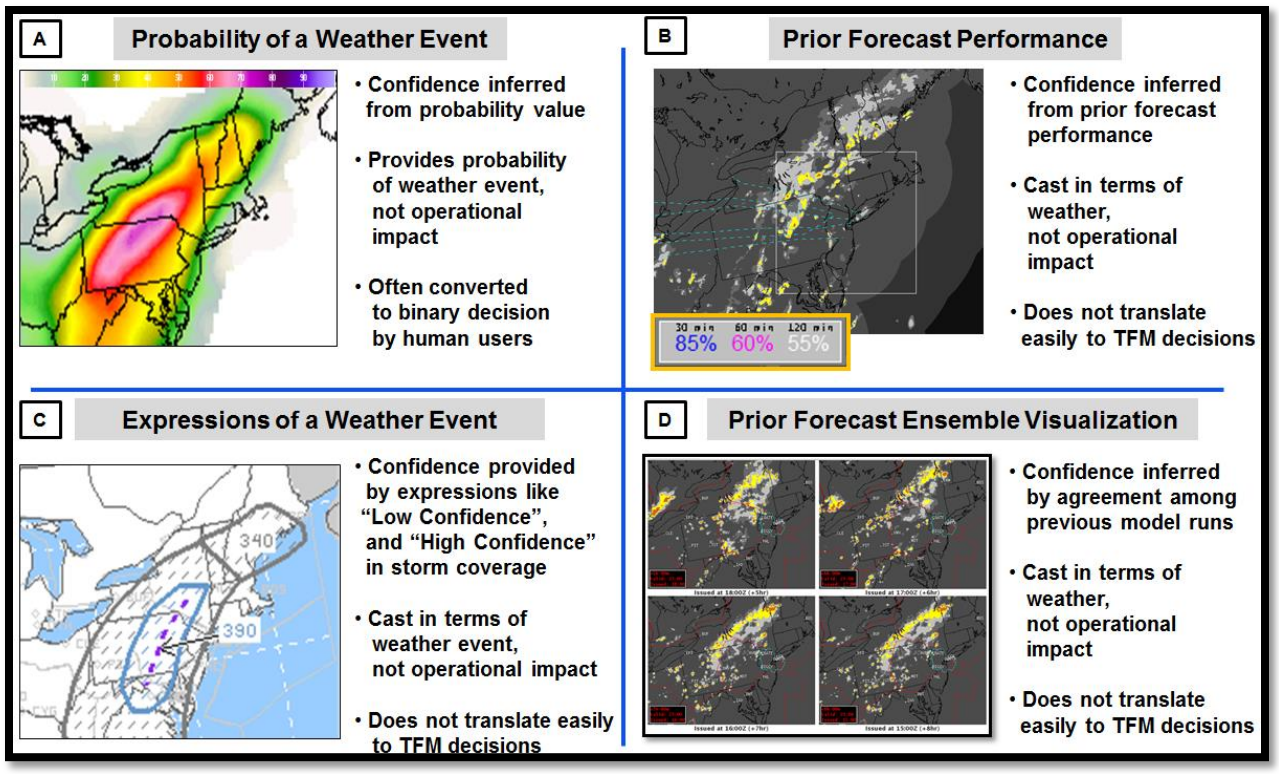

Figure 4. Examples of operational forecasts and their associated forecast confidence estimates. LAMP (A), CIWS (B), CCFP (C), and CoSPA (D).

Beyond translation and confidence in the forecast, there is the need for more comprehensive common situational awareness amongst all decision-makers. Air traffic management and stakeholders need the same translation metric when engaged in day to day management of the NAS. Legitimate differences based on FAA mission statements and industry business models will remain, but the discussions can be more efficient when based on a common set of facts. Managing uncertainty and risk is difficult to do in an operational environment. There is a need for common concepts and vocabulary that will ultimately allow meteorologists and traffic managers to make better use of the forecast models, and to embrace, assess, and enhance the automation that will follow in the years to come.

1.4 ORGANIZATION OF THIS REPORT

This document summarizes work performed by MIT Lincoln Laboratory during the period 1 February 2015 – 30 November 2015 focused on developing and improving algorithms to estimate the impact of convective weather on air traffic flows. Section 2 describes the algorithm used to translate convective weather intensity (Vertically Integrated Liquid [VIL] and Echo Tops) for a defined airspace

region and orientation into a measure of impact called *permeability*. Further, permeability is compared against observed traffic flow rates to build a conversion from permeability into achievable and sustainable flow rates for that airspace. Section 3 describes the model that was developed and refined to forecast permeability and flow rate out to 12 hr in the future. Multiple weather forecast models are combined using that algorithm to produce not only the impact forecast but also the uncertainty bounds on that forecast based on the similarity of the underlying forecasts and a number of other factors. Section 4 summarizes operational decision-making and field evaluations of a prototype implementation of the algorithms at several FAA facilities and airlines. Also discussed are issues related to the operational use of permeability, flow rate, or other impact metrics. Section 5 provides an outline of proposed future work, and Section 6 summarizes the report.

2. WEATHER TRANSLATION INTO TRAFFIC FLOW RATES

In this section, a model to translate weather impacts into an impact measure called permeability will be discussed and the validation of the permeability will be performed with the observed traffic flow rates. Once a correlation is established between permeability and observed traffic flow rates, permeability can be used to predict an airspace impact classification (red, yellow, green), a first order flow rate prediction, or a second order prediction of TMI parameters such as onset, event duration, and cumulative delay discussed Section 4.3.

The translation of convective weather forecasts into an airspace impact is one of the key pieces of information needed to make efficient traffic management decisions in the time-constrained and unpredictable environment that develops when thunderstorms limit capacity across the NAS. The TFI application begins by providing an estimate of airspace permeability. In simple terms, permeability is computed from the overlap of forecasted weather with an airspace resource to determine the amount of usable airspace in the airspace resource. The airspace permeability is then used to assess the operational impact of convective weather on the air traffic operations.

2.1 TRANSLATION MODEL METHODOLOGY

An example of an airspace resource definition is shown in Figure 5. The resource definition consists of three components: airspace crossing; airspace boundary; and airspace traversing trajectories, all of which define a strategic flow through the airspace. The airspace crossing is represented by a line that all aircraft in the strategic flow traverse. The airspace boundary represents the region for which the model will evaluate the weather characteristics to estimate the permeability. Finally, the airspace traversing trajectories represent notional routes perpendicular to the airspace crossing and are the basis for computing the trajectory impacts.

The translation model is based upon: Weather Avoidance Fields (WAF) and Convective Weather Avoidance Polygons (CWAP) developed as part of the Convective Weather Avoidance Model (CWAM)[10]; the definition of airspace resources that are operationally significant and whose capacities are measureable; and the assessment of operational impact of weather on a trajectory.

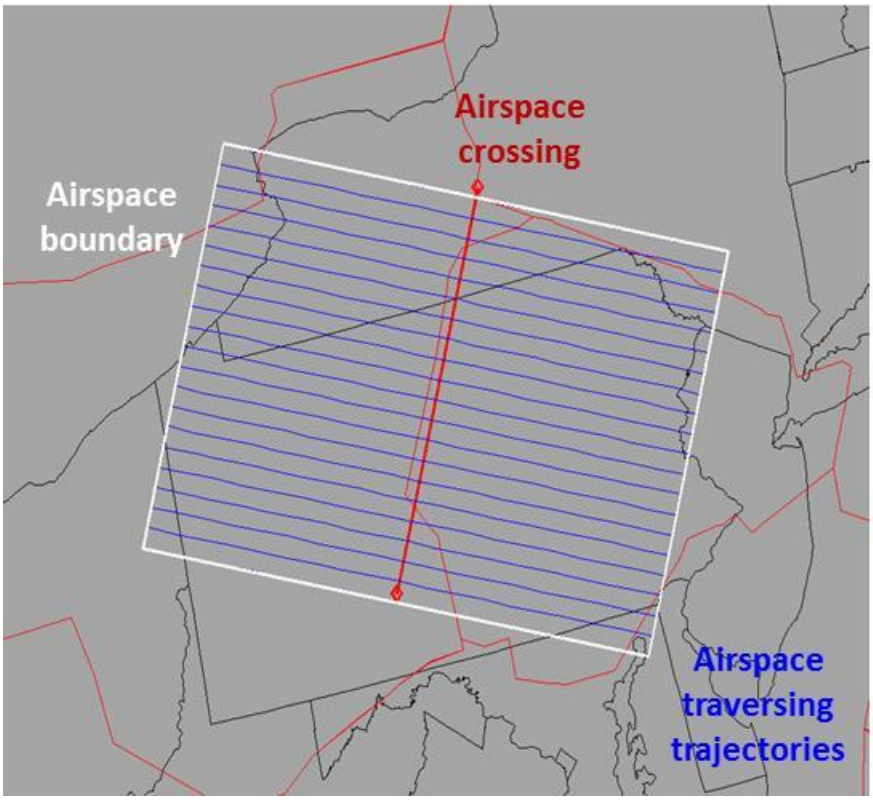

Figure 5. Airspace resource definition for the ZOB/ZNY strategic flow.

The method of assessing the impact of the weather on a trajectory takes into account the scale and severity of storms that impact the flight trajectory. Storm scale is represented by the nominal duration an aircraft flying a trajectory (notional route) spends inside a Convective Weather Avoidance Polygon[11]. Severity is represented by the maximum WAF blockage[12] calculated along the trajectory. Each notional route is then assigned an impact of RED (impassable), YELLOW (uncertain), DARK GREEN (passable with acceptable storm-avoiding deviations), or GREEN (passable) based on a two-dimensional heuristic trajectory impact model, shown in Figure 6. Finally, the permeability of the airspace is estimated by taking a weighted average of the trajectory impacts for all the notional routes that traverse the airspace and scaling into a percentage.

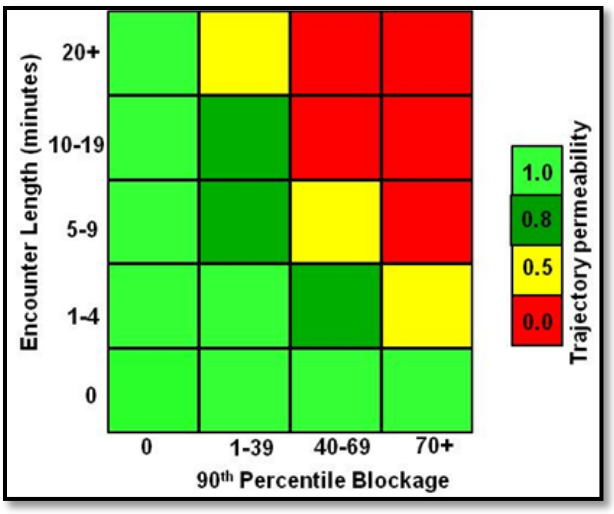

Figure 6. Trajectory impact model used in the airspace classification.

2.2 TRANSLATION MODEL VALIDATION

In order to validate the translation model, it is necessary to demonstrate that the permeability estimate can accurately depict the observed operational behavior. High permeability values (greater than 80) should support high traffic throughput, while low permeability values (less than 50) should represent highly constrained airspace. During times of high permeability estimates it is expected that there will be small, weather-avoiding deviations that will not impact the traffic flow rates. During times of low permeability, while it is possible there may still be some traffic passing through the airspace, the majority of traffic should be rerouted or delayed out of the impacted airspace. For this analysis, we focus on airspace that is roughly the scale of an Air Route Traffic Control Center (ARTCC), and so to validate the model, we will concentrate on the observed en route traffic that transits an impacted ARTCC.

To first order, the translation model can be validated by comparing the permeability to the observed traffic traversing the impacted airspace. However, this validation relies on the implicit and often tenuous assumption that observed traffic in the airspace is determined primarily by weather impacts in the airspace only. This assumption may be violated under several circumstances:

1. Observed traffic through an unimpacted region may be low if there are constraints directly upstream (preventing traffic from entering the airspace) or downstream (preventing traffic from leaving the airspace).

2. Observed traffic through an unimpacted region may be lower than expected if traffic flows through the airspace were constrained by a prior traffic management initiative (TMI). It may take several hours for traffic flow constrained by Airspace Flow Programs (AFP) or a Ground Delay Program (GDP) to return to normal after the programs are lifted, since both constrain traffic by delaying demand on the ground, possibly several hours flight time away from the impacted en route or terminal airspace.

3. Observed traffic through heavily impacted airspace may exceed expectations if creative but difficult to sustain tactical operations are required to reduce large airborne or surface congesting inventory.

Operational behavior can be observed by measuring the flow rate or the number of aircraft that pass through the airspace in a given time period. For validation, we begin by using the Aircraft Situation Display for Industry (ASDI) data feed to identify those aircraft that traverse the entire region defined by the airspace resource. We also compute the permeability estimate from the WAF field generated from Corridor Integrated Weather System (CIWS) data archives of precipitation intensity and storm tops. As one example, Figure 7 depicts the aircraft flying through the airspace that defines the transition between Cleveland ARTCC (ZOB) and New York ARTCC (ZNY). The air traffic controllers managing this resource are handling flights landing and departing from the NYC metro airports. The aircraft shown in black have been associated with this resource by automated algorithms that filter for aircraft entering one end of the airspace and exiting on the opposite end. Aircraft shown in cyan are not associated with the resource: they enter or exit laterally through a side of the region. Figure 7a shows the flights on a summer afternoon without any significant convective weather impacts. Aircraft are entering the western edge of the resource, flying a direct route through the airspace and exiting on the opposite edge. Figure 7b shows the impact of convective weather on the traffic flow in this same region. Significantly fewer aircraft are observed traversing the airspace and those that do are not able to fly a direct route. This additional flight time requires air traffic controllers to spend more time handling each aircraft and thus increasing the workload on ATC. For each flight associated with the airspace resource the algorithm also measured the transition time of the aircraft through the airspace.

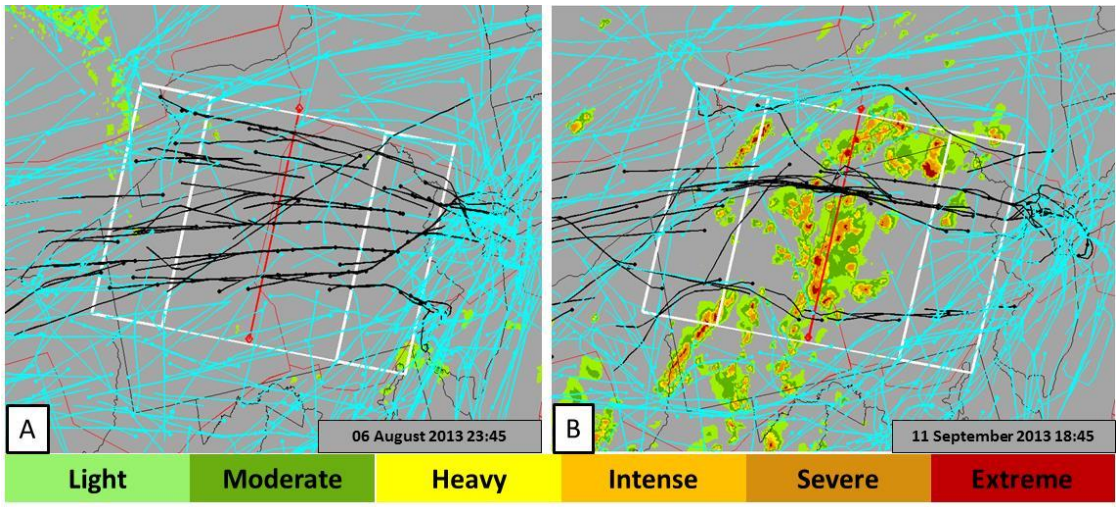

Figure 7. Precipitation and aircraft traversing the airspace resource that defines the transition between ZOB and ZNY. Aircraft flying completely through the resource are shown in black, those not associated are shown in cyan.

Initial validation was performed on ten moderate to severe weather-impacted and 31 minimal to no-impact days from the summer of 2013, focusing on throughput for New York metro-area airports; and the model was shown to have good agreement between the estimated permeability and the observed flow rates. To improve our insight into the relationship between permeability and the achievable, sustainable capacity that is required for strategic planning, our research efforts this past year have focused on three primary areas: improving the validation methodology, expanding the data set of weather impacted days, and examining additional regions of the NAS that have different demand profiles, ATC operational priorities and weather characteristics.

Additional data was collected from a large set of weather-impacted days from the summer of 2014 and 2015 as well as two heavy impact days from 2011 and one from 2012, for a total 122 case days. These included days with a wide range of weather characteristics; from late spring synoptic scale storms to summer midday convection due to heating, to early fall storms with weaker convection. One of the days with significant delays was June 13, 2014. Figure 8 shows the 60-minute flow rates, the transition time[1], and the permeability estimates for that date.

[1] Transition time is the time it takes for an aircraft to cross the airspace resource.

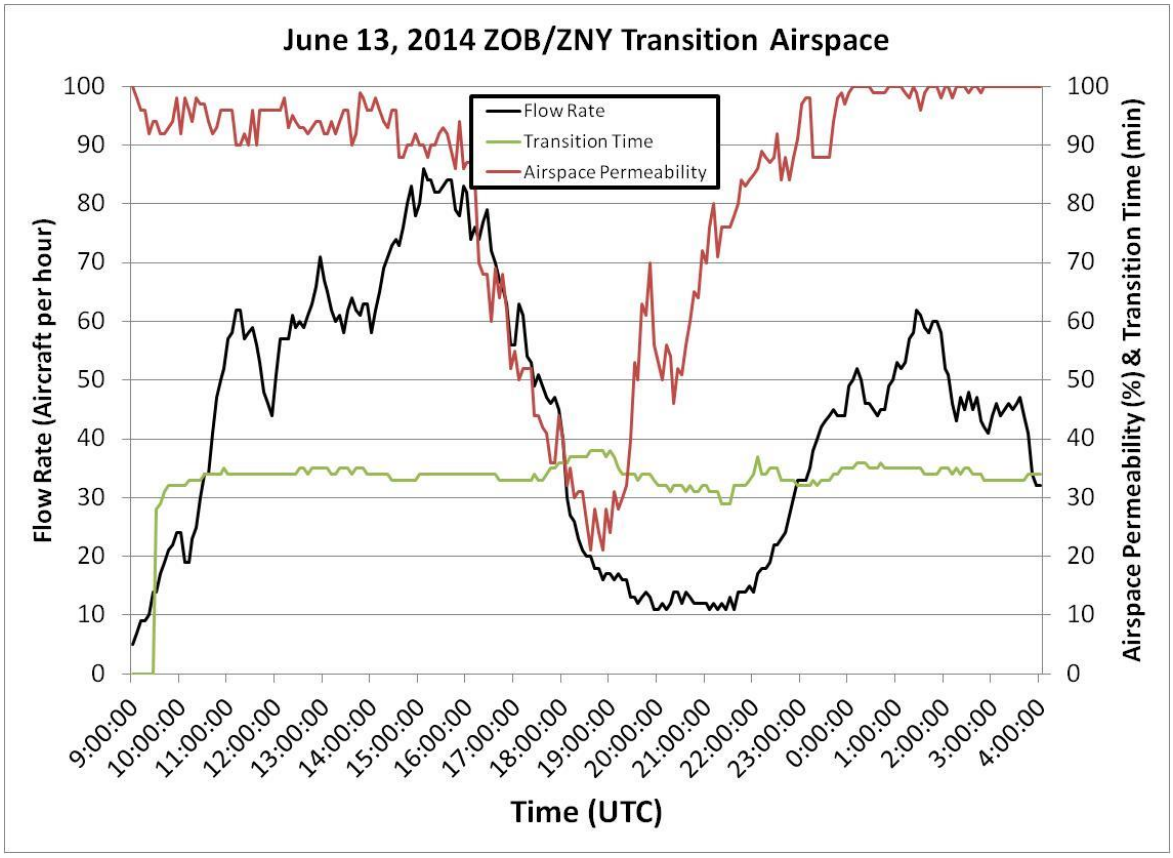

Figure 8. Observed 60-minute flow rate (black), transition time (green), and airspace permeability estimate (red) for June 13, 2014 for the ZOB/ZNY transition airspace ZNY001.

On this day, a cold front was oriented north-south across the ZOB/ZNY transition airspace. Two separate lines of convective weather developed over the airspace during the afternoon and then moved eastward towards the NY metro airports. The airspace permeability estimate for this airspace on this day shows excellent agreement with the flow rates as the weather develops, beginning at approximately 1600Z (noon local time). As the spatial extent and intensity of the weather grows, the observed flow rate and permeability estimate decrease synchronously until 1930Z. Air traffic managers are able to reroute the excess demand north into the Boston ARTCC (ZBW) and south into the Washington DC ARTCC (ZDC), allowing the air traffic to continue to reach the NY metro airports.

At 1930Z, the permeability estimate begins to increase while the flow rate continues to drop, reaching a minimum of 11 aircraft hour after 2100Z. This noticeable discrepancy between the flow rate and permeability is explained through an analysis of the weather images and the ATCSCC program logs. As the weather moves eastward, it exits the ZOB/ZNY transition airspace allowing the permeability

estimate to increase. However, the weather then begins to impact the NY metro airports. The weather impact at the airports is significant enough to shut down all flow into the NY TRACON (N90). With the downstream resources significantly impacted, the flow through ZOB/ZNY cannot resume until the weather clears the airports. With such significant impacts at the NY metro airports, the air traffic managers issued ground stop programs, in essence grounding all flights heading into NY and decreasing future demand into the airspace.

A statistical validation of the impact model was performed for the ZOB/ZNY transition airspace using all 122 case days. The data set was filtered to include only hours between 1800Z and 0000Z, when the airspace experiences the highest demand. Figure 9 is a box-and-whisker plot of the permeability estimates. A correlation between the airspace impact model and the flow rate is clearly visible. As the convective weather impact increases (measured by a decreasing permeability), the flow rate decreases accordingly.

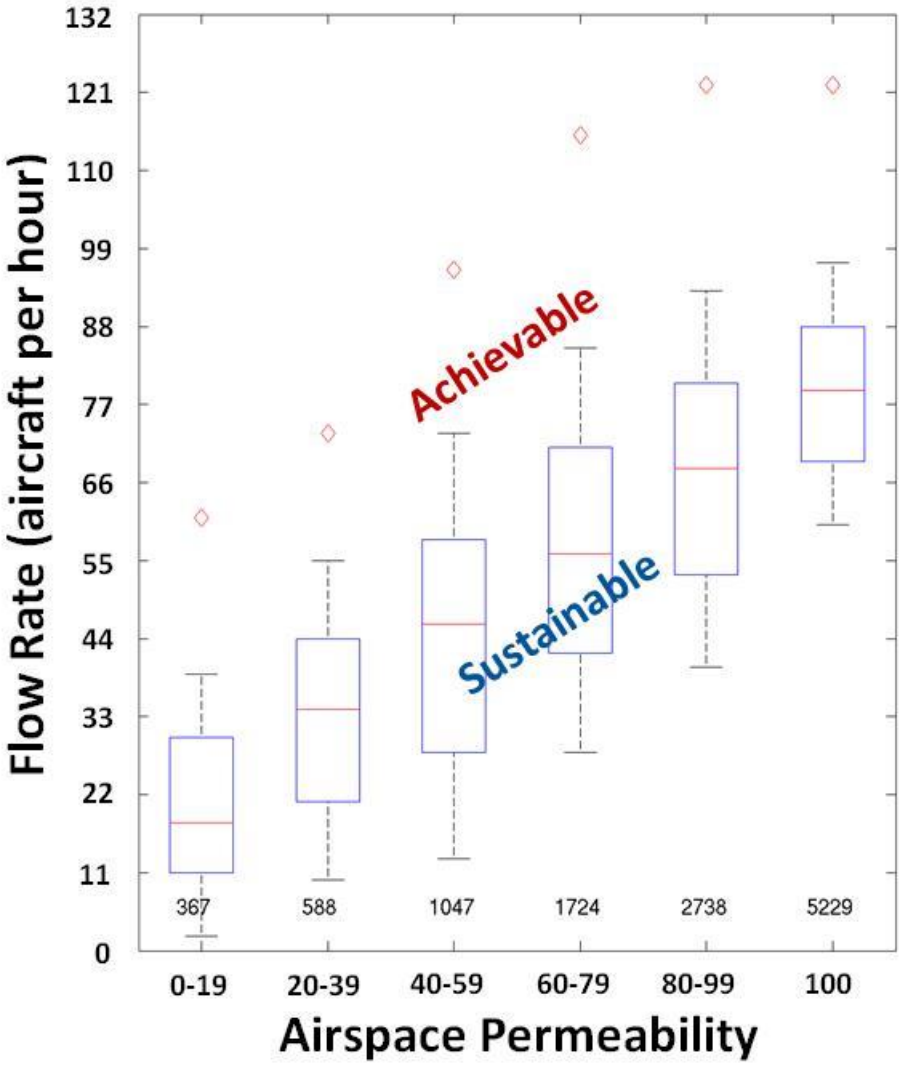

Figure 9. Box-and-whisker plot of the observed 60-minute flow rate for the ZOB/ZNY transition airspace (ZNY001). The red dash is the median flow rate; the box represents the 25th and 75th percentile values; the maximum observed flow rate for each box is shown as a red diamond. The count of observations used in each permeability category is shown above the x-axis. Data are from 122 case days during the summers of 2011, 2012, 2013, 2014 and 2015.

Using the mapping of permeability to flow rate provided in Figure 9 (i.e., median flow, 75 percentile, and maximum observed flow) planners could create traffic management programs that are tailored for the specific scenario of the day. For instance, for short-lived events, air traffic planners may choose to set flow rates near the maximum achievable rate for the permeability estimate forecasted. In

this instance, planners may feel confident in the ability to push the workload of the air traffic controllers and sustain high flow rates due to the limited impact duration of the event. On another day, a planner may decide that the convective weather impact will be long-lived, and it will not be possible to set higher rates due to the difficultly in sustaining a high workload for a long period of time. In this scenario, planners may choose to set rates closer to the median flow rates observed for this airspace.

The validation data contain instances where observed flow rates may not fall within the desired flow range preferred by ATC personnel. This may occur through heavily impacted airspace if creative but difficult to sustain tactical operations are undertaken by air traffic controllers to reduce a large inventory of airborne aircraft. For our validation results this can (and does) lead to larger uncertainty bounds in the correlation of flow rates and airspace permeability. An example of one such case is September 11, 2013. Figure 10 shows the 60-minute flow rates, the transition time, and the permeability estimate for September 11, 2013. At 1730Z the permeability estimate rapidly decreases as the weather develops, dropping below 40% at approximately 1845Z UTC. Due to the lack of a strategic plan on this day, air traffic managers are forced to deal with this excess demand on a severely constrained resource and continue to push aircraft through highly impacted airspace.

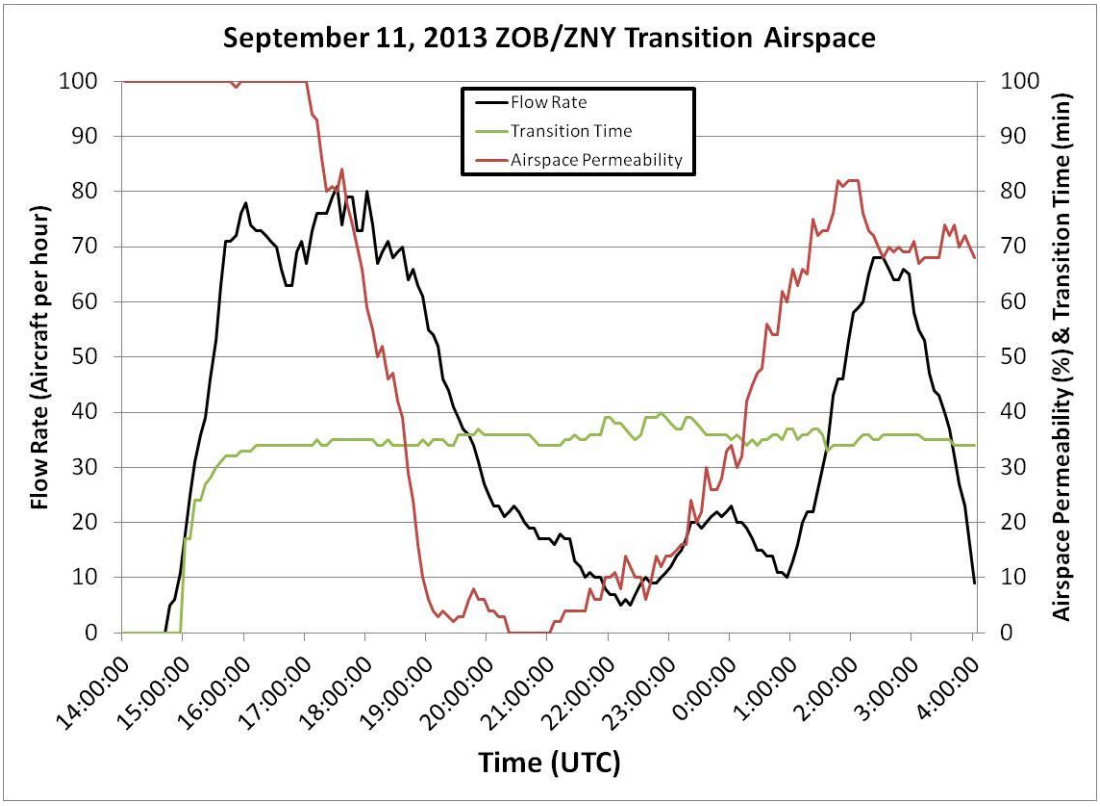

Figure 10. Observed 60-minute flow rate, transition time and airspace permeability estimate for September 11, 2013 for the ZOB/ZNY transition airspace (ZNY001).

Figure 11A depicts the strong convective weather that developed at 1845Z and the high volume departure and arrival streams sharing the same airspace. During the peak of the event, the nominal transition time increases from an average of 34 minutes to approximately 40 minutes as aircraft are vectored around storms or placed into holding while ATC manages the demand through the impacted airspace. It is also important to note that as the weather event ends at 00Z, the flow rate does increase; however, the flow rate lags the increase in permeability by one hour, resulting in unused capacity that is badly needed to begin recovery from the day's impacts. Figure 11B depicts the airspace at 0100Z UTC when the demand is near zero; air traffic managers prevented aircraft from departing for this airspace during the time of impact.

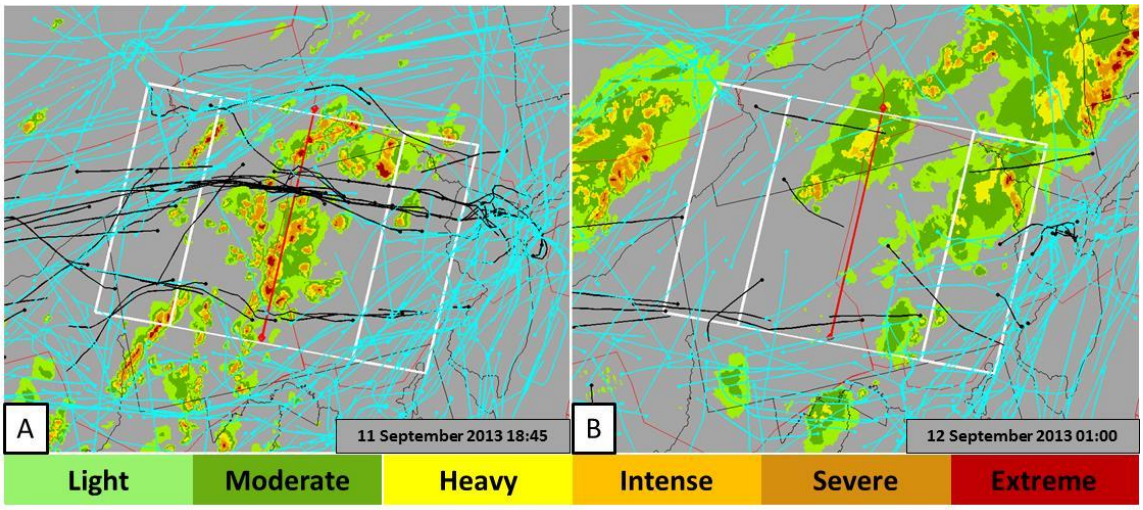

Figure 11. Aircraft trajectories on September 11, 2013 traversing the ZOB/ZNY transition airspace (ZNY001) and observed precipitation intensity. The trajectories in black are associated with the ZNY001 resource. The trajectories in cyan are not associated with the airspace.

Thus far this report has focused on an airspace that overlaps the Cleveland and New York ARTCCs with very heavy demand on the arrival and departure corridors into and out of the metro New York airports. This airspace is notoriously difficult to manage during times of convective weather impacts. The permeability translation model has been extended to 57 regions in the NAS to determine the viability and usefulness of the model across a broad set of air space regions with different demand profiles, air space configurations and typical weather scenarios. Appendix A contains the results for each of the TFI regions.

2.2.1 Improvements to Flow Rate Measurement

In this section, the results of exploring various methods to measure the flow rates will be analyzed. In initial studies conducted prior to this effort, the validation flow rates were estimated with an

instantaneous 15-minute flow rate from the aircraft currently contained within the airspace boundary as described in Figure 5. This was accomplished by first associating each aircraft with the TFI region by identifying those aircraft entering one end of the airspace and exiting on the opposite end as shown in Figure 7. Finally, the transition time across the TFI region was computed for all aircraft associated with the region and the flow rate was estimated as the number of aircraft in the TFI region divided by the median transition time of all those aircraft and multiplying by a constant (15 minutes in this case). This method could produce a significant amount of noise in the data and is not aligned with the common practice of air traffic management to observe and predict flow rates by counting the aircraft crossing a line (airspace crossing in Figure 5) over a 60-minute period.

During this research effort, analysis was performed on computing a flow rate more consistent with typical air traffic management practices. Counting the number of aircraft crossing three distinct lines (entering the TFI region, crossing the center line, and exiting the TFI region) was explored. Counting the aircraft over three distinct time periods (15 min, 30 min, and 60 min) was also explored. Initial results were not very promising, as noted in figures 10 and 11, often the effects of the weather impact, as measurable in flow rates, is not observable until some time after the weather impact begins. This is due to the excess inventory often experienced in these instances that must be tactically managed by air traffic personal until the airspace is cleared. To account for this delayed response, a third variable was added to the analysis that shifted the observed flow rates used in the comparison by 15, 30, and 60 minutes. This variable allowed for comparing the 1815Z, 1830Z, and 1900Z flow rates with the 1800Z permeability estimates. After review it was determined that using the 60 minute count, delayed 60 minutes for the aircraft exiting the TFI region produced the best correlation between permeability and flow rate. Figure 12 depicts the original statistical analysis for the ZJX/ZDC transition airspace (ZDC002) using the 15 minute instantaneous observed flow calculation (left) compared to the new 60 minute flow rate of the aircraft exiting the airspace with a 60 minute delay (right). It can be observed that these results are very similar and will lead to the same conclusions about the validation results.

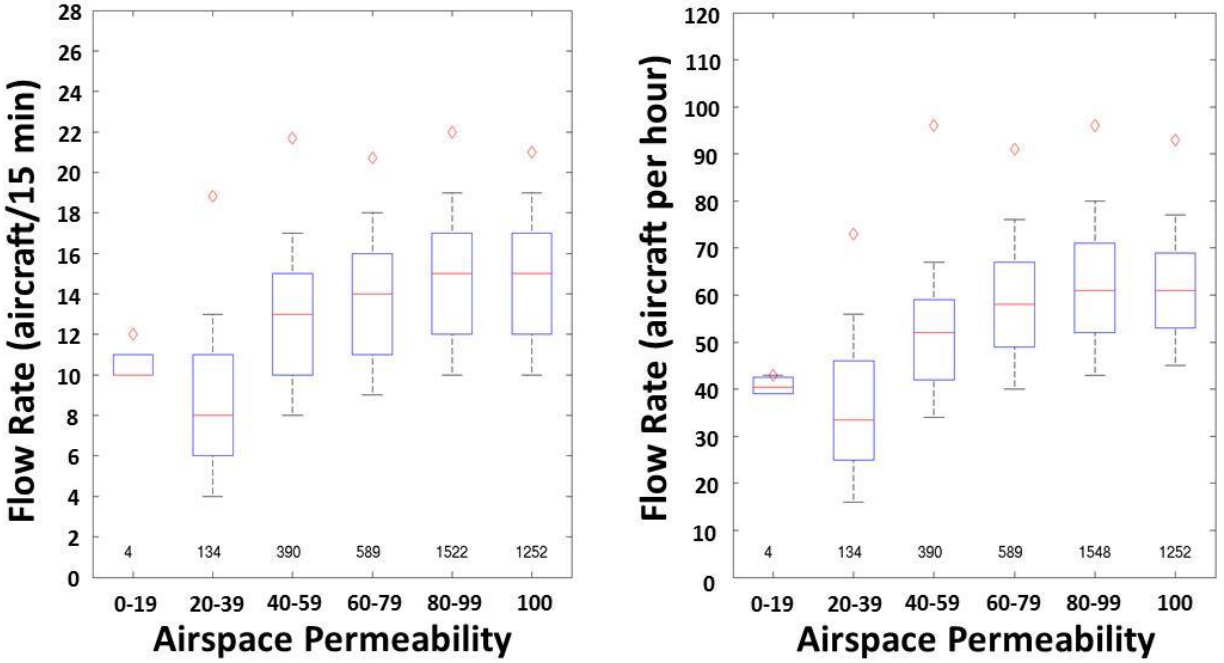

Figure 12. Observed 15-minute flow rate (left) and the observed 60-minute flow rates with 60 minute delay response (right) for the ZJX/ZDC transition airspace (ZDC002). The red dash is the median flow rate; the box represents the 25th and 75th percentile values; the maximum observed flow rate for each box is shown as a red diamond. The count of observations used in each permeability category is shown above the x-axis. Data are from 41 case days during the summer of 2013.

2.2.2 Validation in Regions of Lower Traffic Demand

In this section, we selected two airspace regions from the extended data set in Appendix A to validate the model in airspace regions that may not experience demand as high as the NY region or may have more flexibility in tactical rerouting. It is theorized that for this airspace the flow rate does not decrease due to greater flexibility but there is an increase in the workload of the controllers. Increased workload is discussed in Section 2.3.

The first airspace analyzed (ZKC001) is a region where aircraft are being managed solely by the Kansas City ARTCC (ZKC) traveling in a predominantly east-west flow. This airspace is used heavily by long-haul flights between the east and west coasts. Typically, this airspace has flexibility in aircraft deviations due to weather and does not regularly experience its maximum potential flow rates. This is primarily due to two reasons. First, management of weather impact can be done 'locally' between ZKC controllers under one manager in the same facility. Negotiations can be done in person and not requiring phone conversations between managers at two different facilities. Second, the volume of airspace is quite

large with significant amounts of airspace not used on a regular basis or along pre-planned routes. Figure 13 depicts the airspace crossing line, airspace boundary and typical flow through ZKC. It can be observed that there are large regions of white space denoting a lack of traffic. Also depicted is a box-and-whisker plot of the permeability estimates. Correlation between the airspace impact model and the flow rate is less prominent compared to Figure 9. As the convective weather impact increases (measured by a decreasing permeability), the flow rate does not begin to decrease until the permeability drops below a value of 60 and is not significant until the permeability is in the 0 to 19 range. More data are needed at the low end of the permeability range to validate the calibration for extremely high impacts in this type of airspace.

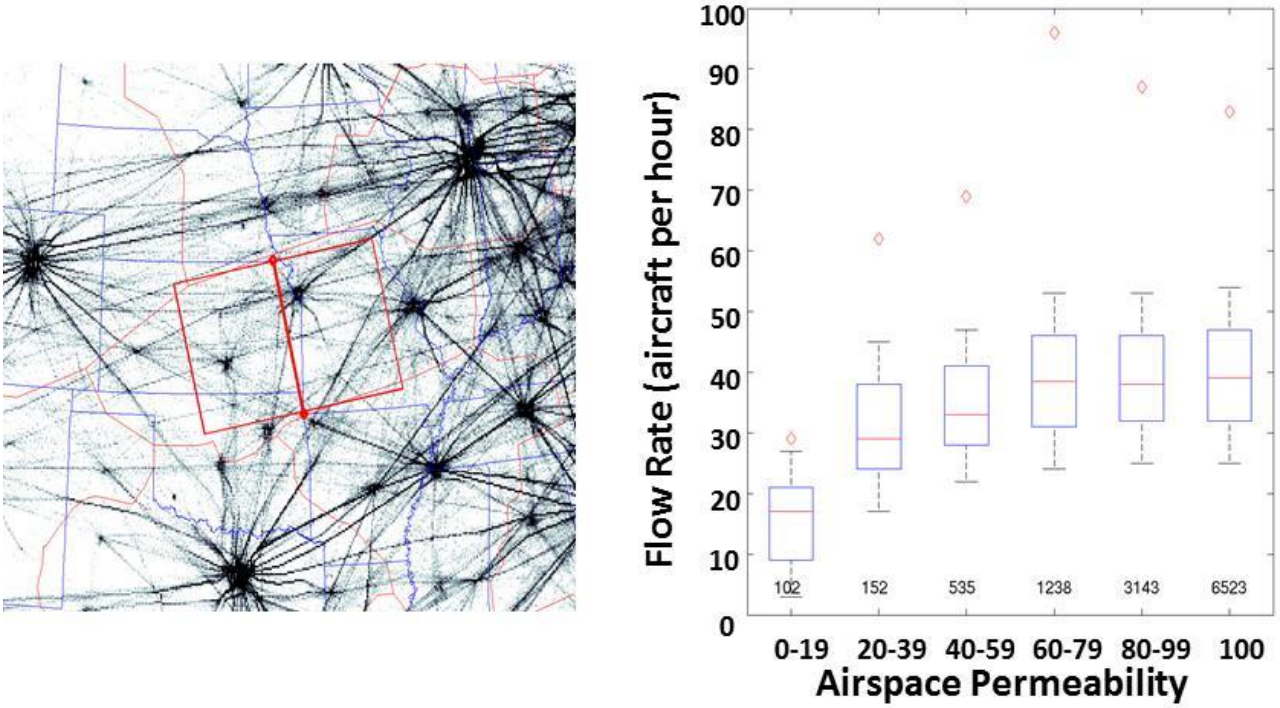

Figure 13. Left: Orientation of the ZKC001 airspace crossing relative to the ARTCC boundaries and common route structures. The airspace covers the primary east-west routes through the Kansas City ARTCC. Right: Observed 60-minute flow rate for the ZKC001 airspace. The red dash is the median flow rate; the box represents the 25th and 75th percentile values; the maximum observed flow rate for each box is shown as a red diamond. The count of observations used in each permeability category is shown above the x-axis. Data are from 122 case days during the summers of 2011, 2012, 2013, 2014 and 2015.

The second airspace analyzed (ZTL002) is a region where aircraft are transitioning between the Atlanta ARTCC (ZTL) and the Jacksonville ARTCC (ZJX) traveling in a predominantly north-south flow. Figure 14 depicts the airspace crossing line, airspace boundary and typical flow through ZTL002. It

can be observed that there are regions of white space between the common routes. Also depicted is a box-and-whisker plot of the permeability estimates. For this airspace there is no correlation between reduced permeability estimates and any reduction in flow rates. A review of the increased workload for the air traffic controllers in this airspace is conducted in Section 2.3.

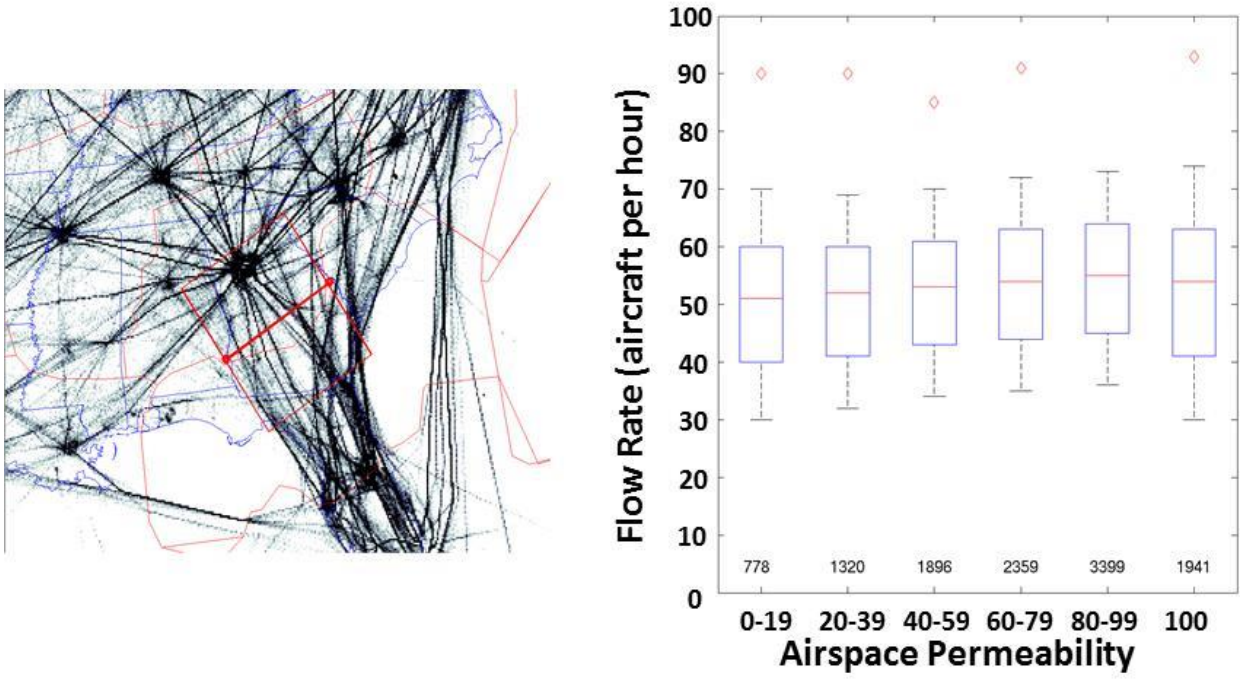

Figure 14. Left: Orientation of the ZTL002 airspace crossing relative to the ARTCC boundaries and common route structures. The airspace covers the transition airspace between the Atlanta ARTCC and the Jacksonville ARTCC. Right: Observed 60-minute flow rate for the ZTL002 airspace. The red dash is the median flow rate; the box represents the 25th and 75th percentile values; the maximum observed flow rate for each box is shown as a red diamond. The count of observations used in each permeability category is shown above the x-axis. Data are from 122 case days during the summers of 2011, 2012, 2013, 2014 and 2015.

Generally speaking, high demand regions have the best agreement between permeability and flow rate, while regions with less demand (allowing for greater flexibility with tactical options such as deviations, reroutes, etc.) have a less significant correlation between permeability and flow rate. This implies that additional analysis may be required and also that users of these types of metrics would need to understand the mapping between permeability and flow rates for different airspace regions.

2.2.3 Comparison of Large vs Small Airspace Results

In this section, we selected an airspace region from the extended data set in Appendix A to validate the model in airspace regions that experience heavy demand throughout the day but are of smaller geographical size than the TFI regions analyzed thus far. The ZNY001 airspace handling the transition between ZOB and ZNY is on the order of magnitude of the size of an ARTCC. Large TFI regions, such as ZNY001, are considered to be optimal for strategic traffic management predicting flow impacts on the 4-12 hour time scale. However, tactical management is done on the 0-2 hour time frame and is typically managed with sectors and measures of sector impact. The TFI region ZNY007 has been configured to capture only the east-west arrival flow traversing through sector ZNY75. This sector manages several arrival streams into the New York metro airports from the west. Figure 15 depicts the airspace crossing line, airspace boundary and typical flow through ZNY007. It can be observed that this is a highly structured air space just west of New York. Also depicted is a box-and-whisker plot of the permeability estimates. Correlation between the airspace impact model and the flow rate is clearly visible. As the convective weather impact increases (measured by a decreasing permeability), the flow rate decreases. It can also be observed that the flow rate decreases faster with decreasing permeability as compared to the larger TFI regions (ZNY001 Figure 9). This behavior is observed for many of the smaller TFI regions and it is speculated that this is due to a couple of reasons. First, smaller TFI regions aligned with sectors are capturing the ability to redirect these flows into neighboring sectors that are within the same facility (ZNY ARTCC) without requiring coordination with neighboring facilities. Second, the flow in smaller TFI regions aligned with departure corridors can be easily cut off by holding aircraft on the ground. It is important to note that although the ability to translate weather impact into flow reductions is possible with smaller TFI regions, the ability to forecast the weather impact beyond one hour becomes much more difficult at the scales due to limitations in the current capabilities of dynamic convective weather forecast models.

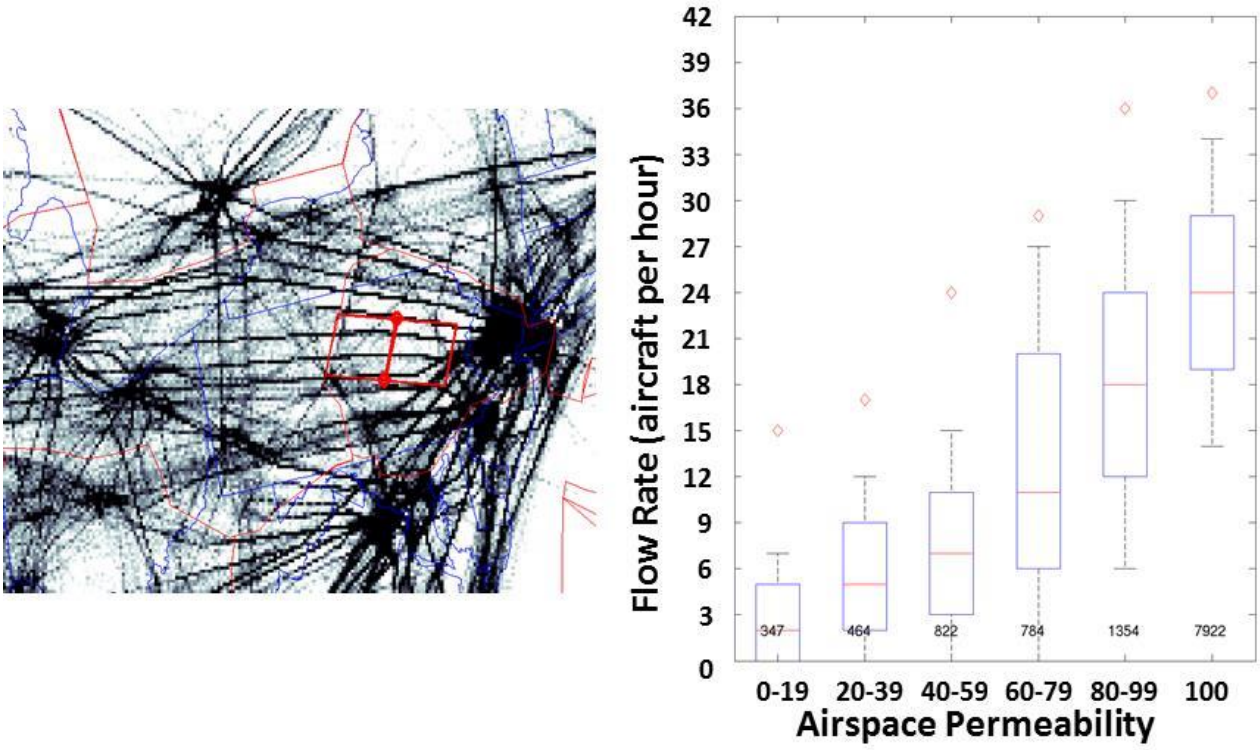

Figure 15. Left: Orientation of the ZNY007 airspace crossing relative to the ARTCC boundaries and common route structures. The airspace aligns with the ZNY75 sector capturing flow inbound into the NYC metro airports. Right: Observed 60-minute flow rate for the ZNY007 airspace. The red dash is the median flow rate; the box represents the 25th and 75th percentile values; the maximum observed flow rate for each box is shown as a red diamond. The count of observations used in each permeability category is shown above the x-axis. Data are from 122 case days during the summers of 2011, 2012, 2013, 2014 and 2015.

2.3 MEASURING WORKLOAD FROM TRAJECTORIES

Initial studies have shown that during some events, or at certain times during an event, or for specific airspace regions (Figures 13 and 14), the measured flow rates were not impacted (reduced) as much as predicted by the model. It is theorized that in these scenarios, air traffic controllers were able to maintain high flow rates at the expense of an increase in workload (i.e., adding more staff or otherwise managing a higher traffic handling rate).

One potential surrogate measure of workload is to relate the transit time of an aircraft through the airspace to the level of workload required from the controllers. An aircraft that flies a straight non-conflict path through an airspace typically requires less controller workload than an aircraft that performs multiple altitude or heading changes.

For this analysis we assume that aircraft that require additional control interaction to perform heading changes can be used as a surrogate for controller workload. To accomplish this, for each aircraft, a metric of Lateral Track Extension (LTE) is calculated, representing the added travel distance beyond a direct routing through the airspace. LTE is computed by measuring the actual distance traveled by the aircraft and dividing by the straight-line distance between the entrance and exit points. Figure 16 depicts the entrance and exit point of aircraft traversing the ZNY001 airspace and a notional direct route (black line) along with the actual aircraft trajectory (blue solid and dashed lines). For the example on the left of the figure, the aircraft follows a well-established route through the airspace making only two heading changes. For this non-weather impacted trajectory the LTE is 1.01 (or 1% increased travel distance). For the example on the right of the figure, the aircraft performs a significant amount of maneuvering to avoid the weather and find the gaps through the weather. There are at least four heading changes requiring controller interaction not including potential conflict resolution with other aircraft perform the same weather avoidance. For this weather impacted trajectory the LTE is 1.11 (or 11% increased travel distance). It is important to note that aircraft in holding can have exceptionally high LTE values that will skew the results in certain scenarios.

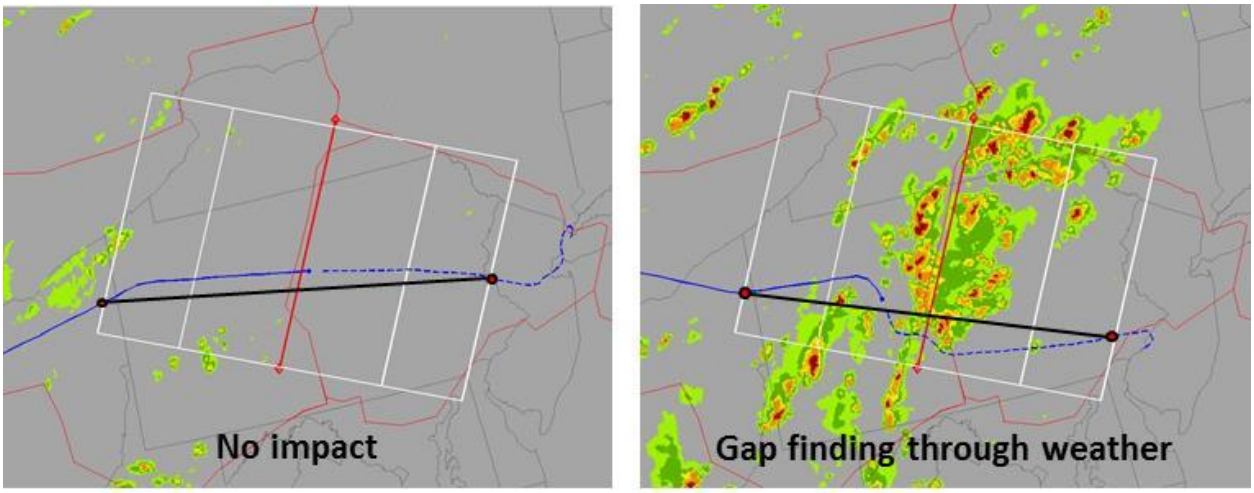

Figure 16. Aircraft trajectory (blue solid line) and aircraft future trajectory (blue dashed line) for aircraft traversing through the ZNY001 (ZOB/ZNY transition) airspace and the observed precipitation intensity. The solid black line represents a notional direct trajectory.

Figure 17 is a box-and-whisker plot of the permeability estimates compared to the Lateral Track Extension for the ZNY001 (ZOB/ZNY transition) airspace. At each five minute update of the permeability of the observed weather, the corresponding median LTE for all aircraft currently associated and contained within the TFI region is computed. A correlation between the airspace impact model and the LTE is clearly visible. As the convective weather impact increases (measured by a decreasing

permeability), the LTE increases accordingly suggesting an increase in the workload of air traffic controllers.

To fully understand the potential value of LTE it is important to understand the relationship between additional controller workload and the flow rates. There is an assumption that air traffic managers make a tradeoff between additional controller workload and reductions in the flow rate. If that is true, then it should be observed that during times when the flow rate does not decrease with increased weather impact, LTE should increase. Figure 18 shows one of these cases for the ZBW001 (ZOB/ZBW transition) airspace. As the permeability decreases from 100% to approximately 50%, LTE increases, suggesting increased controller workload. During these times, the flow rate remains relatively constant with a median of approximately 40 aircraft per hour. As the permeability drops below 50%, the flow rate begins to decrease while the median LTE remains flat near 2.8% and actually begins to decrease with lower permeability. Of course, individual instances of particular aircraft may vary, but the overall statistics suggest that for this airspace the air traffic mangers first begin increasing controller workload by allowing deviations, but at some point the increased workload will induce them to begin to reduce the air traffic flow rates.

At this time, the relationship between LTE as a measure of controller workload and traffic flows is not fully mature. Additional measures of controller workload may need to be investigated such as vertical deviations (altitude changes), and spatial density of aircraft (need for conflict resolution). However, these studies have shown that this is an area that needs additional exploration to provide future guidance on predicting and setting air traffic management programs.

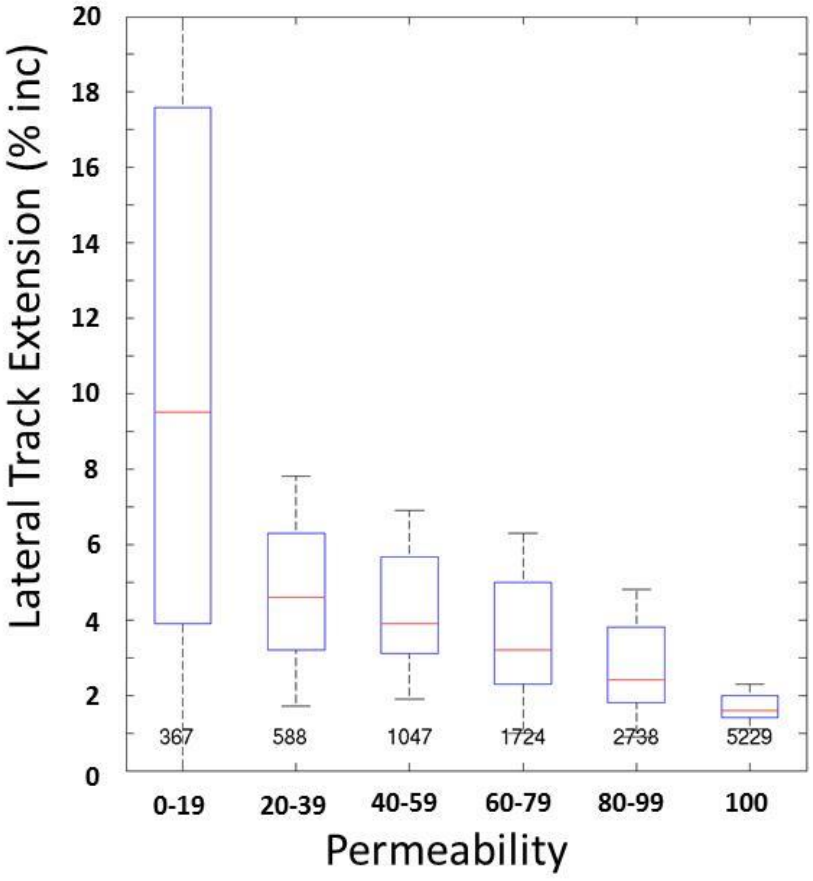

Figure 17. Observed Lateral Track Extension (LTE) for the ZOB/ZNY transition airspace (ZNY001). The red dash is the median flow rate; the box represents the 25th and 75th percentile values; the maximum observed flow rate for each box is shown as a red diamond. The count of observations used in each permeability category is shown above the x-axis. Data are from 122 case days during the summers of 2011, 2012, 2013, 2014 and 2015.

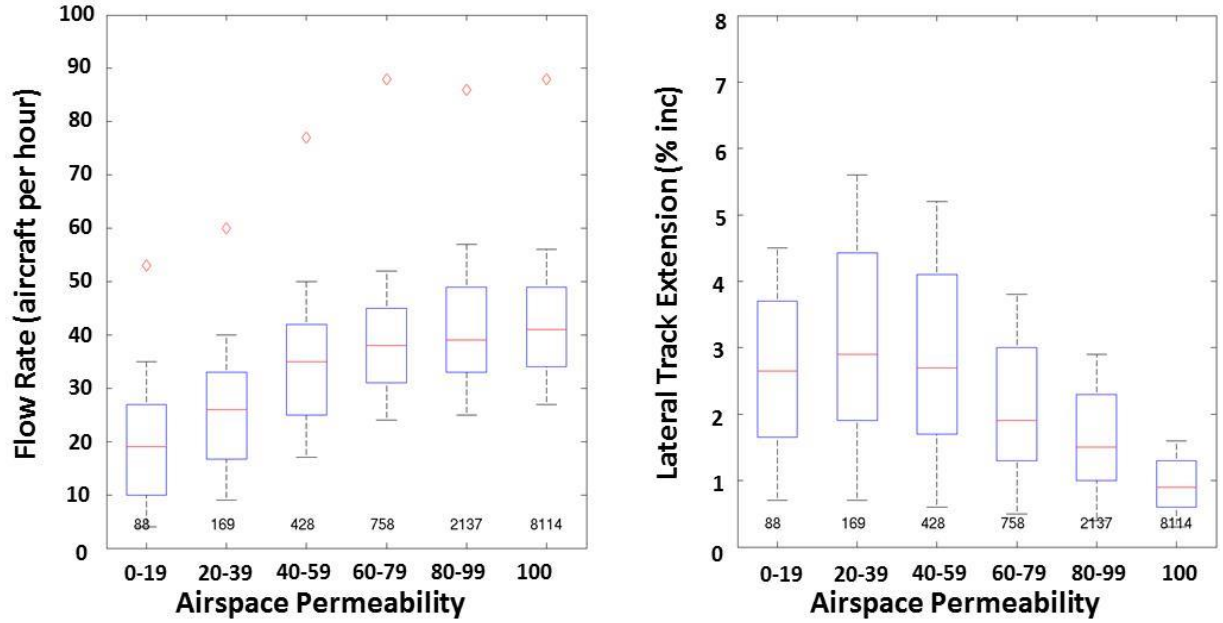

Figure 18. Observed 60 minute flow rate (left) and Lateral Track Extension (right) for the ZOB/ZBW transition airspace (ZBW001). The red dash is the median flow rate; the box represents the 25th and 75th percentile values; the maximum observed flow rate for each box is shown as a red diamond. The count of observations used in each permeability category is shown above the x-axis. Data are from 122 case days during the summers of 2011, 2012, 2013, 2014 and 2015.

3. PREDICTION OF FLOW RATE AND FORECAST UNCERTAINTY

In this section, a methodology for combining multiple forecasts of different types (e.g. deterministic and probabilistic forecasts) into a single forecast of airspace permeability, as well as providing a dynamic measure of forecast confidence will be discussed. In addition to a point prediction of future permeability, this Traffic Flow Impact (TFI) forecast also provides uncertainty information in the form of a *prediction interval*. Prediction intervals represent a range of possible permeability values that are likely to occur at a given time. The width of these intervals also conveys a measure of confidence. Wide intervals imply low confidence in the forecast, while thin intervals imply high confidence. The method described here was applied during the summer of 2015 to key regions of airspace in the NAS.

3.1 PREDICTION MODEL METHODOLOGY

Forecasts used in TFI are categorized as one of two types: Storm Resolving or Probabilistic. Storm resolving forecasts provide a single depiction of two or three dimensional future weather events over a specified geographic area in a high resolution image. These forecasts are deterministic and attempt to represent the future state of actual meteorological quantities. As a result, storm resolving forecasts by themselves contain little or no uncertainty information[2]. In contrast, a Probabilistic forecast assigns likelihood to a particular weather event (e.g. occurrence of thunder storms) and displays the probability of this event at any given point and time. The method described below is intended to be applied to any number of forecasts that fall into these categories. For this report, the following four forecasts were utilized:

1. **Extrapolation Forecasts**: The Corridor Integrated Weather System's (CIWS)[1] extrapolation forecast is a storm resolving forecast that applies motion tracking algorithms to national weather mosaics of VIL and Echo Tops. These tracking vectors are used to advect current weather and predict storm location up to 8 hours into the future. The CIWS forecast has 1km horizontal resolution and a new forecast is issued every 2.5 minutes. The major advantages of extrapolation forecasts are that they have low latency and typically outperform numerical model forecasts at short forecast lead times (~1 – 2 hours). At later lead times however, these forecasts exhibit poor performance.

2. **High Resolution Rapid Refresh (HRRR)**: The HRRR model (http://ruc.noaa.gov/hrrr/) is a 3 km storm resolving model that is capable of providing forecasts of VIL and Echo Tops up to 16 hours into the future. This forecast is issued hourly, and typically exhibits 1 to 2 hours of latency. In contrast to the extrapolation forecast, numerical weather models like the HRRR

[2] Unless that forecast is generated as part of an ensemble of storm resolving forecasts, which is not a case we are considering here.

typically perform worse in short lead times due to model "spin-up" which is often the effect of the model adapting to data assimilation used to initialize the model.

3. **Localized Aviation MOS Program (LAMP):** The LAMP model provides probabilistic forecasts (http://www.nws.noaa.gov/mdl/gfslamp/uncertform.php) of thunderstorms by updating the Global Forecasting System's (GFS) Model Output Statistics (MOS) using observational data (METAR, lightning, radar), output from simple advective models, and geo-climatic data (hi-res topography and relative frequencies). Probabilistic forecasts of thunderstorms are issued hourly on a 20-km grid. Outputs are available in 1 – 2 hour intervals.

4. **Short Range Ensemble Forecast (SREF):** The Storm Prediction Center's SREF Calibrated Thunderstorm Probability field (http://www.spc.noaa.gov/exper/sref/) is created by post processing all 21 members of the SREF along with a three member time lagged ensemble and the WRF-NAM. These forecasts are combined to create a single probabilistic forecast of thunderstorms across the NAS on a 32 km grid. This forecast is issued every 6 hours, and comes in hourly time intervals.

Figure 19 shows an example of each of these forecasts.

To combine these models, the TFI forecast uses a supervised machine learning algorithm that uses features measured from each of these forecasts in a TFI region to predict the *posterior distribution* of permeability conditioned on these forecasts. This posterior distribution describes the range of possible permeabilities and their respective probabilities. Obtaining a full distribution (rather than a point prediction) allows us to infer uncertainty in our prediction and convey this in the form of a prediction interval.

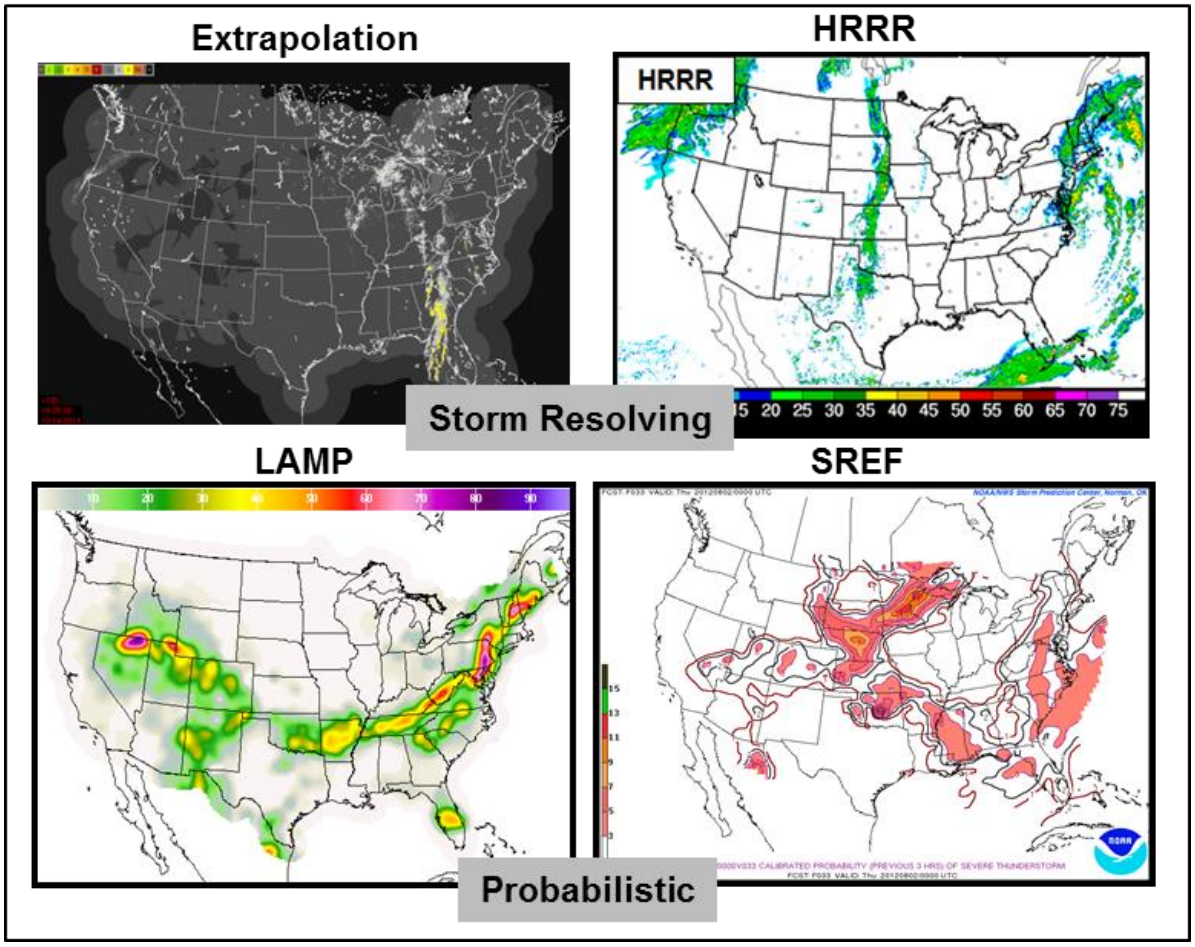

Figure 19. Examples of the four forecasts used in the TFI model. The models include a mixture of storm resolving models (extrapolation and HRRR), together with probabilistic models (LAMP and SREF Calibrated Thunderstorm Probability).

For this methodology to be effective, a historical database of forecasts along with corresponding validation data must be available. In this study, a two year history (2013 and 2014) of data from summer months (May – September) was used for model training. The summer of 2015 was kept separate from training and is used later for validation.

To apply a machine learning methodology, each input forecasts around a TFI region must first be converted into a vector of features with fixed length. Because the forecasts are of different type (storm resolving and probabilistic) different features are extracted depending on the type of forecast. For the storm resolving forecasts (Extrapolation & HRRR), VIL and Echo Tops forecasts are combined to create

a forecast of the Weather Avoidance Field (WAF). This field is processed using the permeability algorithm (Section 2.1) to compute a forecast of permeability for each TFI region. Other features are also computed, such as maximum route WAF, mean storm size within the TFI region, and mean encounter time along each TFI notional route.

In addition to using the latest available forecast, a four-member time lagged ensemble of forecasts was used to create features. As mentioned above, due to the deterministic nature of storm resolving forecasts, they contain little information about forecast uncertainty. A time-lagged ensemble of forecasts is one method of measuring uncertainty from this type of forecast by looking at how the forecast evolves at valid at a fixed time as the forecast is updated. Time lagged ensembles that consistently forecast impacts on an area are, in general, more accurate than ensembles that contain a significant amount of variability. Storm resolving permeability features described above are gathered for each of the four-member time lagged HRRR ensemble as shown in Figure 20. A time-lagged ensemble was not used for the extrapolation forecast.

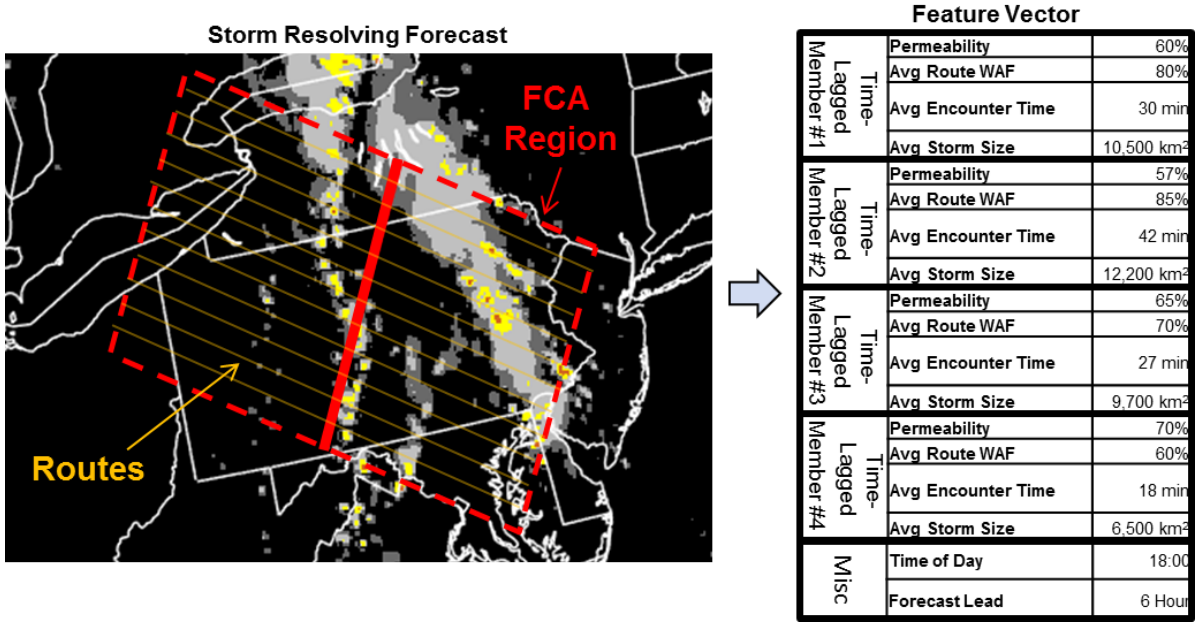

Figure 20. Feature Extraction for a storm resolving forecast. WAF is computed from the HRRR and extrapolation forecast. Within each TFI region, various features are taken from a time-lagged ensemble of forecasts valid at the same time.

For probabilistic forecasts, it is not possible to explicitly create WAF since they do not provide VIL and Echo Tops forecasts (the inputs to the CWAM algorithm). Instead, various statistical properties of the forecasts were gathered in the area surrounding each TFI region. These features include percentiles of

probability (10^{th}, 25^{th}, 50^{th} , 75^{th}, 90^{th}) within the TFI region, areal coverage of probability exceeding various thresholds (10% & 25%) and average probability within quadrants of the TFI region (see Figure 21). These features are meant to convey the impact forecasted on the TFI region, and will later be translated to an estimate of permeability.

Features extracted from each input forecast are represented here by vectors $\boldsymbol{x}^1, \boldsymbol{x}^2, \ldots, \boldsymbol{x}^{N_f}$, where N_f is the number of forecasts (including time lagged ensemble members). Training data of the form $\left(\boldsymbol{x}_1^1, \boldsymbol{x}_1^2, \ldots, \boldsymbol{x}_1^{N_f}, p_1\right), \left(\boldsymbol{x}_2^1, \boldsymbol{x}_2^2, \ldots, \boldsymbol{x}_2^{N_f}, p_2\right) \ldots, \left(\boldsymbol{x}_n^1, \boldsymbol{x}_n^2, \ldots, \boldsymbol{x}_n^{N_f}, p_n\right)$, where $\left(\boldsymbol{x}_i^1, \boldsymbol{x}_i^2, \ldots, \boldsymbol{x}_i^{N_f}\right)$ represents a set of forecast features all valid at the same time, and $p_i's$ are the *observed* permeability at that time. This data was gathered over the summers of 2013 and 2014 around the TFI regions pictured in Figure 22. For each day, a new set of forecast features were measured at the top of each hour (00Z, 01Z, … , 23Z). For each of these times, features were gathered at hourly forecast leads out to 12 hours, with the exception of the extrapolation forecast which is only available out to 8 hours. Because forecasts suffer from latency, and because not all forecasts are generated hourly, the most recently available forecast was chosen to create features for each target time. For example, to create features at 1300Z with a 4 hour lead (target time = 1700Z), we might use a 4 hour extrapolation forecast issued 1300Z (0 latency), a 6 hour HRRR forecast issued 1100Z (2 hour latency), a 5 hour LAMP forecast issued 1200Z (1 hour latency), and an 11 hour SREF forecast issued at 0600Z (Since the 1200Z SREF is not available yet). In this way, our dataset mirrors how the forecasts might be used in an operational setting.

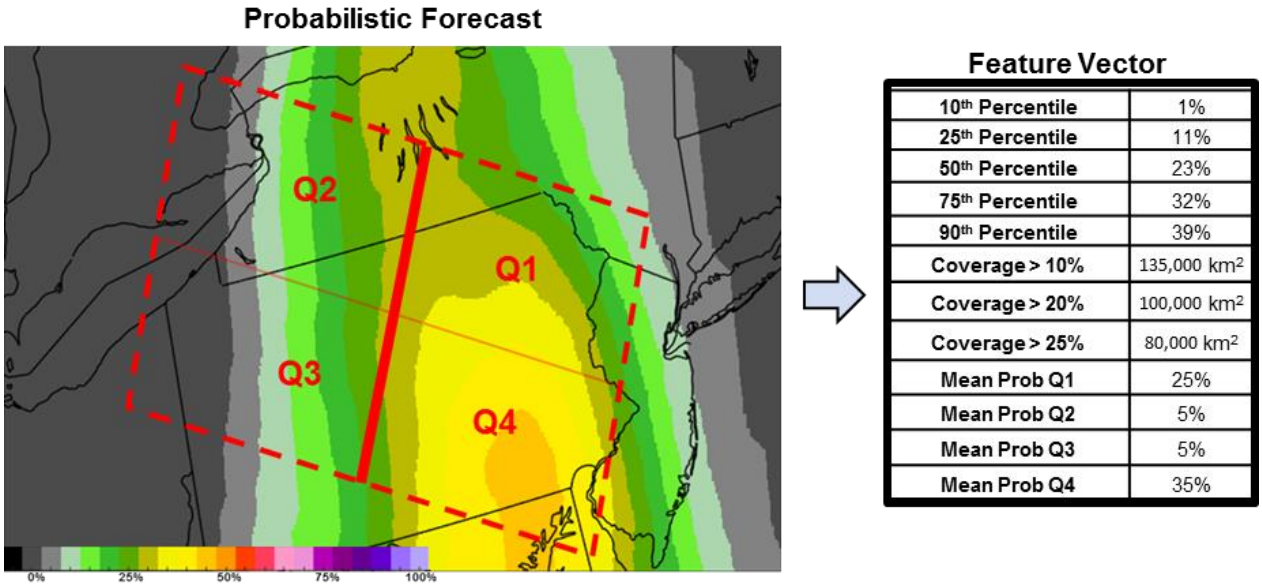

Figure 21. Feature Extraction for a probabilistic forecast. The features listed on the left represent statistical features of the forecast within the TFI region, as well as some descriptions of spatial coverage of the forecasted probability.

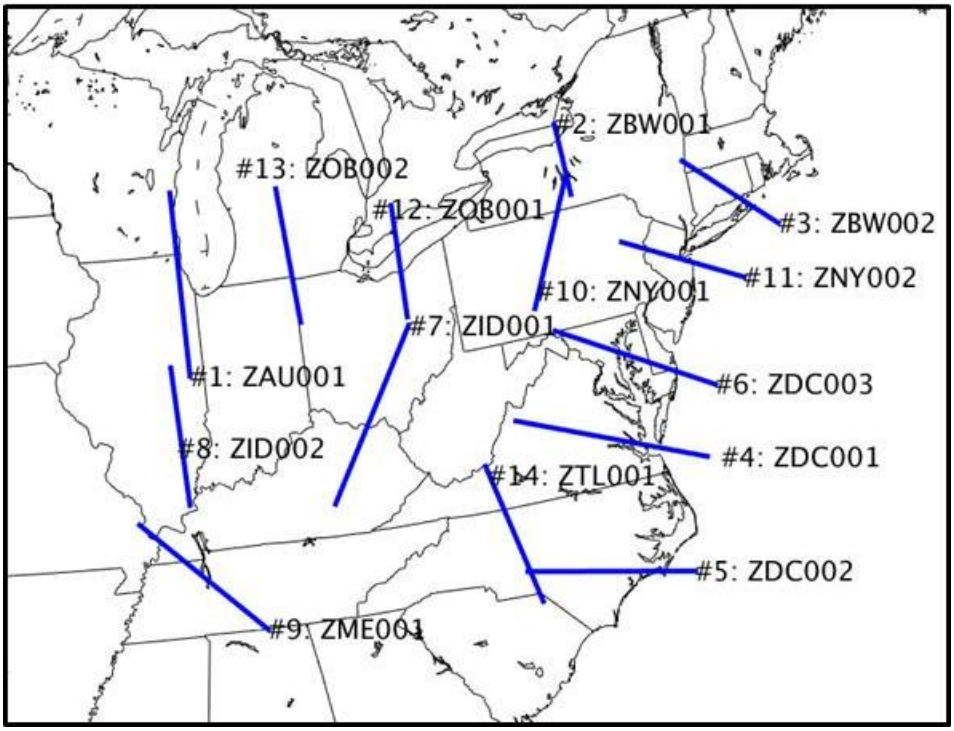

Figure 22. Regions used for training the TFI model.

The observed permeability, p, corresponding to each forecast valid time was measured using VIL and Echo Tops from the CIWS system. The technique outlined below was applied separately for each lead hour 1 – 12 using as many of the forecast features that were available (Note that N_f gets smaller for later leads because the extrapolation forecast is no longer available after 8 hours, and fewer time-lagged HRRR members are available).

The first step in the TFI model is to map features from each input forecast into an estimate of permeability. Prior to model fitting, all forecast features are scaled such that they have mean 0 and unit variance. Forecast features $\boldsymbol{x}^k$ are mapped to a forecast of permeability using a linear combination of the components of $\boldsymbol{x}^k$. The weights in this linear combination are found by fitting a Ridge Regression separately for each forecast type and finding the coefficient vector $\boldsymbol{\beta}^k$ and b_0 that minimize the following objective function:

$$(\boldsymbol{\beta}^k, b_0^k) = \text{argmin}_{(\boldsymbol{\beta}, b_0)} \left(\sum_i \left(p_i - (\boldsymbol{\beta} \cdot \boldsymbol{x_i^k} + b_0)\right)^2 + \lambda_k (|\boldsymbol{\beta}|^2 + b_0^2) \right) \quad k = 1,2, \dots, N_f \qquad (1)$$

where λ_k is a regularization parameter chosen to minimize error on a holdout set and was chosen using a 10-fold cross validation. As a final post-processing step, the outputs obtained from this step are rescaled so the output values $\{\hat{p}_i^k\}$ over the training set span the interval [0%, 100%] (this effectively rescales $\boldsymbol{\beta}^k$ and shifts b_0^k obtained in Eq. 1). In the following, $\hat{p}^k = \boldsymbol{\beta}^k \cdot \boldsymbol{x}^k + b_0^k$ represents the estimate of permeability obtained from forecast k.

Estimates of permeability derived from each forecast are then combined to estimate the posterior distribution of observed permeability p conditioned on the vector of forecasted permeability $\widehat{\boldsymbol{p}} = (\hat{p}^1, \hat{p}^2, \dots, \hat{p}^{N_f})$, i.e. $F(p|\hat{p}^1, \hat{p}^2, \dots, \hat{p}^{N_f})$, where F is the conditional Cumulative Distribution Function (CDF) of p. *Quantile Regression* [13] was chosen as the method for estimating the conditional quantiles of p (these characterize the conditional CDF). Quantile Regression seeks to find a function $f_\tau(\widehat{\boldsymbol{p}})$ that estimates the 100τ% percentile of the random variable p as a function of $\widehat{\boldsymbol{p}}$ by minimizing the following functional over the training set $\{(\widehat{\boldsymbol{p}}_i, p_i)\}$:

$$f_\tau = \text{argmin}_{f \in H} (\sum_i \rho_\tau (p_i - f(\widehat{\boldsymbol{p}}_i))). \qquad (2)$$

Here, ρ_τ is the "check-mark" function defined as $\rho_\tau(t) = \begin{cases} \tau \cdot t, t > 0 \\ -(1-\tau) \cdot t, t \leq 0 \end{cases}$, see Figure 23.

The minimum in Eq. 2 is taken over a suitable set of functions H. Typically H is chosen to be all linear functions of the components of $\widehat{\boldsymbol{p}}$, however here we introduce non-linear interaction terms between the different forecasts into the model by using an H covers all second order polynomials of the inputs $\widehat{\boldsymbol{p}}$, i.e.

$$H = \left\{ f : f(\boldsymbol{p}) = c_0 + \sum_{i=1}^{N_f} c_i p^i + \sum_{i=1, j=i}^{N_f} d_{i,j} p^i p^j \right\}$$

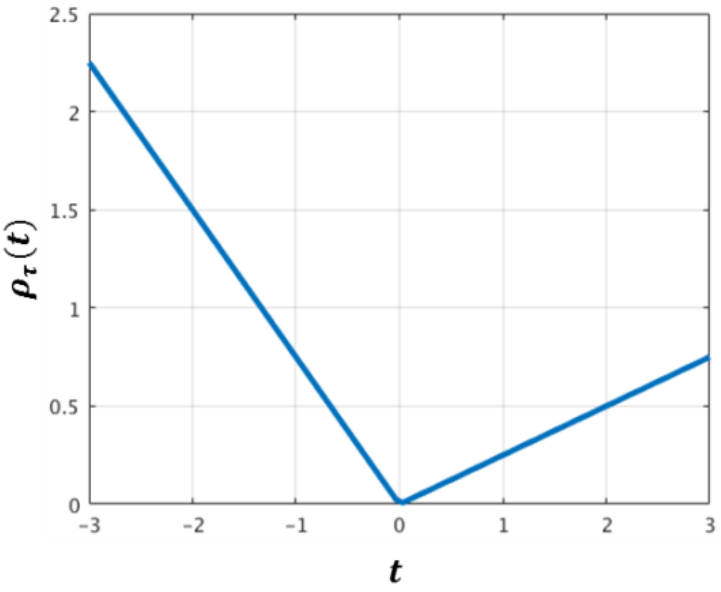

Figure 23. The "checkmark function" $\rho_\tau(t)$ used in the quantile regression objective function. Plot shows $\tau = 0.25$.

The optimal values of the coefficients c_i and $d_{i,j}$ for the forecast models considered here was found using the interior point (Frisch-Newton) algorithm [14].

The two steps described here – the translation of weather features into permeability estimates followed by a combination of permeability forecasts into conditional quantiles – can also be viewed as a feed forward neural network with multiple input layers (one for each of the N_f forecasts) feeding one hidden layer that contains the vector $\left(\hat{p}^1, \hat{p}^2, \ldots, \hat{p}^{N_f}\right)$. The output layer of the network contains quantiles of the distribution of permeability. A summary of this model is shown in Figure 24.

Because both layers of the TFI model were trained separately, care must be taken not to "double-dip" in the training set (that is, using the same training example in both layers will cause overfitting in the second layer). If left unchecked, this can lead to poor generalization on a holdout set. To avoid this, a stacking methodology similar to that described in [15] was used.

An example TFI forecast made using this methodology is shown in Figure 25. All of the model inputs are shown in the top plot and show an overall drop in permeability across the TFI region ZNY001 (shown in Figure 25). The bottom plot shows the TFI forecast. The center line represents the median of expected permeability ($f_{0.5}(\hat{\boldsymbol{p}})$), and the upper and lower curves that make up the prediction intervals are given by the 20$^{\text{th}}$ ($f_{0.2}(\hat{\boldsymbol{p}})$) and 80$^{\text{th}}$ ($f_{0.8}(\hat{\boldsymbol{p}})$) percentiles, respectively. With these choices of quantiles, we

are asking that our prediction intervals capture at least 80% - 20% = 60% of all observations. This target for prediction interval accuracy will be important when performing validation.

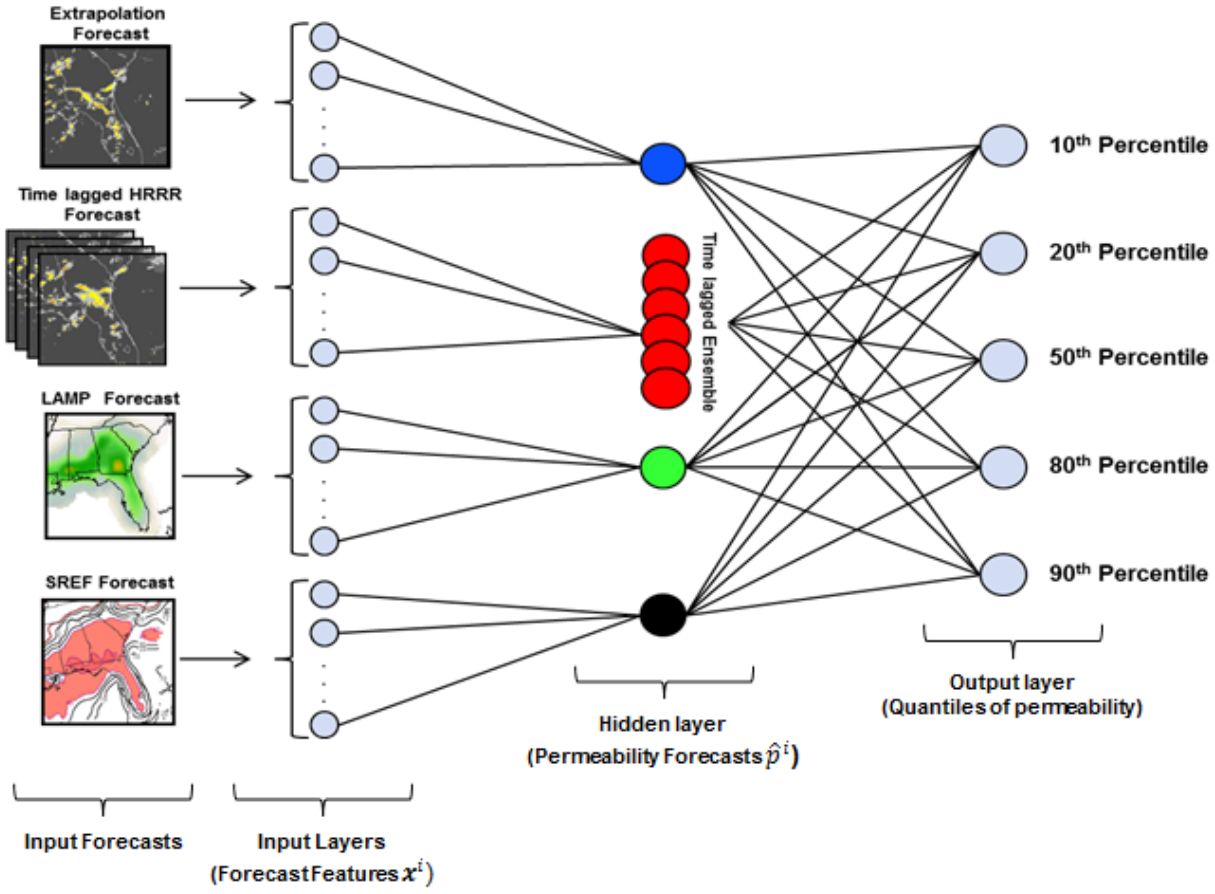

Figure 24. TFI forecast model.

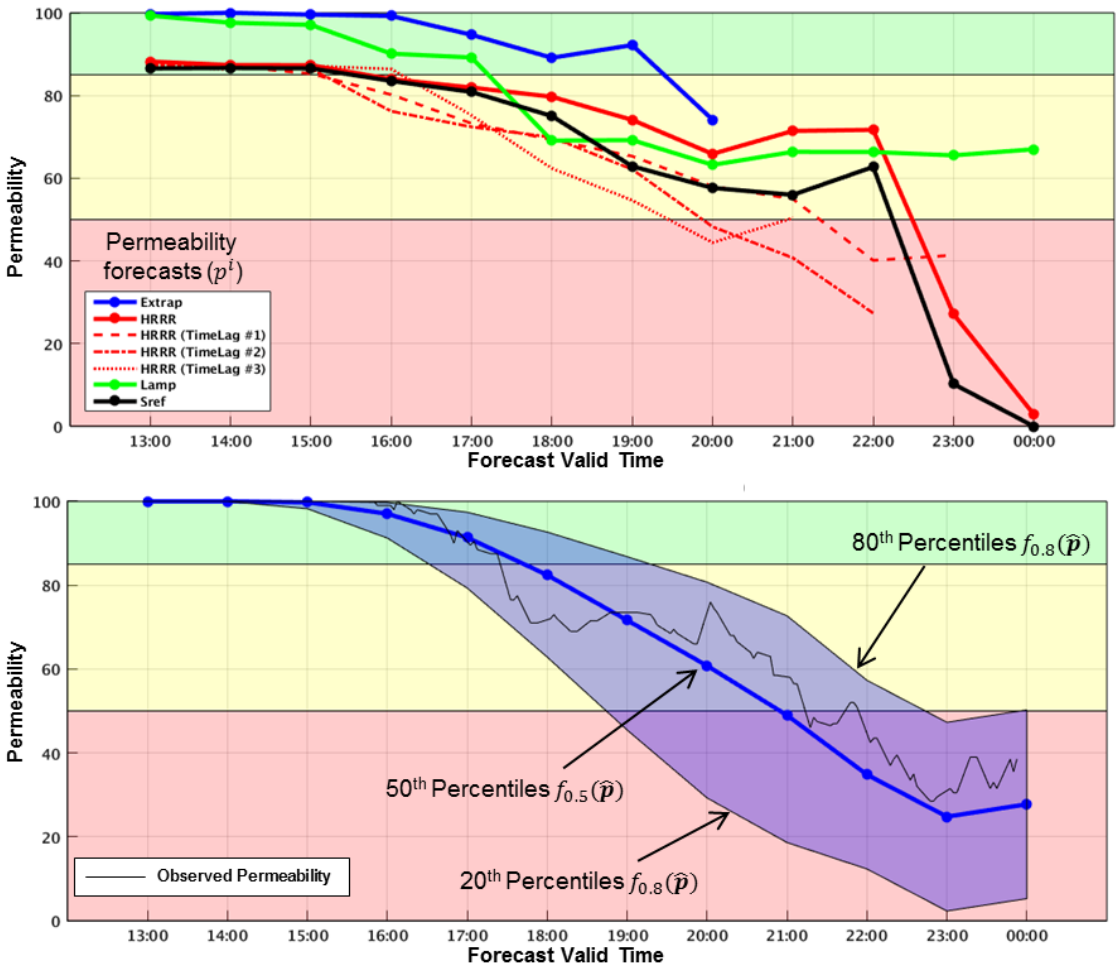

Figure 25. Example of TFI model forecast. Top: permeability estimates derived from individual models (p ̂)using the extrapolation forecast, 4 members of a time lagged HRRR ensemble, the LAMP and SREF forecasts. Bottom: TFI forecast from median prediction (f_(0.5) (p ̂)) and the prediction intervals from 20th (f_(0.2) (p ̂)) and 80th (f_(0.8) (p ̂)) percentiles.

3.2 PREDICTION MODEL ASSESMENT

The TFI model was assessed using data from the summer of 2015 (recall training data came from the summers of 2013 and 2014). We begin by examining a case study, and then will provide performance statistics for the entire summer.

Figure 26 shows a sample of verification for a storm impacting New York airspace on July 14th 2015. This plot shows the sequence of 1, 4 and 8 hour TFI forecasts made over a period of 60 hours

(updating every 15 minutes). The x-axis represents the valid time of each forecast. Note that this plot is different than the plot in Figure 25 since each point here comes from a forecast with a different issue time. The black curve in each plot shows the observed permeability measured at each time.

Not surprisingly, the 1 hour forecast shows the greater skill and thinner prediction intervals than that seen in the 4 and 8 hour forecasts. Prediction intervals appear much wider when the forecast intensifies (i.e. permeability drops into yellow and red regions). The main drop in permeability at roughly 2100Z on the 14th was detected well across lead times, and the transition was mostly captured by the prediction intervals at 4 and 8 hour leads. At around 1600Z on the 14th, the 8 hour forecast was late in detecting a drop in permeability, but quickly caught up when storms began to intensify. Both the 4 and 8 hour forecasts decayed the storms too quickly on the 15th, as both had permeability returning to 100% earlier than what was observed.

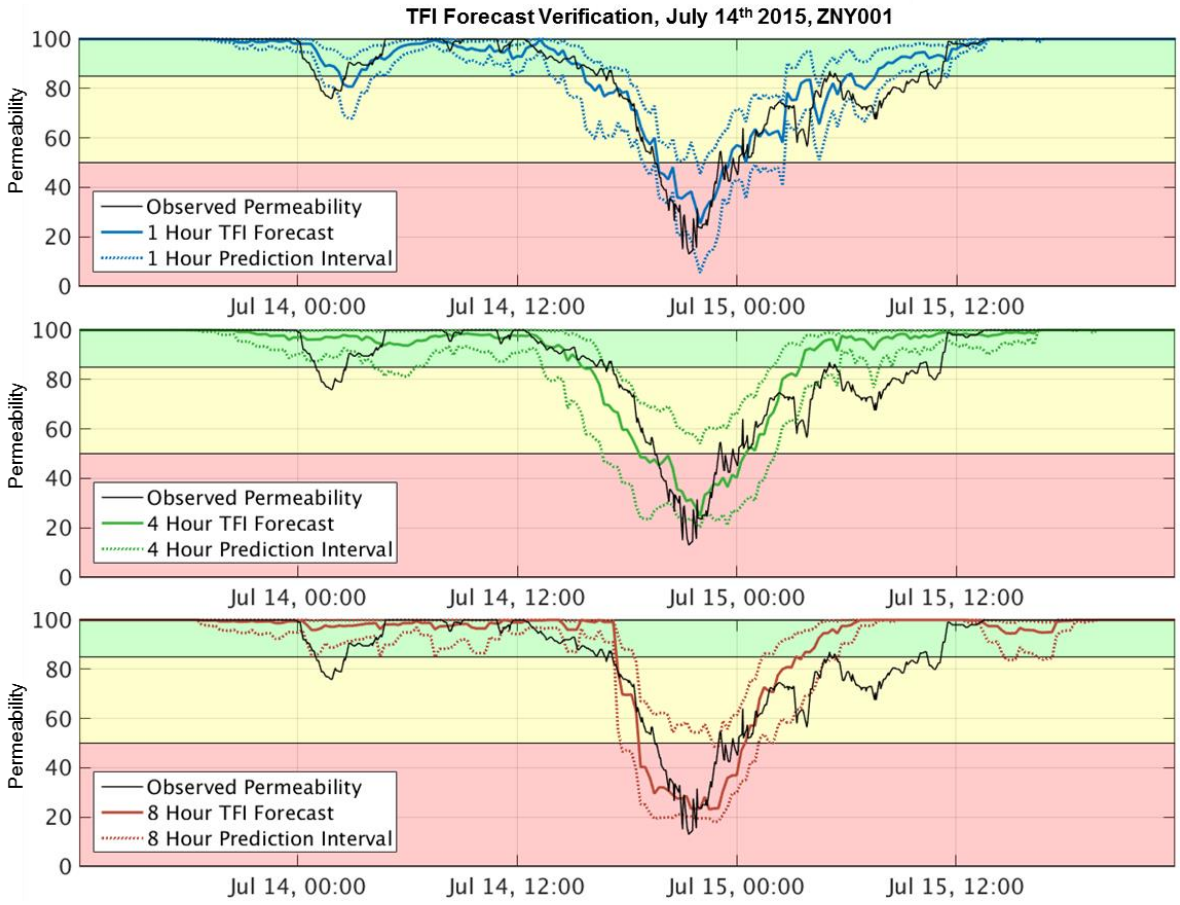

Figure 26. TFI verification on July 14th – July 15th for the TFI region ZNY001. The three plots show the 1, 4, and 8 hour TFI forecasts valid at the times on the x-axis. The black curve shows the observed permeability at those times.

To quantitatively assess model skill, the following metrics are used. In the following, N denotes the number of forecasts used in verification, and $\mathbf{1}(\cdot)$ denotes the indicator function.

- Correlation Coefficient $r = \mathrm{cov}(\mathrm{p}, f_{0.5}(\hat{\boldsymbol{p}})) \Big/ \sigma_p \sigma_{f_{0.5}(\hat{\boldsymbol{p}})}$

  The correlation coefficient is a measure of how related observed permeability is to the median curve in the TFI forecast. We will also compare this to the correlation coefficient of the individual forecasts ($\breve{p}_i^k$). Correlation was chosen over other metrics like Mean Squared Error (MSE) or Mean Absolute Error (MAE) because it is less sensitive to the rescaling performed on the permeability estimates obtained from individual models.

- Prediction Interval Coverage (PIC): $\frac{1}{N}\sum_i \mathbf{1}(\mathrm{f}_{0.2}(\hat{\mathbf{p}}_i) \leq p_i \leq \mathrm{f}_{0.8}(\hat{\mathbf{p}}_i))$

  The Prediction Interval Coverage (PIC) measures the proportion of time that the forecast prediction interval $[\mathrm{f}_{0.2}(\hat{\mathbf{p}}_i), \mathrm{f}_{0.8}(\hat{\mathbf{p}}_i)]$ contains the observed permeability p_i. Because the 20th and 80th percentiles were used as lower and upper bound, one should expect a PIC of at least 60%. Note that we say "at least" and not "equal to" because for a large proportion of samples, the majority of the posterior distribution is concentrated at $p = 100\%$, and hence a prediction interval containing 100% might capture more than the targeted 60%.

- Prediction Interval Width (PIW) $\mathrm{f}_{0.8}(\hat{\mathbf{p}}_i) - \mathrm{f}_{0.2}(\hat{\mathbf{p}}_i)$

  The Prediction Interval Width (PIW) computes the distribution of interval widths in the TFI forecast. It is important to consider PIC and PWI as a pair because obtaining a "perfect" PIC of 1 is easy if prediction intervals are allowed to be large. A skilled prediction interval will be thin while maintaining a PIC near the target of 60%.

The square of the correlation coefficient, r^2, for the all forecasts is shown in Figure 27 as a function of TFI lead time. Because the dataset is dominated by cases with no weather impact, cases with observed permeability of 100% were removed prior to computing correlation. In terms of correlation, the TFI forecast offers a clear improvement over the permeability estimates derived from individual forecasts[3]. This improvement is most striking in the 3 and 4 hour lead time, where there is no clear "winner" amongst the forecasts. Skill of TFI steadily drops as lead increases, as do HRRR, LAMP and SREF.

[3] Note that this isn't meant to be a reflection or comparison of the individual forecasts as a whole, but merely an observation about the scalar quantities $\hat{p}^k$ engineered for the purpose of the TFI forecast. These forecasts offer far more information than what is captured in the permeability metric.

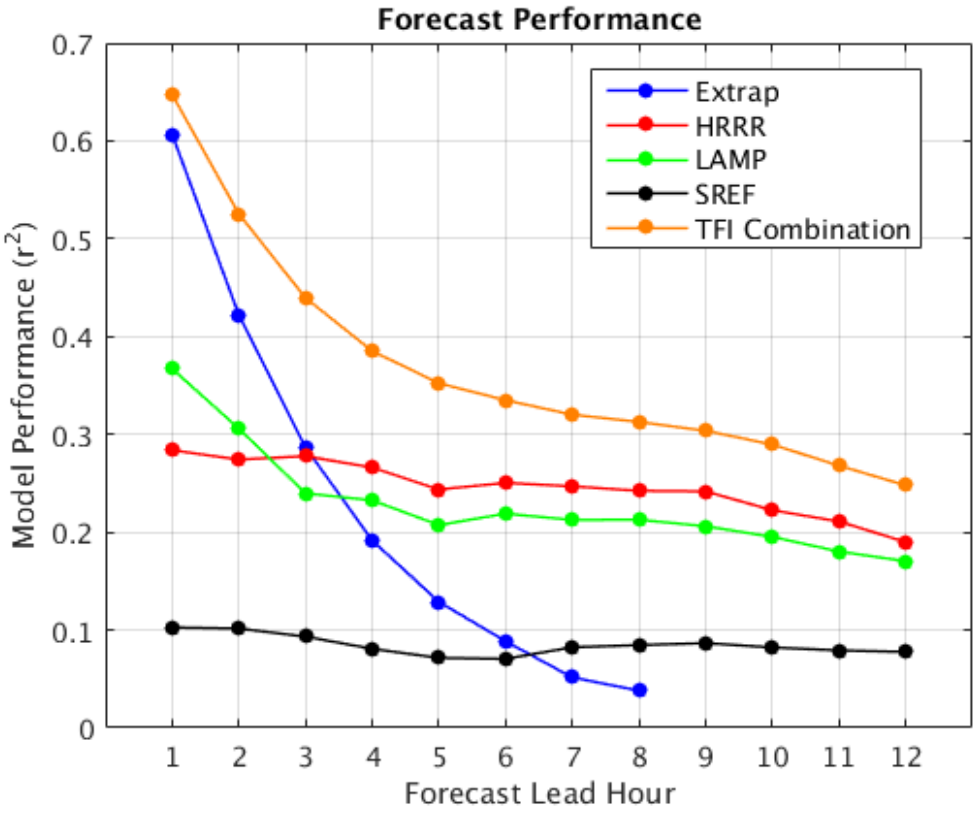

Figure 27. Skill of TFI permeability forecast along with all input forecasts measured as the square of correlation coefficient between forecasted and observed permeability. The TFI forecast shows improvement in skill over all input forecasts.

It is also interesting to examine at the interrelationships between other forecasts in the TFI model. In the early lead times, permeability measured form the extrapolation forecast dominates over the other input forecasts, but quickly loses skill past 3 hours. As the skill of the extrapolation forecast drops, the HRRR and LAMP become the most skillful at predicting permeability. Permeability estimated from the SREF probabilistic forecast showed the least skill of the four forecasts considered here. We believe that this is mostly due to infrequent updating of the SREF compared to the other forecasts considered here (which are updated at least hourly compared to the SREF which is updated every 6 hours). This results in SREF forecasts that are on average much older than the other forecasts. This point also helps explains why SREF curve in Figure 27 is relatively flat, while the other forecasts decrease in skill as lead time increases (since each TFI lead time is an average over a mixture of SREF lead times). One possible conclusion of this is that frequently updating forecasts are better suited for estimating permeability (and airspace capacity) than are forecasts that update infrequently. Note that the translation of weather

forecasts into a specific metric (permeability) enables us to quantitatively compare model performance as shown in Figure 27. Such relationships have been postulated qualitatively in the past; this represents the first analysis providing a quantitative assessment of the relative performance of each forecast component.

Turning now to the skill of the predicition intervals, the left panel in Figure 28 shows PIC as a function of forecast lead. As discussed above, the forecasts should ideally have PIC scores at or above 60%. Results are stratified by TFI forecast intensity (median curve) of "low" (Upper 95% of forecasted permeability) , "medium" (bottom 1% to 5% of forecasted permeability) and "high" (bottom 1% of forecasted permeabiltiy). The PIC for TFI forecasts in the medium and high categories are near the target 60%, while PIC is higher (around 80%) for low impact forecasts that make up the large majority of the dataset. Forecast lead hour does not seem to have much effect on PIC. The medium impact forecasts appear to be the most difficult for prediction intervals to capture, especially in the earlier lead times when compared to low and high impact. One possible reason for this might be that medium impact cases represents periods where the weather is transitioning from low to high impact. Capturing the timing of these transistions is a common problem in forecasts and so it is not surprising that TFI struggles most for this category.

The interval widths are shown on the right of Figure 28 as box and whisker plots (center line represents mean width, box represents interquartile range, and whiskers are extremes). Prediciton interval width grows quickly with respect to lead time within the first 4 hours, and remains relatively flat in later lead hours with modest increase. This trend mirrors that of the decrease in correlation coefficient seen in Figure 27 for the TFI forecast. Interval width also grows as forecast intenstiy increases, since medium and high impact forecasts show greater spead than low impact forecasts. This is consistent with interval widths observed in the case study shown in Figure 26.

These results suggest that quantile regression is an effective technique for finding prediciton intervals that achieve a given accuray goal (for us, 60%). In experiments, higher accuracy goals (80%, 95%) were explored, and achieved in terms of PIC, albeit with the cost of wider prediction intervals. For 95% accuracy, some prediction curves were observed to span the entire 0% - 100% range of permeabilities, making them not very useful as a decision support tool. It was decided that 60% was an appropriate balance between performacne and interval width, although further tuning might be necessary as forecasts improve and this tool evolves.

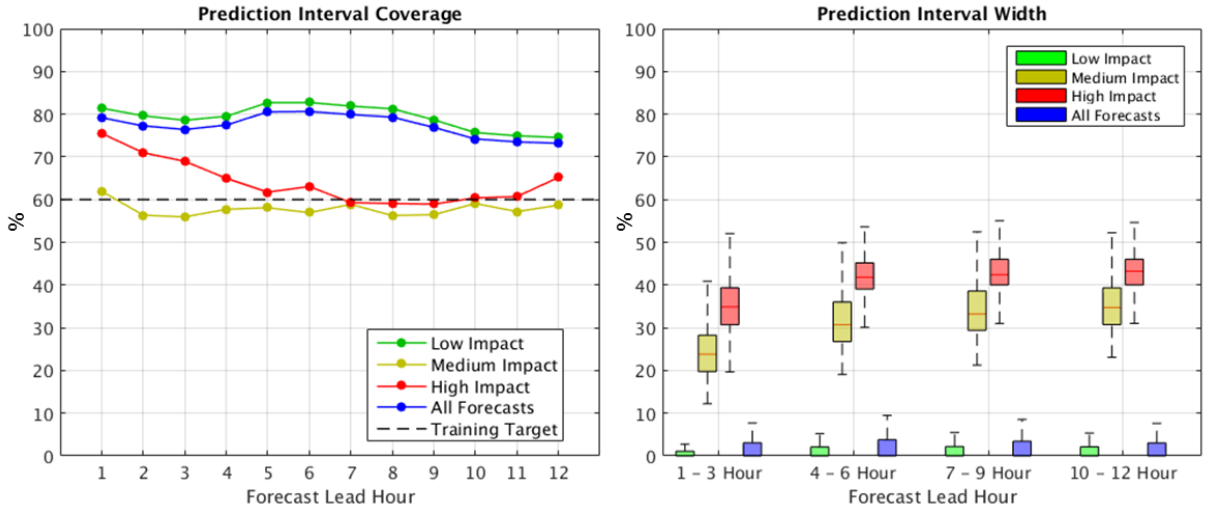

Figure 28. Performance of TFI prediction intervals. Left: percentage of times that the prediction intervals captured the observation is shown for each lead 1 -12, stratified by forecast intensity (Low, medium and high). TFI prediction intervals capture near or better than 60% of observations (black dashed line) which is consistent with the percentiles used to define the interval limits. Right: distribution of interval widths as a function of lead hour and forecast intensity. Interval widths grow with both lead hour and forecast intensity.

This page intentionally left blank.

4. PROVIDING OPERATIONAL GUIDANCE

This section provides a description of the current operations and infrastructure used for strategic traffic flow management and decision-making, a description of the Traffic Flow Impact tool developed for presenting the translated forecasts and forecast uncertainty information to the decision maker, and a review of the operational observations conducted during the summer of 2015.

The translation of convective weather forecasts into an airspace impact is one of the key pieces of information needed to make efficient traffic management decisions in the time-constrained and unpredictable environment that develops when thunderstorms limit capacity across the NAS. The TFI application is developed to provide Air Traffic Control System Command Center (ATCSCC) users with a way to mitigate the risk in the strategic planning of significant convective weather events by providing forecasts of airspace resource constraint and flow rate guidance, with a measure of forecast confidence for these quantities.

4.1 CURRENT OPERATIONS AND STRATEGIC TRAFFIC FLOW MANAGEMENT

Two strategic planning concepts that are currently active within Traffic Flow Management (TFM) are the Airspace Flow Programs (AFP) and National Playbook Reroutes. The TFI concept and tool presented in this report is focused on these two primary traffic management initiatives.

The translation of convective weather forecasts into an airspace impact is one of the key pieces of information needed to make efficient traffic management decisions in the time-constrained and unpredictable environment that develops when thunderstorms limit capacity across the NAS. The TFI application is developed to provide ATCSCC users with a way to mitigate the risk in the strategic planning of significant convective weather events by providing forecasts of airspace resource constraint and flow rate guidance, with a measure of forecast confidence for these quantities.

4.1.1 Airspace Flow Program (AFP) Planning

Airspace Flow Programs were created in the summer of 2006 to provide enhanced en route traffic management during severe weather events. The AFP identifies a constraint within the en route system and develops a real-time list of aircraft destined to fly through the constrained area. Once created for a specific NAS constraint, the AFP provides a set of timing, rate and scope information to the users consisting of:

- Anticipated Cumulative Program Period
- Anticipated Program Rate
- Departure Scope (i.e. the scope of the facilities affected by the program)

The goal is to model a program around the constraint that reduces the flow rate, allowing traffic to maneuver through potential convective weather while minimizing the delay. The following are the key steps in determining an AFP.

1. Prior to the first Strategic Planning Telecom (SPT) of the day, the National Operations Manager (NOM), Planner and Severe Weather En-Route Specialists review early morning weather forecasts to assess the threat of NAS constraints due to convection. (Note: The National Aviation Meteorologist (NAM), who is stationed on the operations floor at ATCSCC, is consulted and notifies the Planner of any potential severe weather constraints.)

2. Predicted demand through the specified airspace is then examined using the Traffic Flow Management System (TFMS) to determine the operational objectives for en route planning.

3. This discussion is coupled with considerations of terminal operations at east coast destination airports to assess overall risk, determining traffic rates without under-delivering aircraft to the destination terminals. (Note: If AFPs are considered, GDPs at terminals are discussed in tandem. If GDPs are likely, they must be published before the AFPs due to a programming glitch within the TFMS software.)

The above discussions become the basis for determining whether an AFP is needed within the Collaborative Decision-Making (CDM) community on the first few SPTs of the day.

4. The Planner **manually collects various pieces of meteorological and aviation information** concerning the potential constraint to determine if an AFP is appropriate. The information gathered varies depending on the individual Planner, but generally consists of **perceived throughput loss** (based on various weather models, i.e., SREF, LAMP, HRRR and CCFP) as well as input from the early SPTs with airline industry and other FAA facilities.

5. **The three key defining properties of the AFP (Rate, Cumulative Period, and Scope) are chosen manually** and modeled on the Flight Schedule Monitor (FSM) in order to assess the amount of average and total delay the AFP will create.

6. This gathered information is then shared on the next SPT for the collective CDM community to discuss and finalize. (Note: Once agreed upon, the AFP (Figure 29) is published by ATCSCC and an assigned Estimated Departure Clearance Time (EDCT) is assigned to each aircraft scheduled to pass through the constrained region of airspace. AFPs manage demand-capacity imbalances through the issuance of EDCTs to flights traversing the AFP.

7. **Manual reassessment of weather forecast and predicted demand** is performed every two hours prior to the next SPT to determine if a revision or cancellation of the AFP is needed.

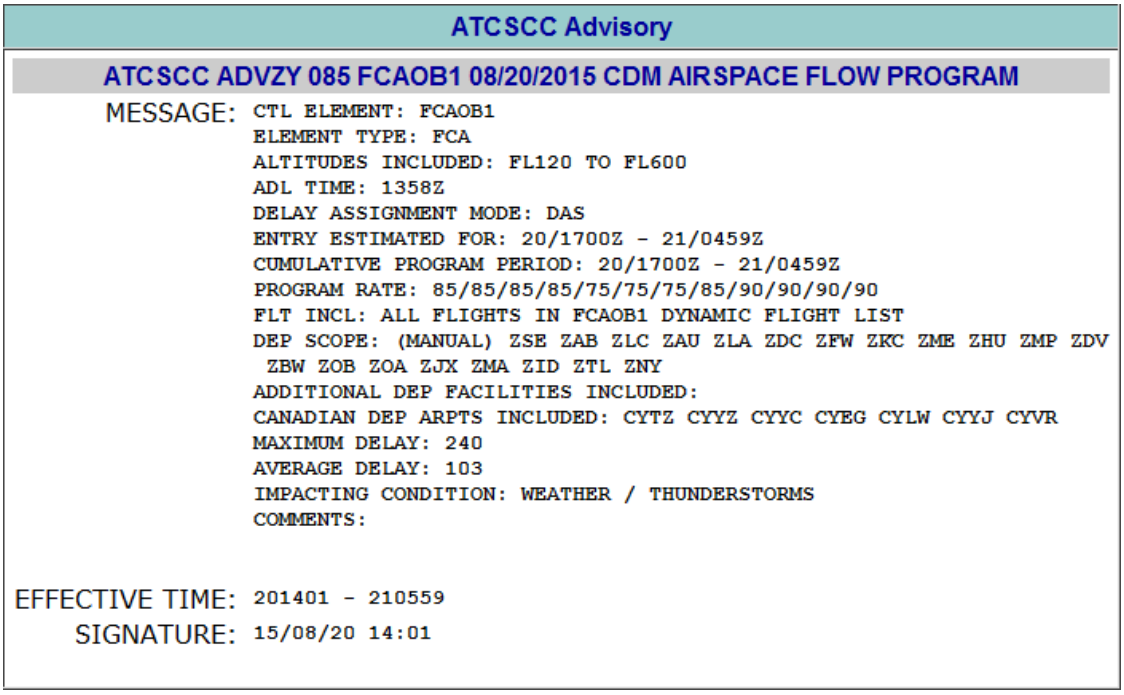

Figure 29. A sample AFP issued on 20 August 2015 which details AFP OB1 which lies along the eastern ZOB boundary.

4.1.2 National Playbook Reroute Planning

The National Playbook is a collection of Severe Weather Avoidance Plan (SWAP) routes that have been pre-validated and coordinated with impacted ARTCCs[16]. The FAA, in collaboration with industry, designed the National Playbook to mitigate the impact of potential severe weather, military operations, communications issues, or other situations that may affect coordination of routes across the NAS. This tool was developed to give the ATCSCC, other FAA facilities, and industry a common product to review various scenarios for planning and common situational awareness. The National Playbook is comprised of standard reroute scenarios that occur each convective season, depending on where the constraint lies across the NAS. Each of the planned playbook routes includes resource- or flow impacted-facilities and specific routes depending on the facility involved. Figure 30 is one example of the pre-coordinated reroutes that exist in the National Playbook.

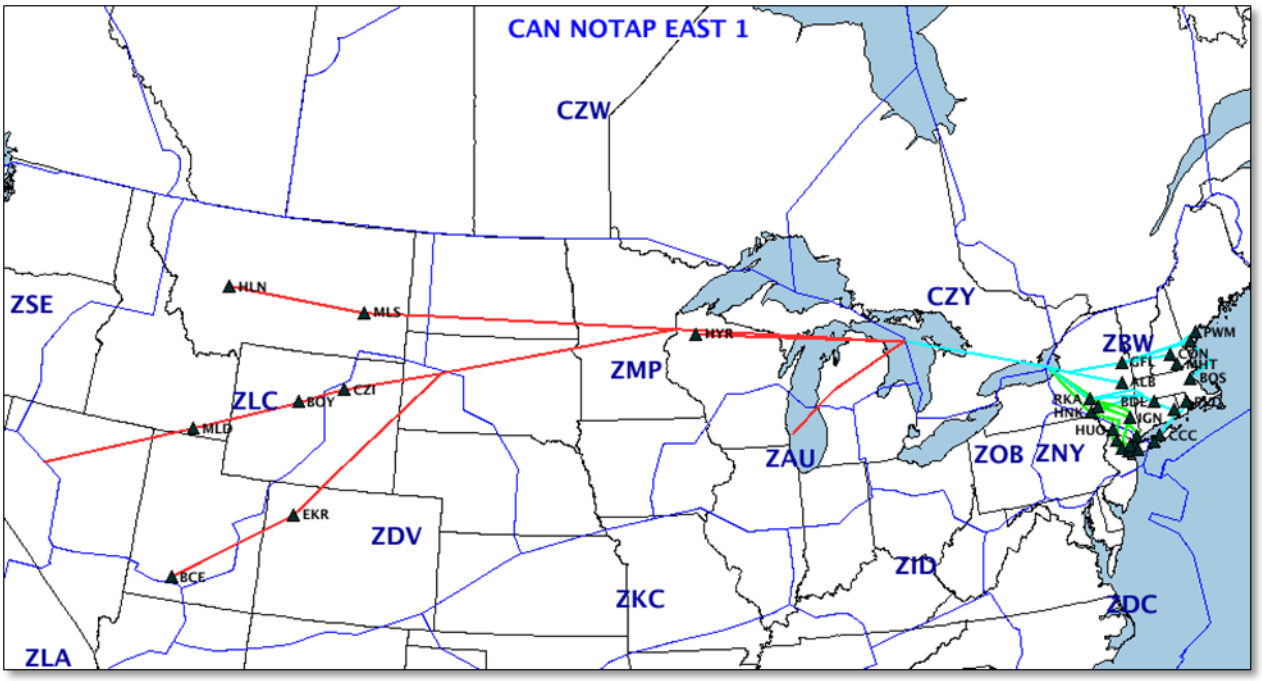

Figure 30. Sample pre-coordinated reroute which exists in the National Playbook. This CAN NOTAP EAST 1 is designed for west to east transcontinental flights bound for New York or Boston Centers. The reroute allows airlines to bypass potential severe weather across the mid-section of the NAS and any associated EDCTs by flying north through Canadian airspace.

Identical key steps that were outlined in Section 4.1.1 are followed when considering National Playbook routes to mitigate delay. **Manual translation** of weather forecast and scheduled demand information is performed to identify the need for playbook reroutes, AFPs, or a combination of the two delay-mitigation strategies.

4.1.3 Current Supporting Infrastructure

Traffic managers use weather products such as the CCFP, CIWS, and CoSPA, and various mesoscale forecast models (Section 1.1) to assess convective weather. Traffic managers use weather forecasts to manually translate and determine the impact on en route capacity. CCFP provides only 4- to 8-hour low resolution convective weather forecasts. CIWS provides 0- to 2-hour convective weather and winter precipitation forecasts. CoSPA provides a full 0- to 8-hour deterministic outlook of weather-only information. The various other models such as SREF and LAMP provide probabilistic guidance only, with no translation.

Traffic managers use TFMS and Flight Schedule Monitor (FSM) to review predicted demand and plan AFPs, and use Flight Schedule Analyzer (FSA) to monitor if an AFP is delivering the planned rate. Traffic managers can use Time Based Flow Management (TBFM) to review predicted delays to determine if an existing AFP needs to be revised.

4.2 TRAFFIC FLOW IMPACT TOOL DESCRIPTION

As previously stated, the Traffic Flow Impact (TFI) application can provide objective, automated translation of convective weather forecasts and uncertainty information to traffic managers and airline operators involved in strategic air traffic flow planning. Figure 31 depicts the graphical interface that was developed during the summer of 2014 and provided to the operational decision makers during the summer of 2015. With a quick glance of the TFI tool, Command Center planners, meteorologists, and ARTCC traffic flow managers could be alerted to potential flow-constrained areas - caused by convective weather. The primary display format for the TFI tool is the CoSPA 0-8 hour forecast shown graphically on the top, and a timeline of the impact category for the chosen airspace regions shown across the bottom. In the scenario shown in figure 31, the user could quickly identify that for TFI region ZNY001 (ZOB/ZNY transition airspace) the flow would begin to be impacted at 1700Z and from 1900Z to 00Z would be severe enough to warrant some form of flow constraint through a TMI.

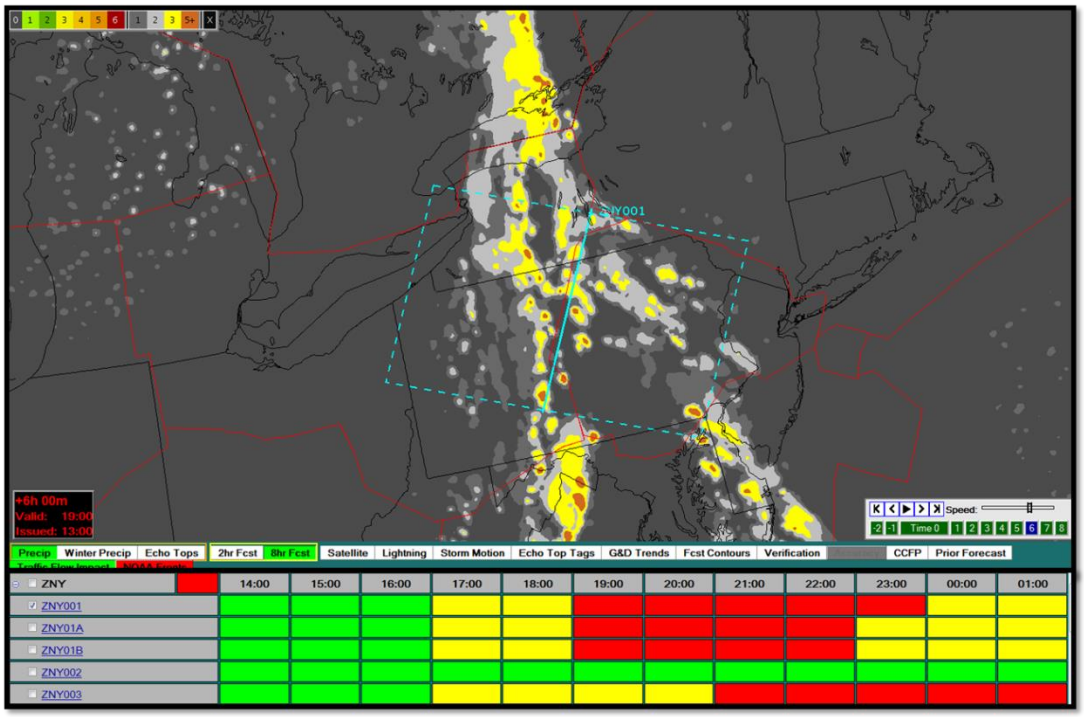

Figure 31. CoSPA deterministic forecast display (weather graphics window) with TFI impact timeline beneath for 20 August 2015. The timeline highlights forecasted convective impact for a TFI region ZNY001.

In addition, TFI provides drill-down graphs (Figure 32) that plot vital time-based airspace throughput permeability and forecast uncertainty information for individual TFI regions, allowing traffic managers and planners to strategically formulate low-risk management plans for the area(s) of concern. The example in Figure 32 represents a forecasted convective impact on the ZOB/ZNY transition airspace. The plot of valid forecast time (12 hours) versus permeability (percent) was developed to allow traffic managers to quickly assess potential impact and translate that impact into timely TMIs. The solid blue line and accompanying data points in Figure 32 display the translated weather impact forecast. The blue shading represents forecast uncertainty, providing a range of possible outcomes based on the current forecast. The current TFI application updates every fifteen minutes, continuously ingesting new data from multiple sources including CoSPA, HRRR, SREF, and LAMP.

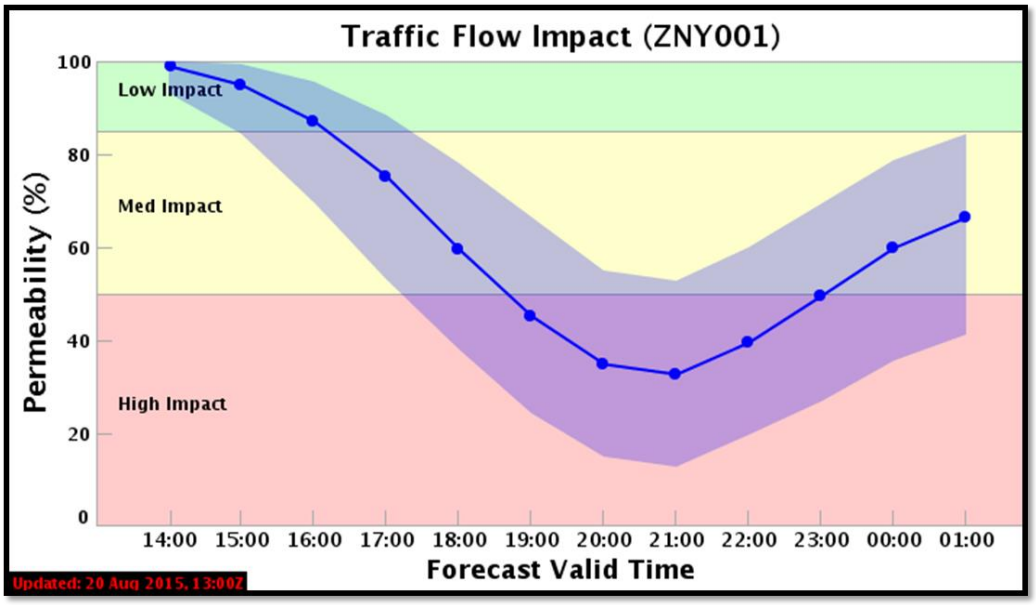

Figure 32. Traffic Flow Impact drill-down plot of permeability across a TFI region in ZNY on 20 August 2015. The graph represents a projection of potential convective impact affecting the region over the next 12 hours.

4.3 SETTING TRAFFIC MANAGEMENT INITIATIVE PROGRAM PARAMETERS

As discussed in Section 4.2, traffic planners are tasked with creating a set of traffic management initiatives that will manage demand on impacted air space by either removing the future air traffic (or some portion) from the airspace or limiting the number of flights through the air space to create delay for all aircraft planning to fly through the airspace. All TMIs require traffic planners to set critical TMI parameters such as the start time of the program, the duration of the program as well as the allowable traffic flow rates. In many instances, traffic planners will spend a significant amount of time debating

with one another along with the users of the airspace (airlines) and those whose workload will be impacted during the event (local ATC personnel) over a single parameter such as the start time of the event. The attractiveness of the method presented in this report is the permeability forecast time line, shown in Figure 32, allows a traffic planner to not only set a program rate, but to also very quickly see the most likely start time and range of possible start times for each event given proper thresholding of the permeability to reflect when the allowable flow will drop below the expected demand.

Figure 33 depicts a notional TFI permeability forecast out to 12 hours and the TMI parameters that a traffic planner could extract from the tool. Defining permeability thresholds that could be translated into types of TMI programs would allow traffic planners to quite easily identify the program onset time, duration and maximum delay (impact) expected for the event. The determination of these thresholds requires additional study and interaction with experienced TMI planners as well as an understanding of the typical traffic demand profiles compared to the observed traffic flow rates and the correlation to permeability. Accordingly, steps to develop and evaluate TMI-specific metrics are included in the future directions covered in Section 5.

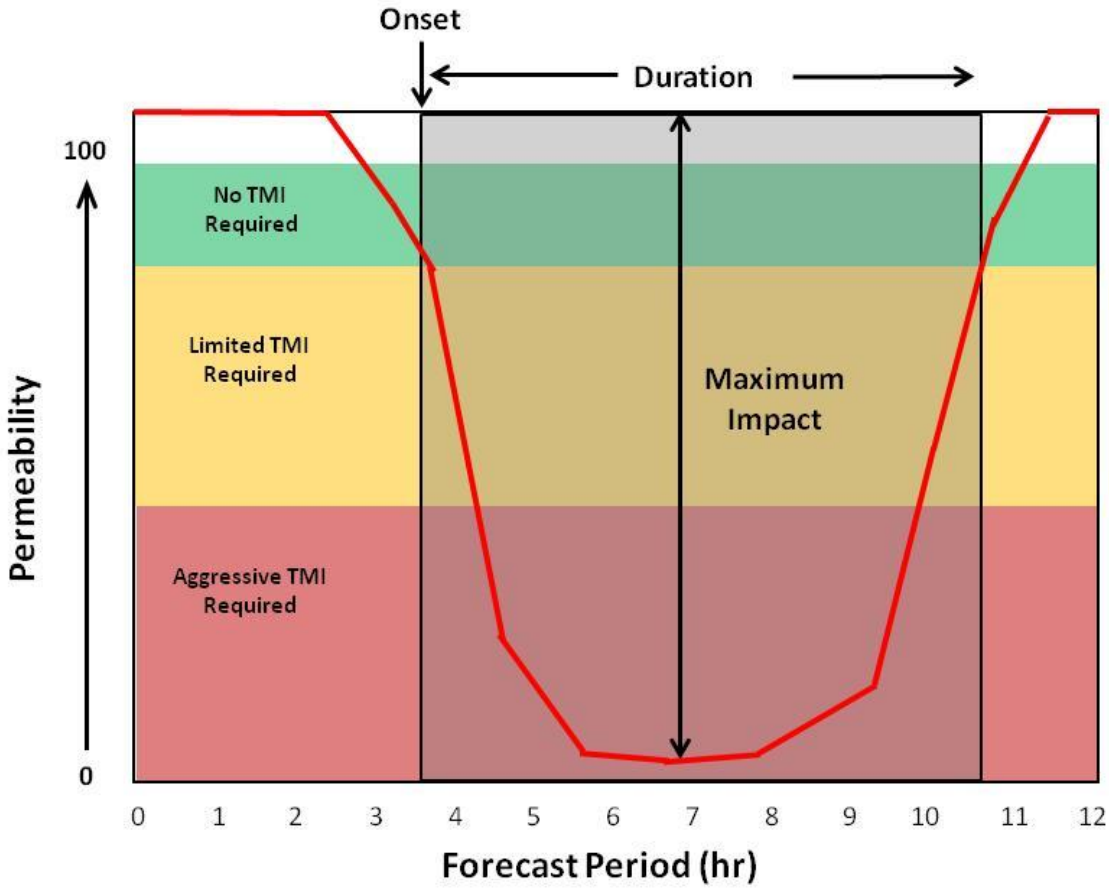

Figure 33. Notional TFI permeability forecast out to 12 hours and a Traffic Management Initiative (TMI) defining an onset, duration, and maximum impact (flow rate) for an event. The green represents permeability values not requiring TMIs, the yellow region defines events requiring limited TMIs, and the red region defines events requiring aggressive TMIs.

4.4 OPERATIONAL EVALUATIONS FROM SUMMER 2015

The objective of the summer operations observation and evaluation period was to gain valuable insight into the potential operational usefulness of the Traffic Flow Impact forecast and guide the development of the algorithms and validation process. Input from experienced operational traffic flow managers familiar with the complexity of the NAS and who perform the daily decision making that impacts the National Airspace System (NAS) performance is critical to developing future advanced methods and products that improve NAS performance.

The CoSPA field demonstration was conducted from 13 April to 31 October 2015. This demonstration involved FAA and National Weather Service facilities, commercial airlines, universities, and the private sector. During the field demonstration the 0- to 8-hour CoSPA VIL and ET forecasts were viewable by operational users 24/7 via web-only displays. Given the importance of convective forecasts to air traffic management in the NY Metroplex, MIT LL meteorologists conducted three separate field operational evaluations covering four days when storms were forecast to develop across the Eastern U.S. The MIT LL convective observation team gathered data from each of the four separate convective events displayed in Figure 34. MIT LL observers simultaneously visited four FAA Air Route Traffic Control Centers (ARTCC) and the Air Traffic Control System Command Center (ATCSCC) that are considered the primary decision makers in the strategic planning process. The ARTCCs chosen were Boston (ZBW, Boston Center), Washington DC (ZDC, Washington Center), New York ARTCC (ZNY, New York Center), and Cleveland ARTCC (ZOB, Cleveland Center). Five airline operations centers (Delta, Southwest, American, United, and JetBlue) were also visited during field observations. However, MIT LL observers were not present at every airline on each of the four days. MIT LL observers embedded at each facility documented the use of CoSPA in the strategic planning process for planning Airspace Flow Programs, Ground Delay Programs, and Enhanced Reroute Planning. The TFI application was also made available to traffic planners during the summer beginning on 9 July 2015. MIT LL observers performing the CoSPA field evaluations also observed and documented use of TFI. Since TFI was a new application available to traffic planners, MIT LL personnel performed training during the months preceding the July release and conducted in-situ training during the CoSPA field observations.

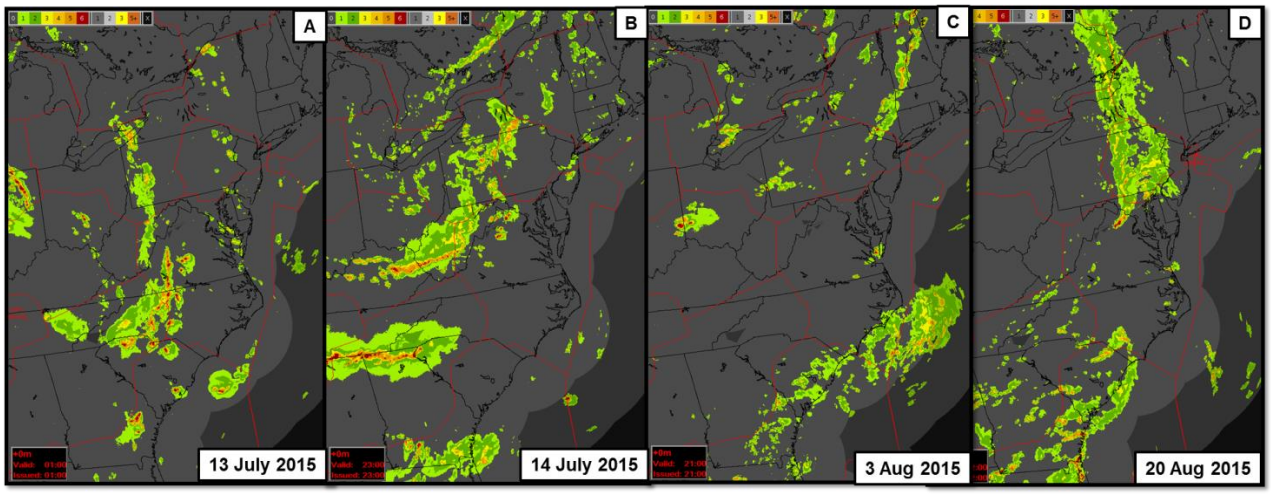

Figure 34. 2015 CoSPA Operational Observation case days: 13-14 July (A and B), 3 August (C), and 20 August (D). Observers resided primarily in the Traffic Management Unit (TMU) or operations area of each facility and airline in order to gather observations on the use of CoSPA and TFI. If appropriate, MIT LL observers posed questions concerning how TMI decisions were made, what information was used to support the decisions, and other questions relating to the objectives listed above. Observers recorded information using a standardized data entry form that included fields for facility, user position, time, and detailed notes on each event and the discussions that took place. Shortly after each observation period, Lincoln staff convened to correlate the data entry form information with the archived CoSPA and TFI information. This enables, for example, a statistical comparison of the timing of TMI decisions with the status of the TFI information (e.g. did the forecast enter the high impact region?) and also compare how information was used simultaneously at the various facilities involved in the TMI decisions.

The first field visits of 2015 involved two consecutive days of observations on 13 and 14 July. User evaluation of TFI was observed on both days at FAA and airline operation centers. The majority of views of TFI were registered at ZOB and ATCSCC. JetBlue air traffic managers were also highly engaged in evaluation of TFI during both days of observations. Command Center planners and specialists reviewed TFI on each of the mornings during the strategic planning period (~1000-1600Z). The focus for use on both days was to evaluate the necessity of AFPs based on the convective forecasts presented. Figure 35 displays the AFPs that were being considered across the Northeast and Mid-Atlantic regions on these two days. Users specifically concentrated on the starting and ending times of the forecasted convective events in order to determine the length of the TMI. Users were observed viewing the drill-down plots of the TFI application (Figure 36) in order to track the convective impact on the embedded timeline.

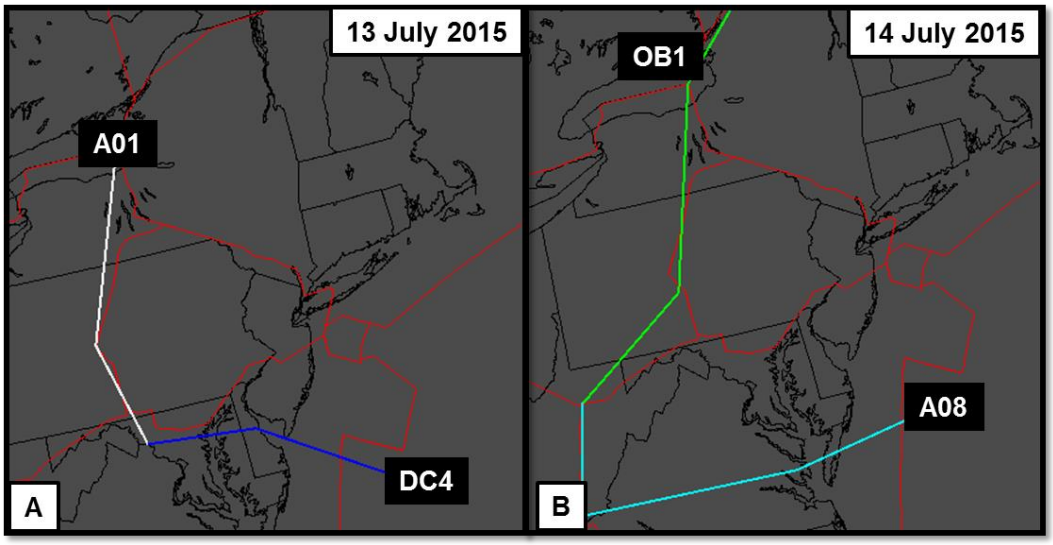

Figure 35. Airspace Flow Program boundaries used on 13 and 14 July to manage forecasted thunderstorms across the Northeast and Mid-Atlantic regions.

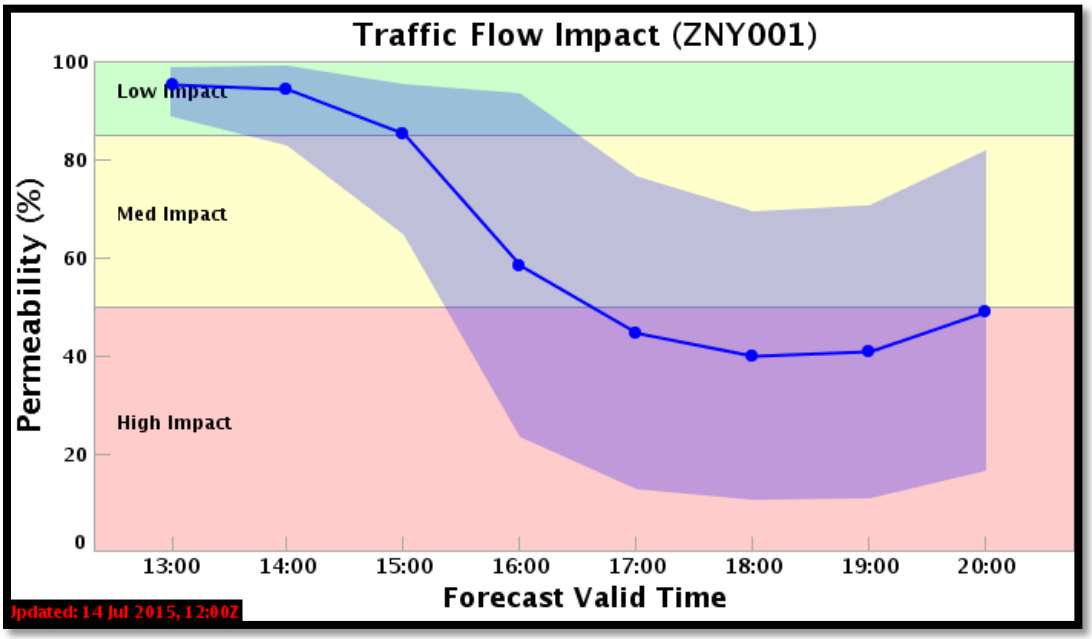

Figure 36. TFI drill-down display plot for 1200Z forecast on 14 July 2015 across the TFI region ZNY001 which lies along the border of ZOB and ZNY.

August 3rd was the second observation day of 2015 and evaluation of TFI continued at all FAA facilities. JetBlue was once again part of the evaluation, along with two other airlines: American and Southwest. ATCSCC, ZOB and ZDC were all engaged in evaluating TFI during the strategic planning period on this day. Traffic managers and dispatchers at JetBlue also continued their evaluation of the new application. AAL and SWA saw limited use of both CoSPA and TFI. This was the first live exposure to both products at these facilities and MIT LL staff used the evaluation to perform additional instructional training. Three AFPs were used to manage traffic on this day, JX7, OB1 and A08 (Figure 37).

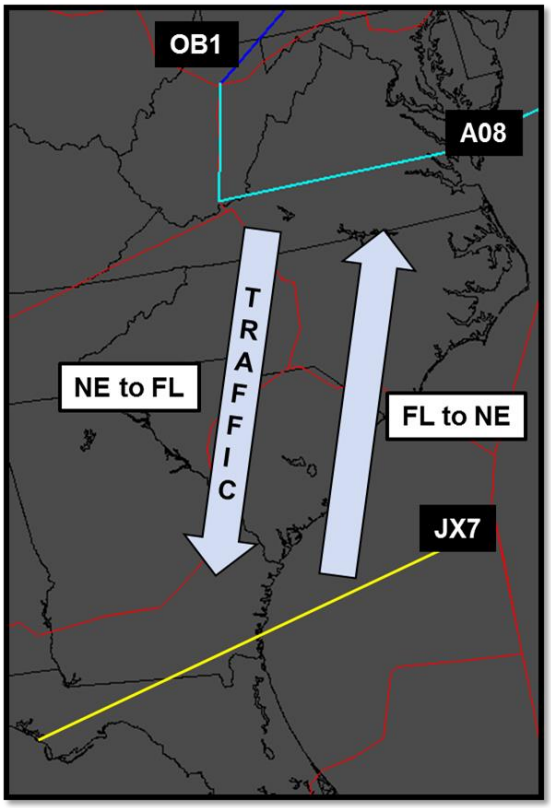

Figure 37. The three AFPs that were issued on 3 August 2015: OB1, A08 and JX7.

There are typically only two AFPs issued during severe weather events, however, on this day, storms were forecast to erupt along a wide swath in the east, including across northern Florida. Air traffic between JX7 and A08 constitutes a major flow between the Northeast terminals (BOS, EWR, LGA, JFK) and Florida. There are multiple segments between each of these cities per day and the preference is not to have JX7 and A08 in place at the same time. If this were to occur, delay would increase exponentially between the two AFPs as flights passed southbound through JX7 on the flight segment and then incur

additional delay on the second flight segment as the flight returned to the Northeast passing through A08. Figure 38 shows the 1300Z CoSPA VIL truth and 5 hour forecast (valid 1800Z) that the Command Center planners and specialists were viewing on the morning of August 3rd. The 5 hour CoSPA forecast (Figure 38B) indicates that storms will remain across central and western Florida while new storms begin to initiate across southern VA and northern NC at 1800Z. The CoSPA forecast along with the TFI plots for these regions (Figure 39) allowed traffic managers to more precisely estimate when to end the Jacksonville AFP (JX7) and begin the Washington Center AFP (A08). The planner and NOM at ATCSCC suggested that TFI could potentially be a useful application to evaluate such strategic timing decisions.

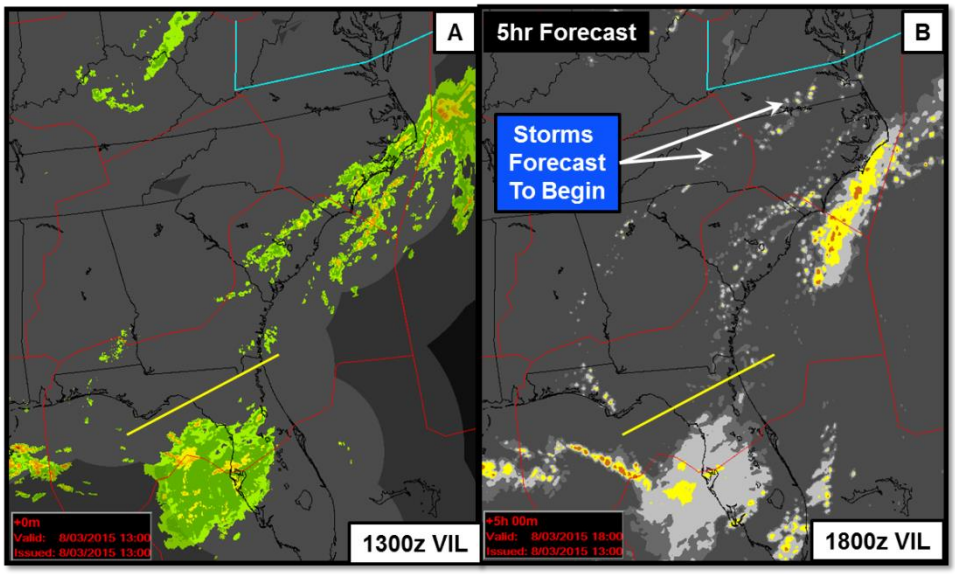

Figure 38. 1300z VIL truth and 5 hour CoSPA forecast on 3 August 2015.

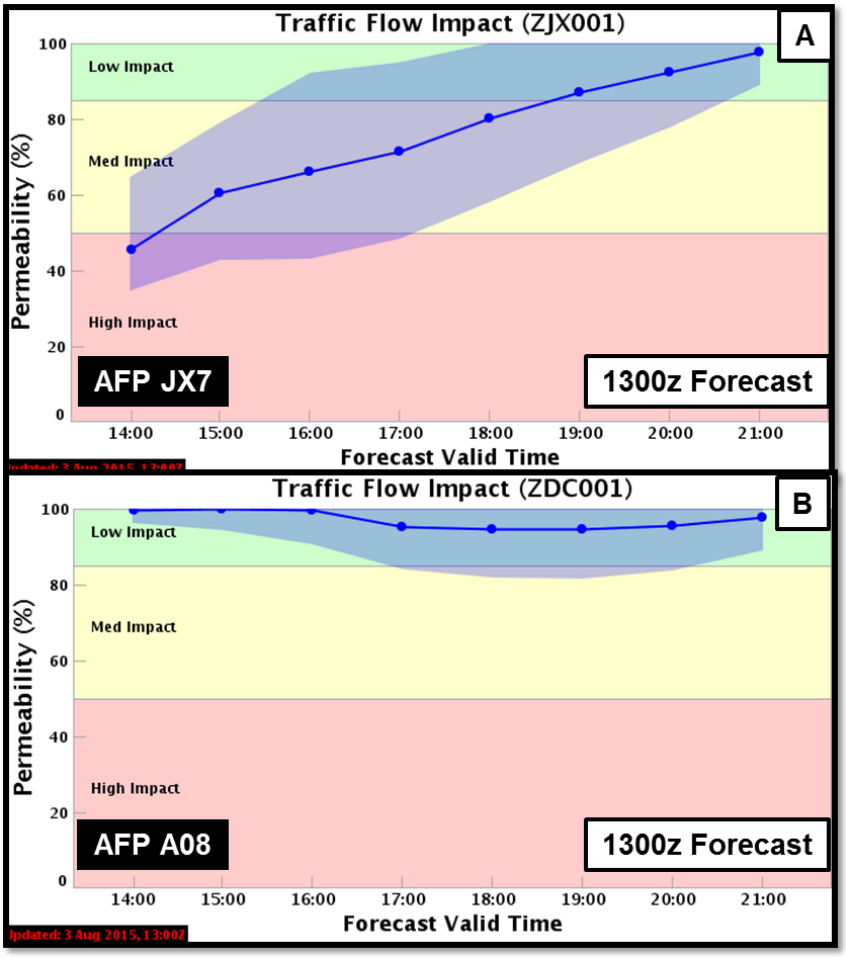

Figure 39. 1300Z TFI forecast plots for ZJX001 and ZDC001 representing AFPs JX7 and A08 respectively.

The third and final observation took place on 20 August, 2015 and utilized all previous FAA facilities plus JetBlue and United Airlines. Six more direct references to TFI at Command Center were noted during the strategic planning period. TFI was evaluated during the AFP planning process to determine timing and severity of the TMI needed. One observation from a terminal traffic manager in the 4-6 hour timeframe noted use of TFI to plan a potential GDP prior to the AFP issuance. Figure 40 highlights the 1300Z 8 hour CoSPA VIL forecast which was evaluated in conjunction with TFI for this specific hour. The NOM on duty at ATCSCC agreed that TFI "could have been very useful for planning". After the strategic planning was complete that morning he deduced that "current AFP rates are set too high". He was concerned that the rates which were agreed upon by FAA facilities and airlines during the morning conferences were not going to be impactful enough based on the coverage and intensity of the

thunderstorms he was witnessing. He deduced that the rates TFI was suggesting in the morning may have been more representative of the reduction needed to restrict traffic. Figure 41 displays the 1300Z TFI forecast (blue plot) along with the actual permeability verification (black plot) for the TFI region ZNY001 which represents AFP OB1. Multiple ground stops for all NY terminals were issued on this day which is often indicative of over-delivery of demand based on restrictions due to convective weather.

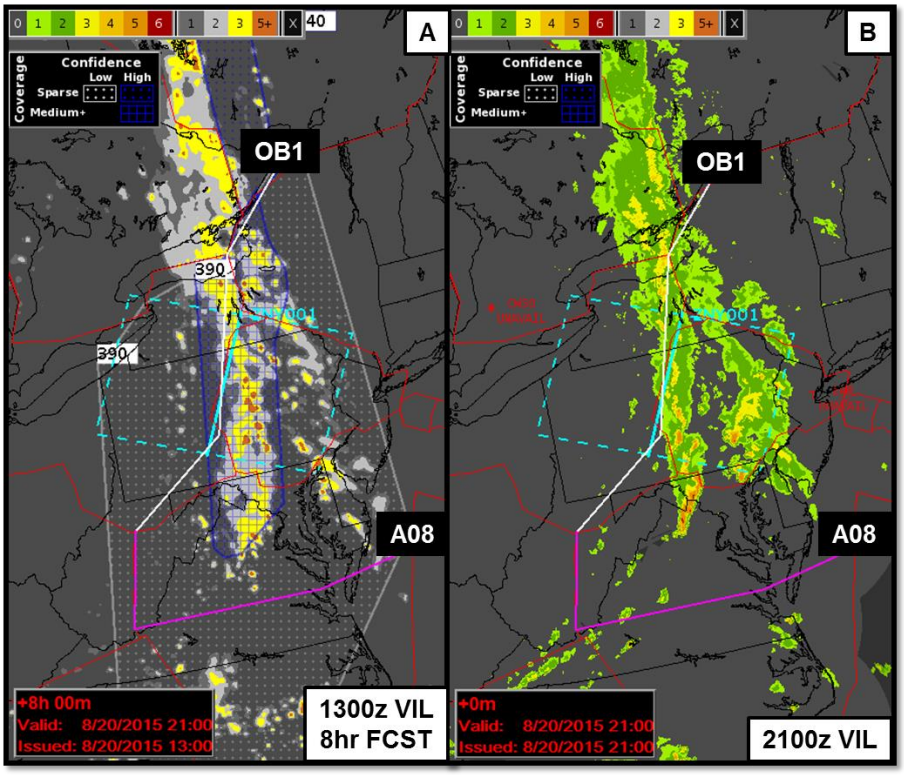

Figure 40. The CoSPA VIL 8 hour forecast (valid at 2100Z) and the 2100Z VIL truth on 20 August 2015. Shown in the plots are AFPs OB1 and A08 along with the TFI region ZNY001 highlighting the restricted airspace due to thunderstorms. Also plotted in (A) is the CCFP 8 hour forecast overlay.

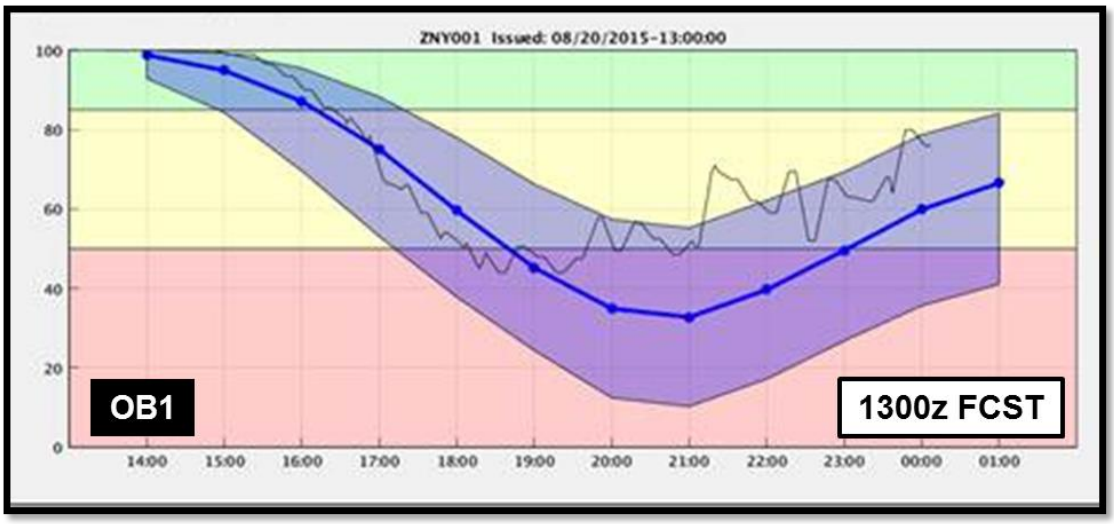

Figure 41. The 1300Z TFI forecast (blue) and verification plot (black) on 20 August 2015 for the ZNY001 region for AFP OB1.

5. RECOMMENDATIONS FOR FUTURE WORK

The analysis of the Traffic Flow Impact (TFI) Flow Constrained Area (FCA) forecast presented in this report has demonstrated the validity of the TFI forecast approach and the strengths and limitations of the current underlying technology. The next steps focus on refinements and improvements to the concept and technology that will support the development and full integration of TFI into the Traffic Flow Management System (TFMS) as a decision support capability. Many of these steps are independent and can be performed in parallel. Where dependencies exist, they are identified.

1. Flow rate forecasting. Traffic management planners must specify flow rates through FCA boundaries when defining strategic Traffic Management Initiatives (TMI). The mapping of permeability to capacity is a function of the underlying structure of the impacted airspace controlled by the FCA – this represents a type of site adaptation. The task of mapping permeability into flow rates may be broken up into several steps:

1. Define mappings for fixed 'standard' FCA, such as ARTCC boundaries (TFI site adaptation)
2. Develop a model to map permeability of arbitrarily defined FCA to flow capacity through pattern matching of standard FCA mappings defined in step 1
3. Refine the TFI forecast uncertainty model to incorporate weather and flow rate uncertainty
4. Implement the algorithm to display 0-12hr flow rate forecasts, including uncertainty
5. Evaluate and refine the use of flow rate forecasts in a laboratory or operational environment

2. Event forecasting. The definition of a TMI includes several key pieces of information: the start time, stop time, and flow rate by hour. The TFI impact forecast can be translated into a forecast of the onset, duration, and severity of a convective weather event that may impact airspace associated with an FCA. Forecasts of onset, duration, and severity of impact events correspond closely to the TMI decision parameters of start time, stop time, and flow rate. The event forecast task includes the following steps:

1. Working with subject matter experts, create objective definitions for onset, duration, and severity based on TFI permeability
2. Develop an initial version of an event forecast uncertainty model
3. Evaluate and refine TFI forecast performance for each event metric (onset, duration, severity) through statistical analysis and in human-in-the-loop laboratory or operational environments.

3. TFI forecasting for coupled FCA / CTOP TMI planning. The Collaborative Trajectory Options Program (CTOP) requires the ability to couple up to four FCAs into a single TMI. The TFI ConOps and forecast tool can be extended to support the identification of FCAs that that may be combined into a CTOP TMI to mitigate forecast convective impacts. Similar to #1 and #2 above, this would also involve statistical and human-in-the-loop evaluations and refinement.

4. ConOps for integration of the TFI forecast with Operational Response Development (ORD). The TFI forecast provides explicitly-defined forecast and uncertainty information that is particularly tuned to weather conditions at the time of decision making. TFI impact forecasts, including uncertainty bounds, provide a clear and concise set of parameters that can bound the TMI search space for ORD what-if simulations. The links between TFI forecasts, TFI uncertainty, and TMI parameter selection are explicit and so are likely to be readily understood and interpreted by users. In contrast, TMI parameters that are automatically generated from historical data, in which the parallels between past and present may be opaque to the decision maker, may be more challenging to interpret in operations. Accordingly, there is a need for more research and development to explore how TFI and other concepts can contribute to effective ORD. This task can proceed concurrently with **TFI forecasting for coupled FCA / CTOP TMI planning**, but the two capabilities are related.

5. Best practices for uncertainty mitigation. There are no validated best practices to guide the decision maker in the use of uncertainty information in traffic planning. Nor is there evidence that 'what if' simulation will result in better decisions. While the uncertainty information conveyed by the TFI forecast is explicit and directly linked to TMI planning, there is not yet sufficient data to fully understand how decision makers interpret and use the information. Likewise, there is a need to gather the evidence needed to provide users with specific guidance about the most effective ways to interpret and use TFI forecasts to plan TMI. This task has three steps (steps 2 and 3 may proceed in parallel):

1. Define appropriate TMI decision metrics that take into account forecast and execution uncertainty information available from the TFI forecast to evaluate the quality of TMI decisions

2. Test the impact of different uncertainty information / presentation on decision timeliness and quality via serious gaming of several real-world scenarios

3. Perform laboratory and field evaluations of TFI uncertainty forecasts coupled with post-event assessments of decision quality

6. Airspace impact forecasts for progressive decision making and operational bridging. The spatial scale over which convective weather impacts can be forecast within operationally acceptable accuracy is correlated to the forecast horizon. At horizons greater than 4 – 6 hours, impact forecasts may be accurate only for FCA that control ARTCC-scale strategic flows. At shorter forecast horizons, impact forecasts may be sufficiently accurate for smaller FCA that control tactical flows. Sector and individual trajectory impact forecasts may be sufficiently accurate for operations at the 30 – 60 minute forecast horizon. Understanding the relationship between forecast horizon and appropriate spatial scale has

important implications for progressive decision-making. This task has three related subtasks that may proceed in parallel:

1. Evaluate forecast skill as a function of FCA scale, down to the sector level

2. Explore the relationship between large-scale FCA forecasts at long forecast horizons and shorter horizon forecasts of smaller scale FCA and sectors within the large-scale airspace

3. Develop a ConOps for progressive decision making that incorporates forecast skill at increasingly finer spatial / temporal scales

This page intentionally left blank.

6. SUMMARY

This report has presented the methodology and validation results of research to predict the impact of convective weather on traffic flows using a flow-based permeability measure. The work was broken down into four areas: translating convective weather into a metric, called permeability, that estimates the reduction in flow due to that weather; predicting the permeability and uncertainty in the forecast using multiple forecast products and expressing uncertainty with prediction intervals; providing operational guidance to front-line traffic planners with the Traffic Flow Impact (TFI) tool; and recommendations for future work to assist in advanced operational guidance methods.

The translation model was developed to capture impact on large scale traffic flows on the order of the size of the typical ARTCC. A series of notional routes (straight line trajectories perpendicular to an airspace crossing line) are used to capture the convective impacts on an air space. The permeability is computed by taking the aggregated impact on all the routes across the TFI region. The model was validated by computing the permeability on true weather and capturing the true traffic flows as measured by the observed air traffic. The results have shown good agreement between the permeability estimate and measured flow rates for major air traffic resources with heavy demand during the afternoon and evening hours. Therefore, the permeability estimate forms the basis for a weather impact assessment that air traffic planners could use to anticipate the constraints on the air traffic control system. By translating convective weather forecast information into an impact metric that can be easily interpreted for selecting TMIs and setting the TMI parameters (e.g., time of onset, level of impact [permeability and flow rates], and duration), it is hypothesized that more effective and timely TMIs can be formulated and assessed in operations. These results suggest that the permeability translation model discussed in this report is an effective methodology to translate the convective weather into a metric that can be easily interpreted as an impact on air traffic resources.

A forecasting capability was also developed as part of this effort to predict TFI permeability 0-12 hours into the future at a set of user selectable TFI regions. This tool utilizes multiple forecasts for making this prediction, including the CIWS extrapolation forecast, a time-lagged ensemble of VIL and Echo Tops forecasts from the HRRR, the LAMP probabilistic forecast of thunderstorms and the SREF calibrated thunder storm probability. Features are extracted from each of these forecasts and combined to predict future permeability and to create a prediction interval made up of the 20th and 80th percentiles of the expected distribution of permeability using quantile regression. Data from the summers of 2013, 2014 and 2015 were used to develop, train and validate the TFI forecast. Permeability estimates made using the quantile regression showed higher skill than permeability estimates made from any of the individual forecasts. Prediction intervals grew with forecast intensity and forecast lead time, but was able to maintain the target 60% accuracy in capturing observed permeability. These results show that the TFI forecast can combine multiple forecasts and translate them into a single forecast of airspace permeability that comes with a measure of uncertainty (prediction intervals). Additionally, we believe that communicating forecast uncertainty as expressed using those same decision variables provides an

objective, quantitative basis to better understand and communicate the risks and benefits of various levels of TMI strategies. However, more research and evaluation is needed to verify these hypotheses and ensure that decision support information meets user needs.

During the summer of 2015, the Traffic Flow Impact tool was provided to front-line operational decision makers during the operational evaluation demonstration period which began on 9 July 2015 and ran through the end of October. The objective of the summer operations observation and evaluation period was to gain valuable insight into the potential operational usefulness of the Traffic Flow Impact forecast and guide the development of the algorithms and validation process. Input from experienced operational traffic flow managers familiar with the complexity of the NAS and who perform the daily decision making that impacts the National Airspace System (NAS) performance is critical to developing future advanced methods and products that improve NAS performance. The MIT LL convective observation team gathered data from each of the four separate convective events. Feedback from the operational decision makers was very positive. Experienced ATCSCC planners commented were observed consulting the TFI tool and commented on ways the tool could have helped improve the operational decisions made of specific days with significant weather impact that resulted in excessive amounts of delay.

Finally, this report discussed the next steps for improving the concept, supporting the technological development, and moving towards the full integration of TFI into the Traffic Flow Management System (TFMS). Six focus areas are recommended for future work including improvements to flow rate forecasting, event forecasting, coupling TFI forecasts to FCA/Collaborative Trajectory Options Program (CTOP) Traffic Management Initiative (TMI) planning, integration of TFI forecasts with Operational Response Development (ORD), defining best practices for uncertainty mitigation, and forecasts for progressive decision making with operational bridging. Most of these steps are independent and can be performed in parallel. Continued input from Subject Matter Experts (SMEs), human-in-the-loop laboratory experiments or serious gaming, along with field evaluations would greatly enhance the future efforts.

APPENDIX A

A statistical validation for each of the 57 TFI regions created for this study was performed and is summarized in this Appendix. Each figure consists of four images and uses the data for all 122 case days, unless otherwise noted.

The top left image depicts the TFI region as defined in Section 2.1 The airspace crossing is shown with a red line; the airspace boundary is shown in a thick white line; and the notional airspace traversing trajectories are shown in the thin white lines. The states are depicted with a thin black line and the ARTCC boundaries are shown in a thick black line.

The top right image is a box-and-whisker plot of the 60-minute flow rates as described in Section 2.2.1 by the time of day. The red dash is the median flow rate for the entire data set during that hour, and the box represents the 25th and 75th percentile values. In general, the higher nominal flow rates are observed in the afternoon for most TFI regions, while the higher flow rates for ZJX and ZMA are observed during the morning hours.

The bottom left image is a box-and-whisker plot of the observed 60-minute flow rate as described in Section 2.2.1 for the airspace binned by increments of 20% permeability. The red dash is the median flow rate, and the box represents the 25th and 75th percentile values. The maximum observed flow rate for each box is also shown in a red diamond. The data are filtered to include only the hours when the airspace experiences the highest demand. For all TFI regions, except those over the Florida peninsula (ZJX, ZMA) the filtering begins at 1800Z and ends at 0100Z. For ZJX and ZMA the data is filtered between 1300Z and 2100Z. The far right column is permeability estimates equal to 100, implying no weather impact.

The bottom right image is the median 60-minute flow rates as described in Section 2.2.1 by hour categorized into four impact categories. The categories are No Weather (permeability equal to 100), Low Impact (permeability between 85 and 99), Moderate Impact (permeability between 50 and 84) and High Impact (permeability less than 50). The reduction of flow rates by impact category can be observed for most TFI regions, as well as those times of day which will experience the High Impact category (later afternoon).

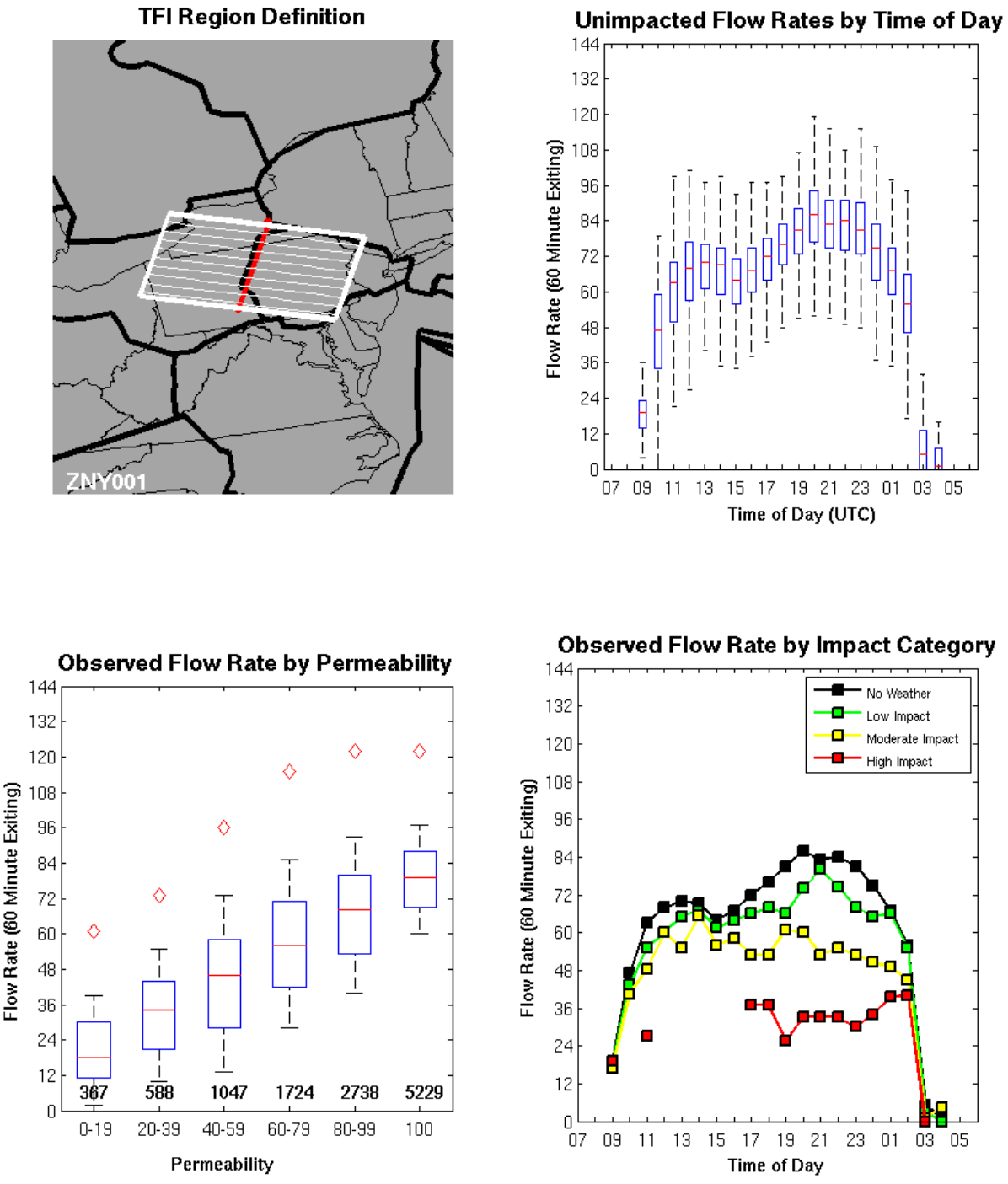

Figure A-1. Traffic Flow Impact region ZNY001: Transition air space between the Cleveland ARTCC and the New York ARTCC over central Pennsylvania.

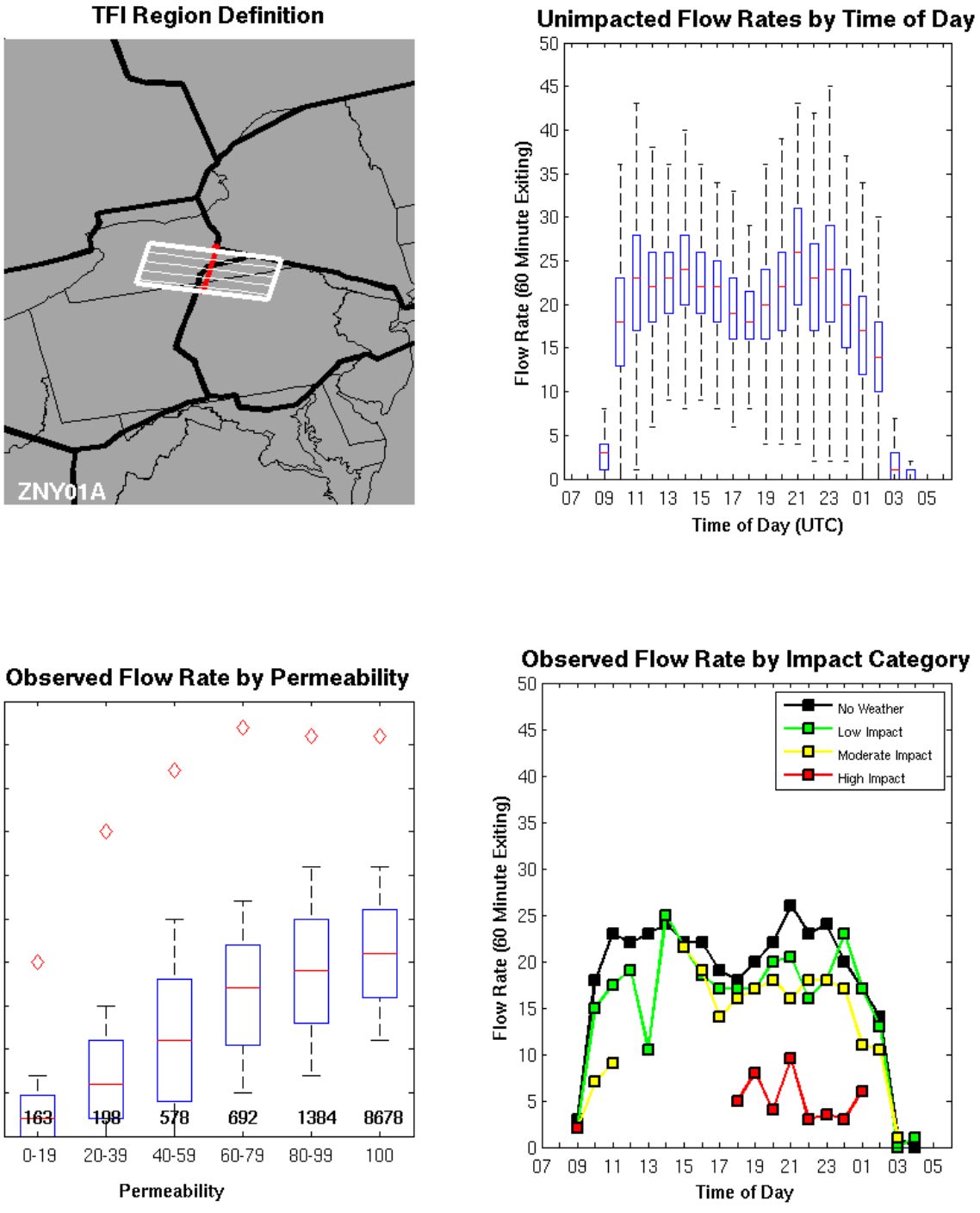

Figure A-2. Traffic Flow Impact region ZNY01A: Transition air space for west bound departures between the New York ARTCC and the Cleveland ARTCC over south central New York

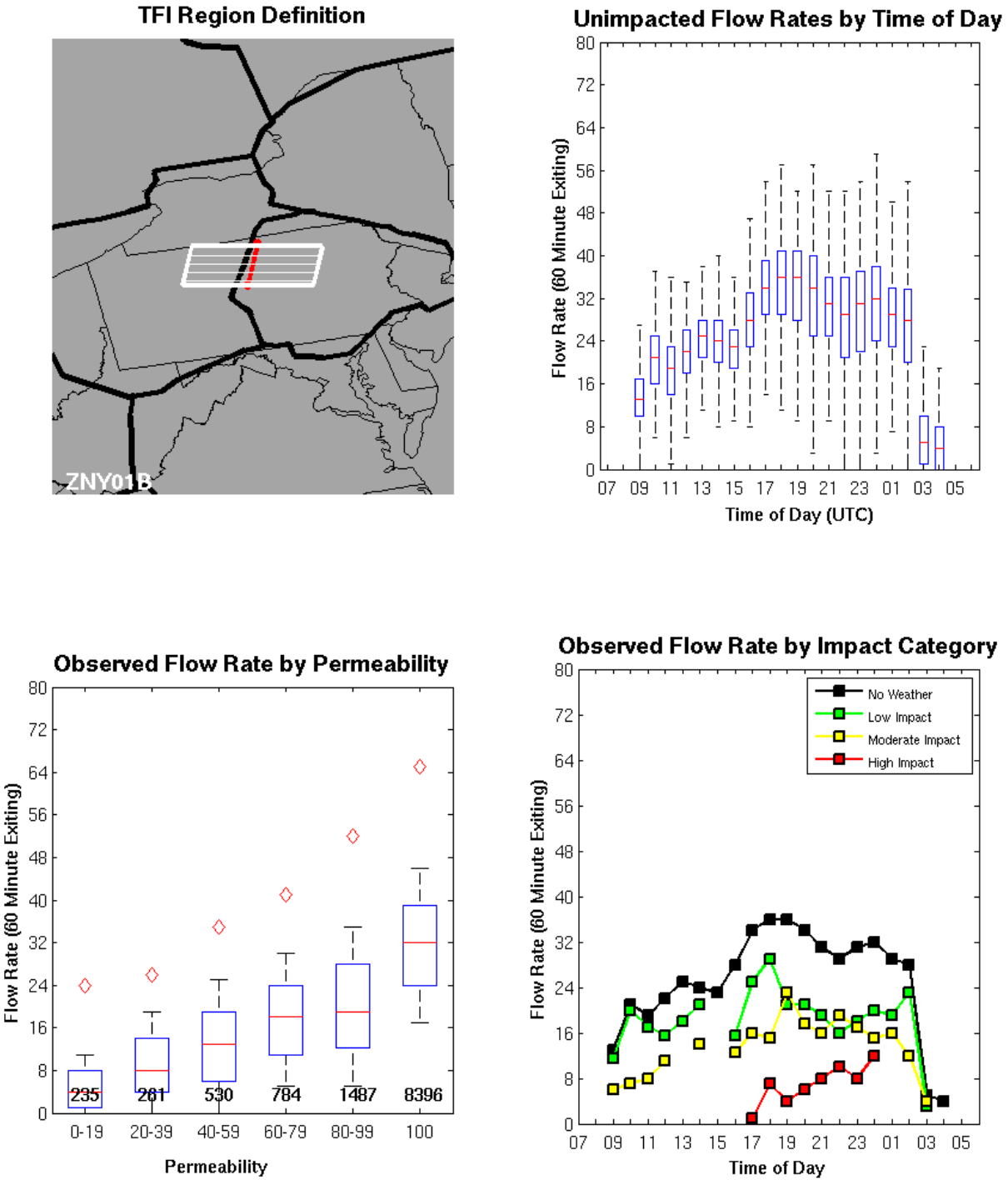

Figure A-3. Traffic Flow Impact region ZNY01B: Transition air space for east bound arrivals between the Cleveland ARTCC and New York ARTC over north central Pennsylvania.

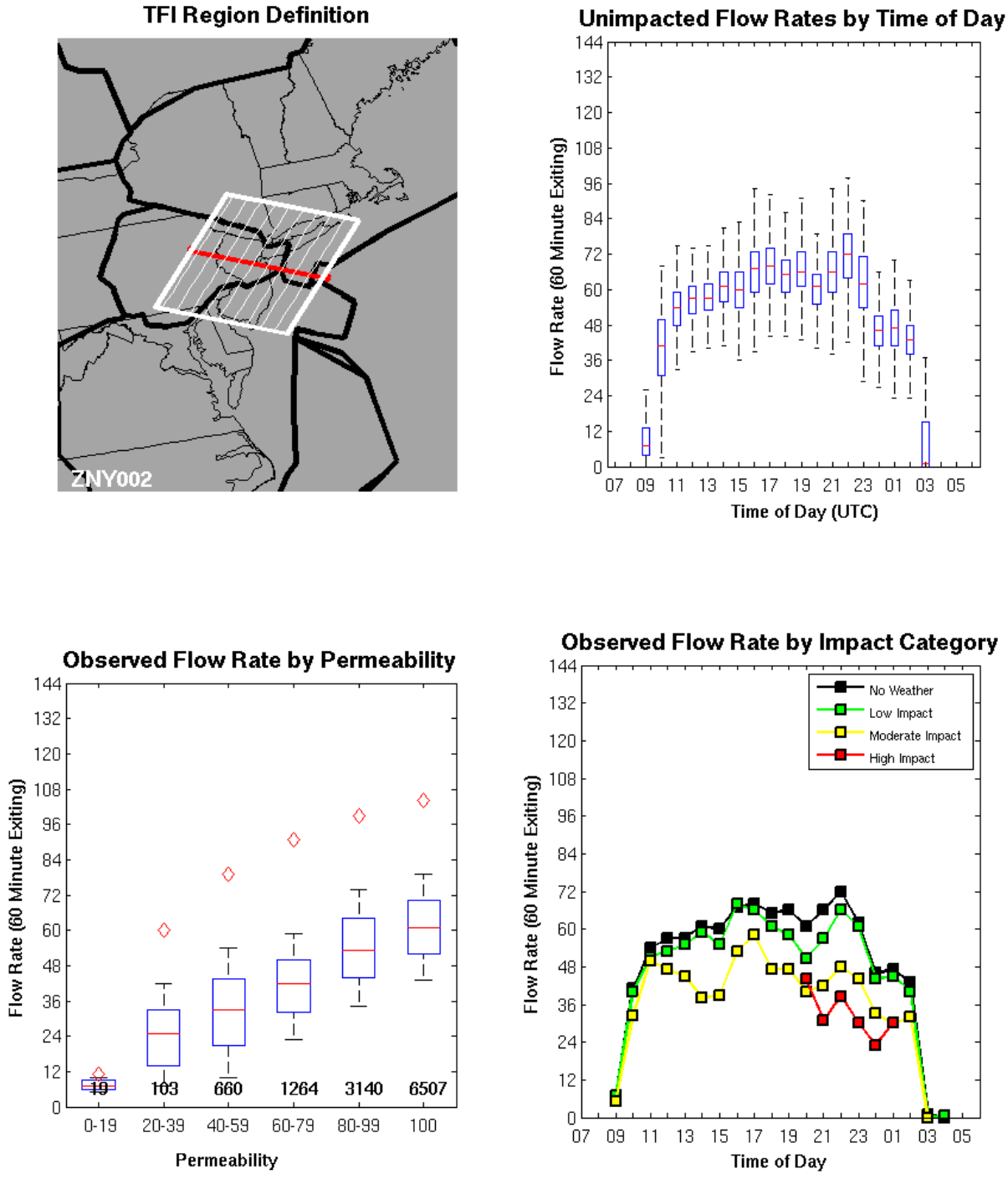

Figure A-4. Traffic Flow Impact region ZNY002: North-south traversing en route flow over the metro New York airports.

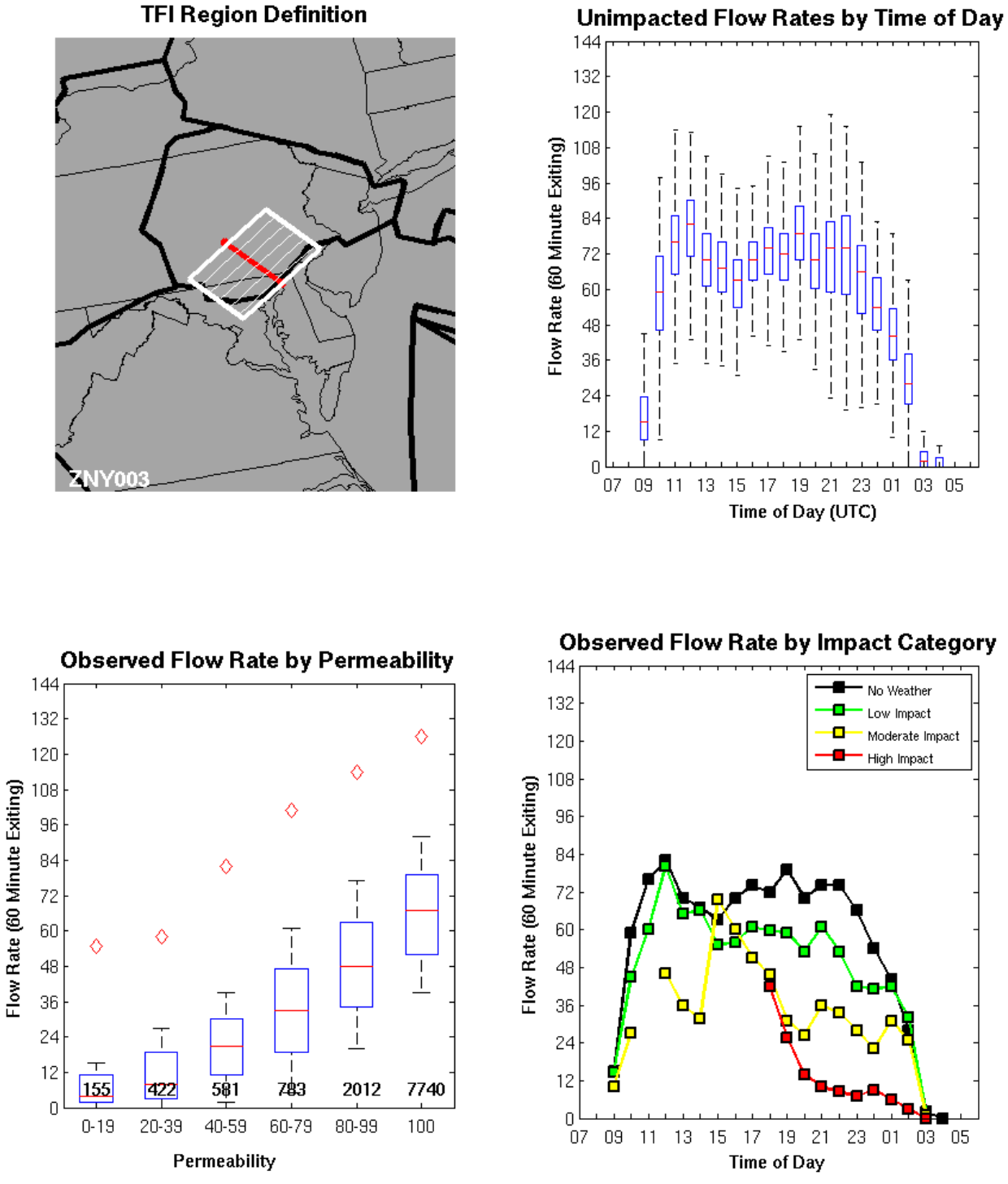

Figure A-5. Traffic Flow Impact region ZNY003: Departure flow from the metro NY airports heading southwest into ZDC.

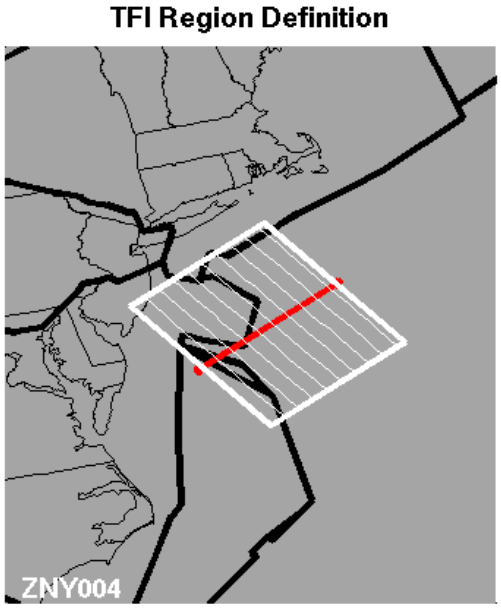

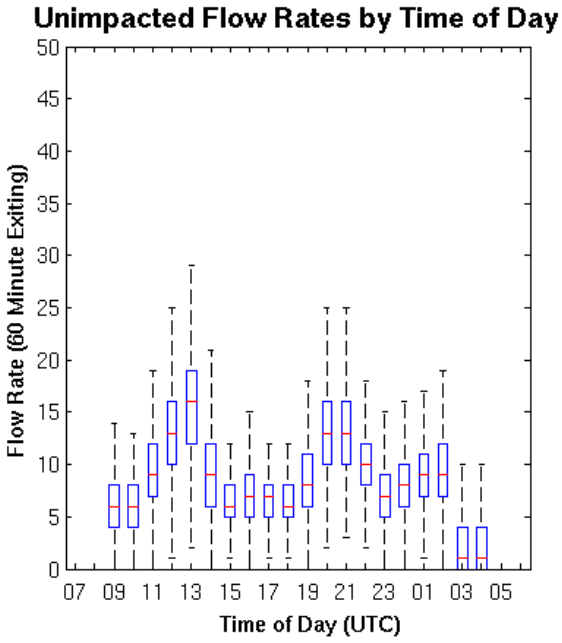

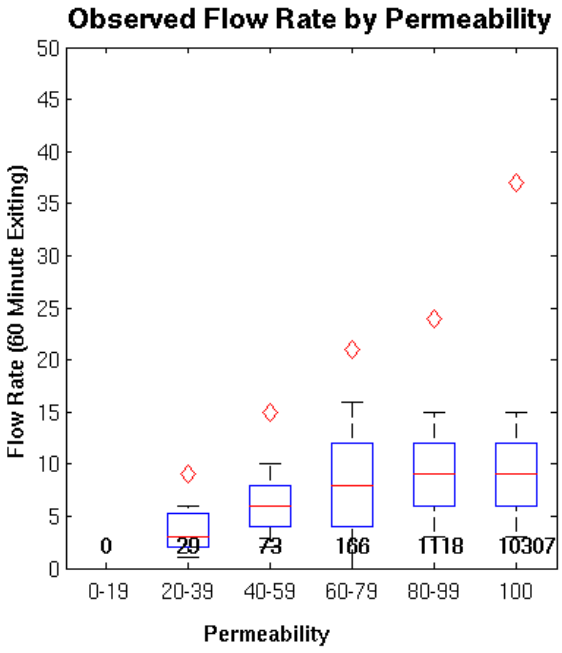

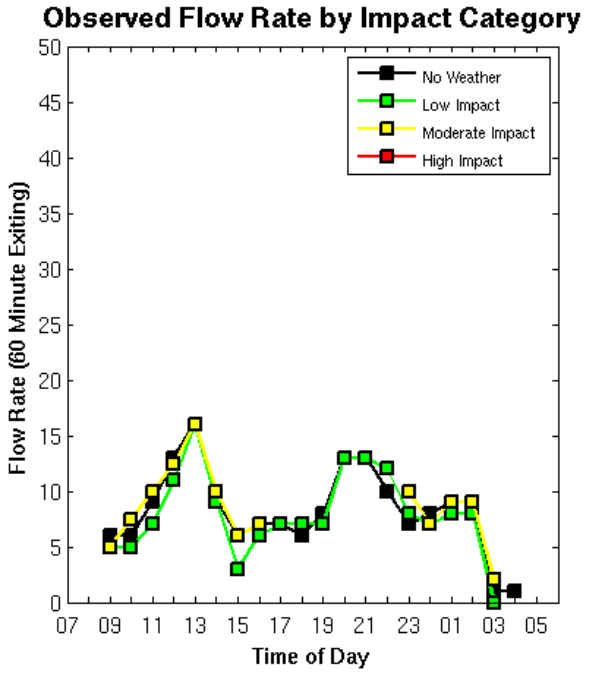

Figure A-6. Traffic Flow Impact region ZNY004: Traffic flow entering and exiting the NY metro airports over the Atlantic Ocean to the southeast.

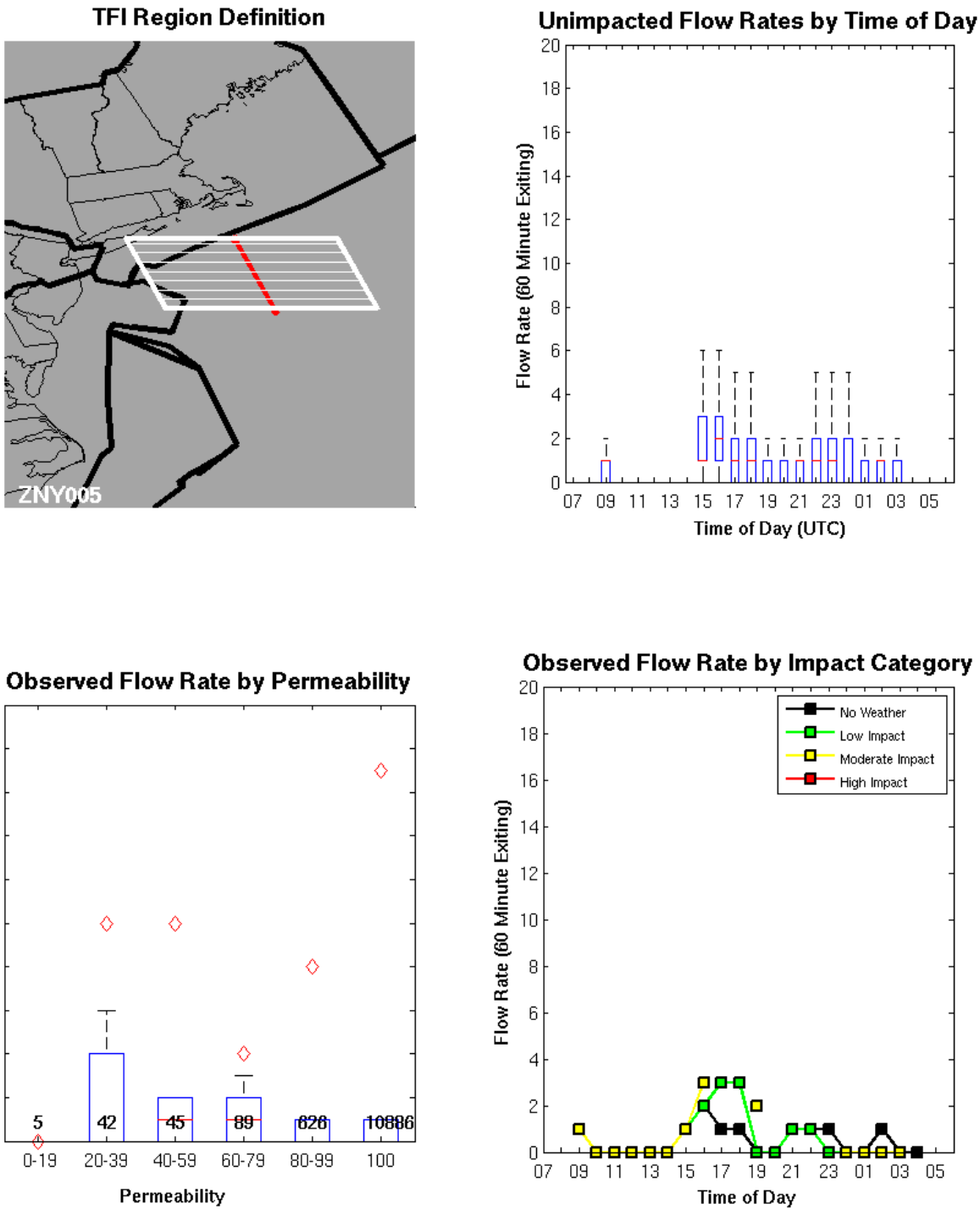

Figure A-7. Traffic Flow Impact region ZNY005: Traffic flow entering and exiting the NY metro airports over the Atlantic Ocean to the east.

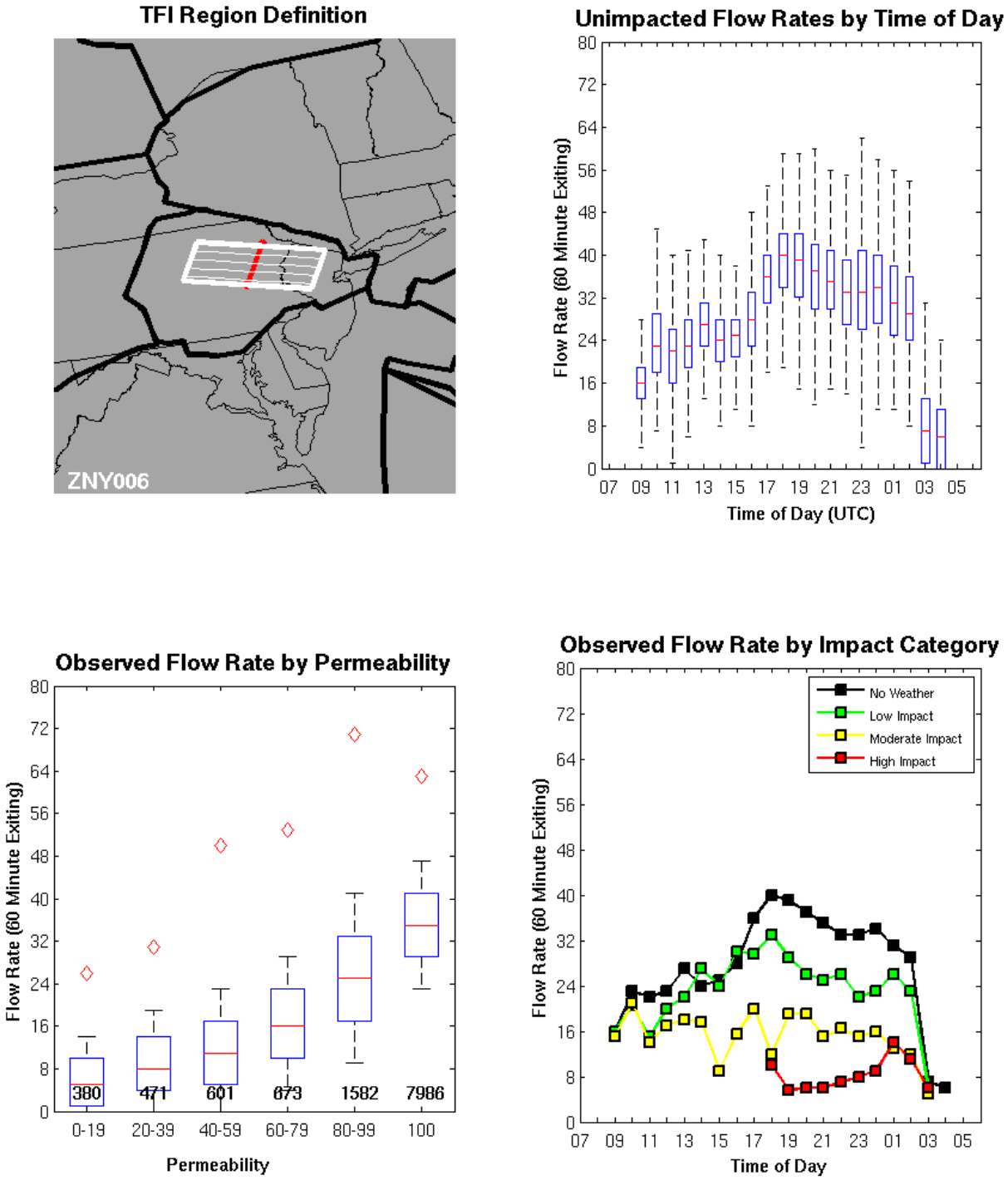

Figure A-8. Traffic Flow Impact region ZNY006: Arrival flow to the metro NY airports from the west over eastern Pennsylvania.

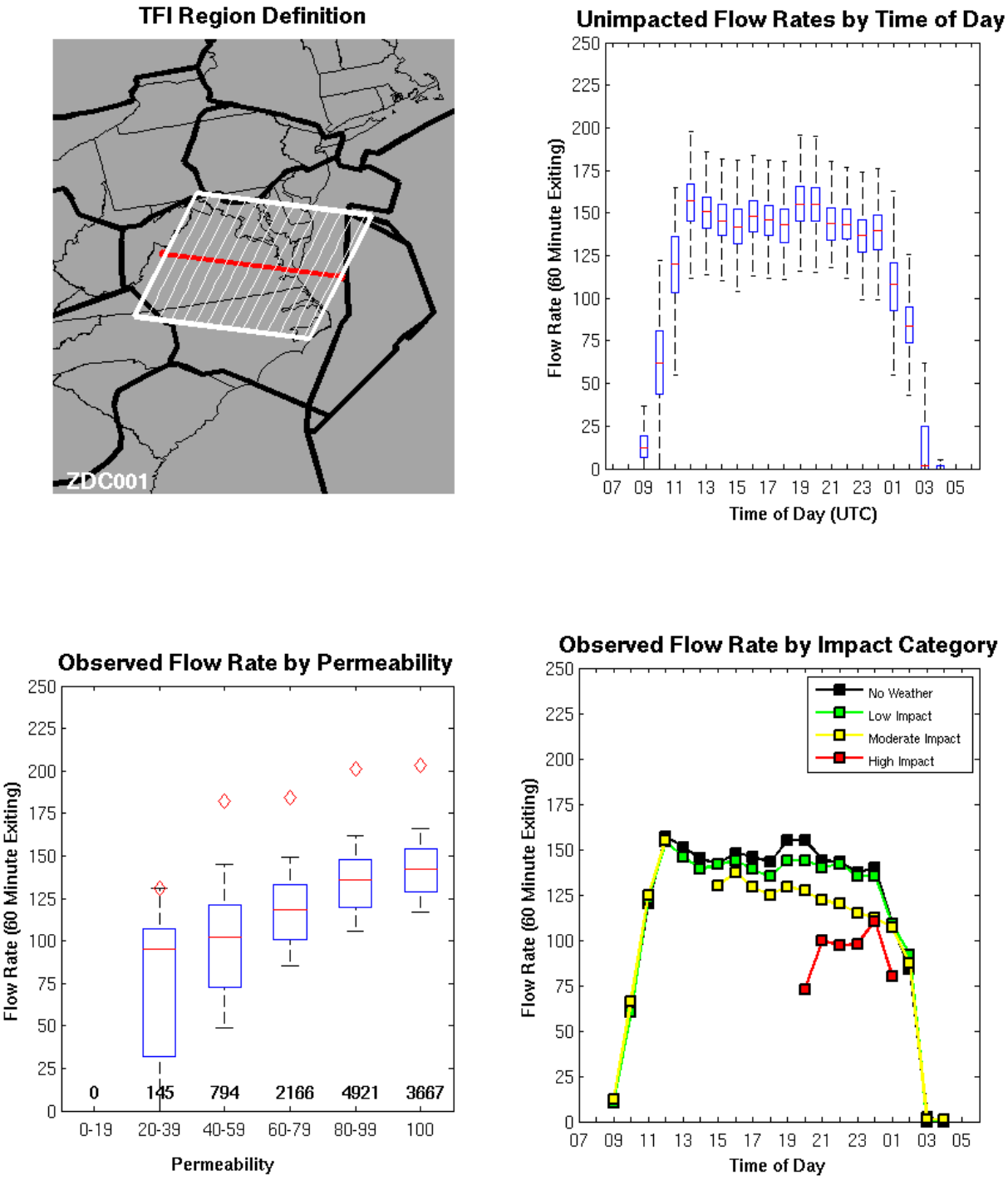

Figure A-9. Traffic Flow Impact region ZDC001: Traffic flow through ZDC on a north-south trajectory.

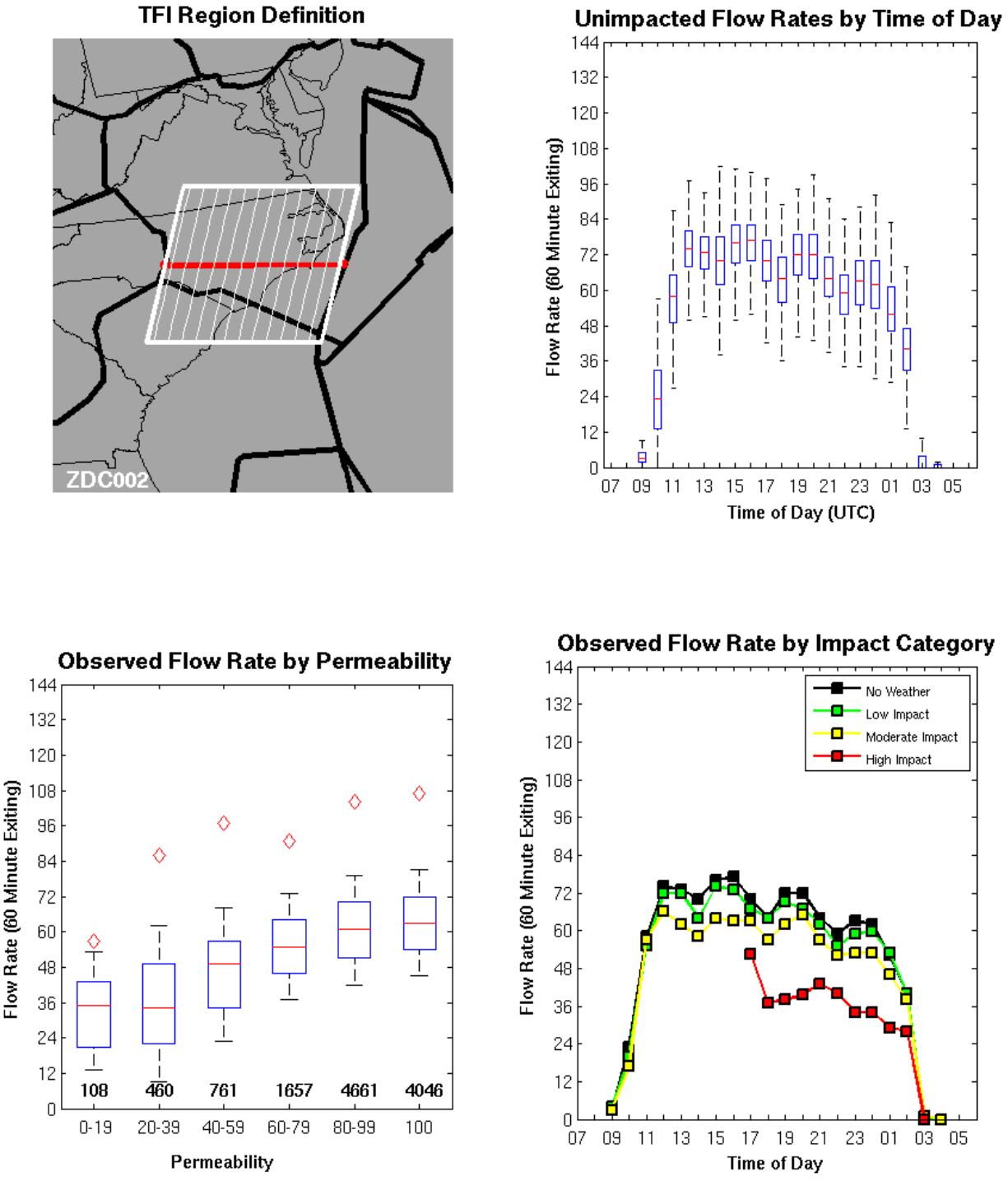

Figure A-10. Traffic Flow Impact region ZDC002: Traffic flow transitioning between ZJX to ZDC .

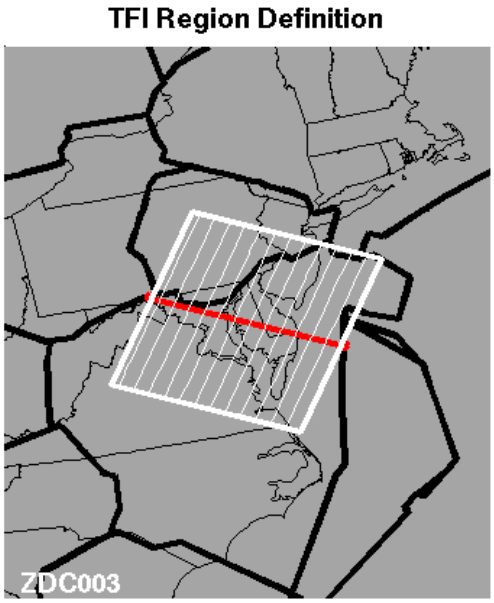

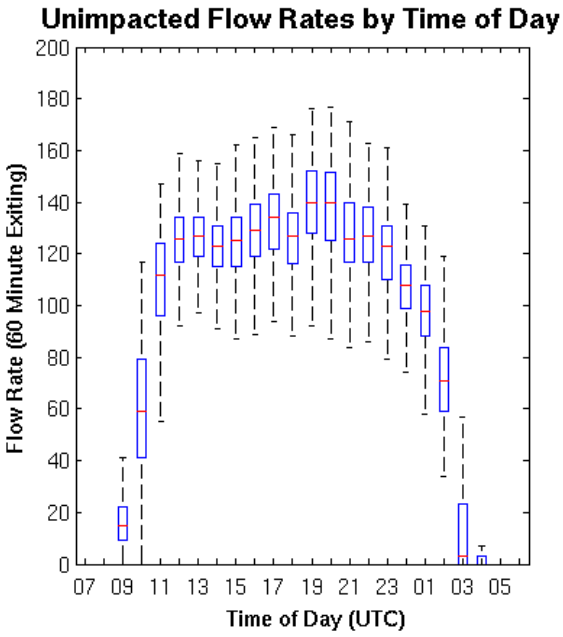

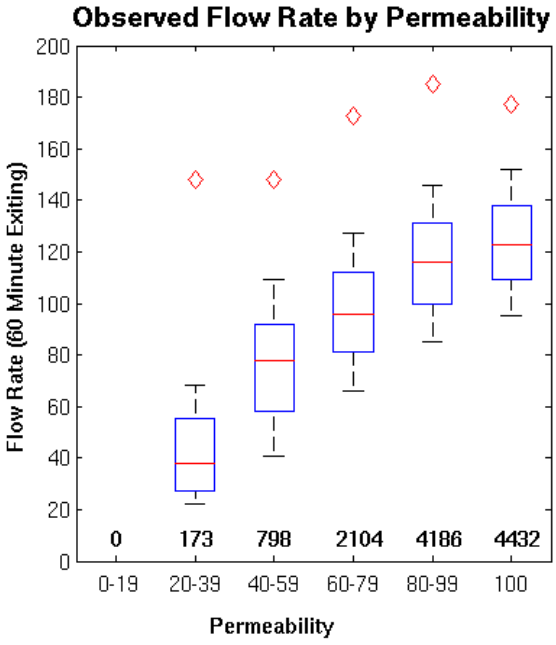

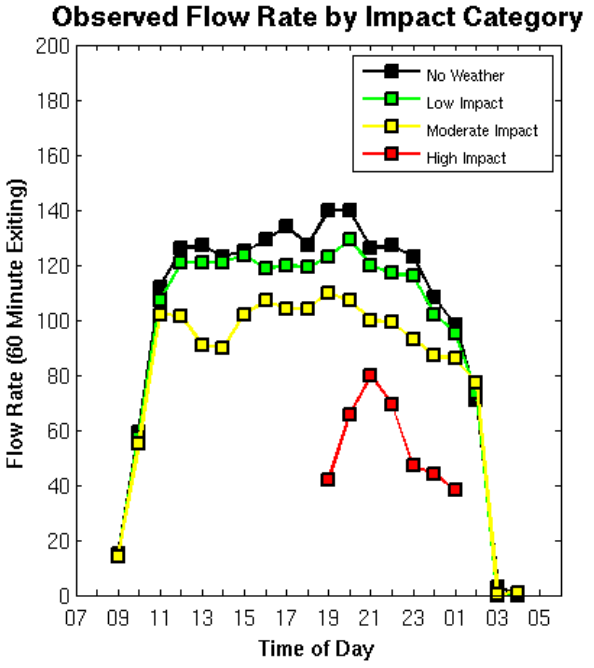

Figure A-11. Traffic Flow Impact region ZDC003: Traffic arriving into the NY metro airports along with overflights heading the New England .

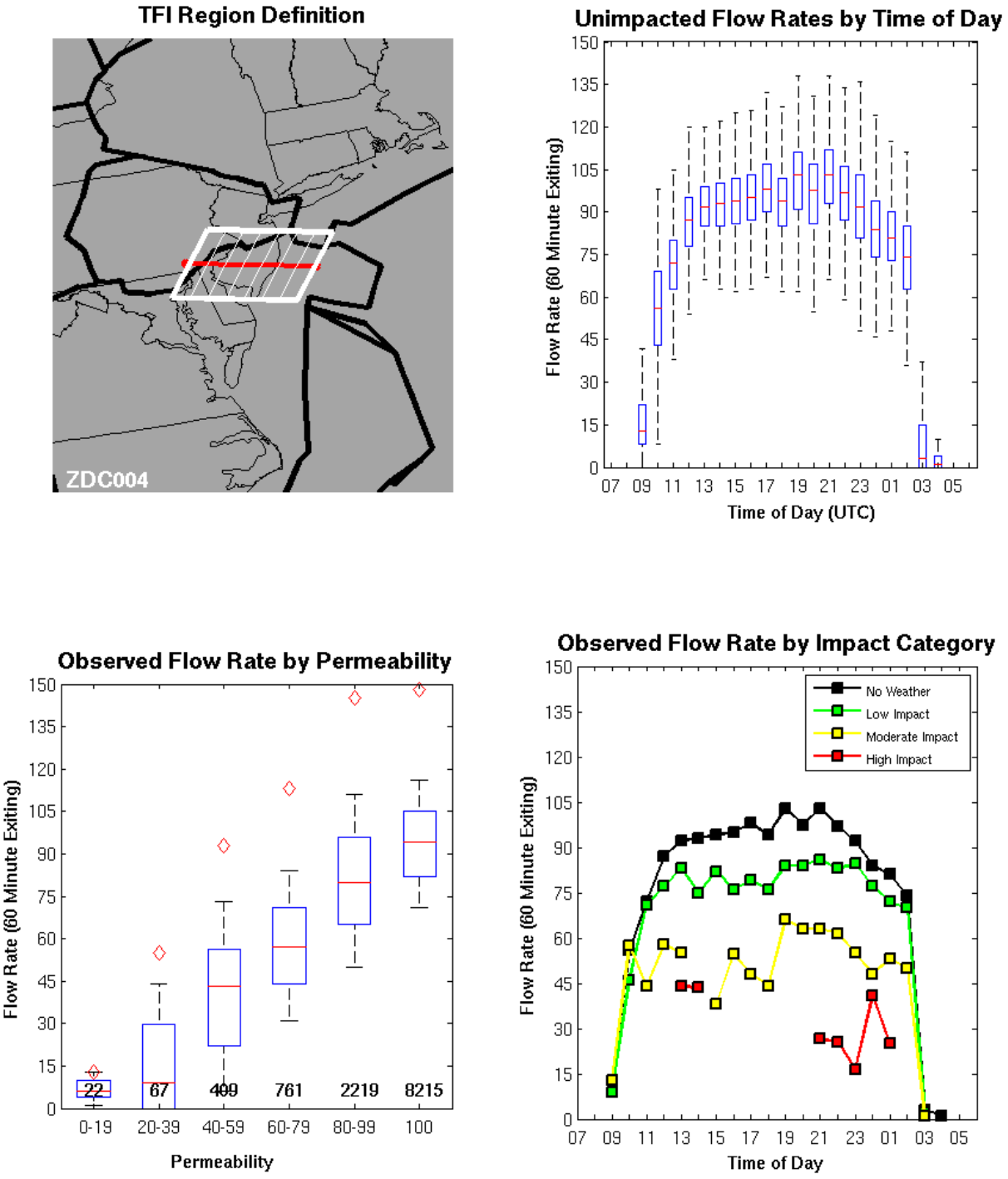

Figure A-12. Traffic Flow Impact region ZDC004: Air traffic primarily destined for the NY metro airports.

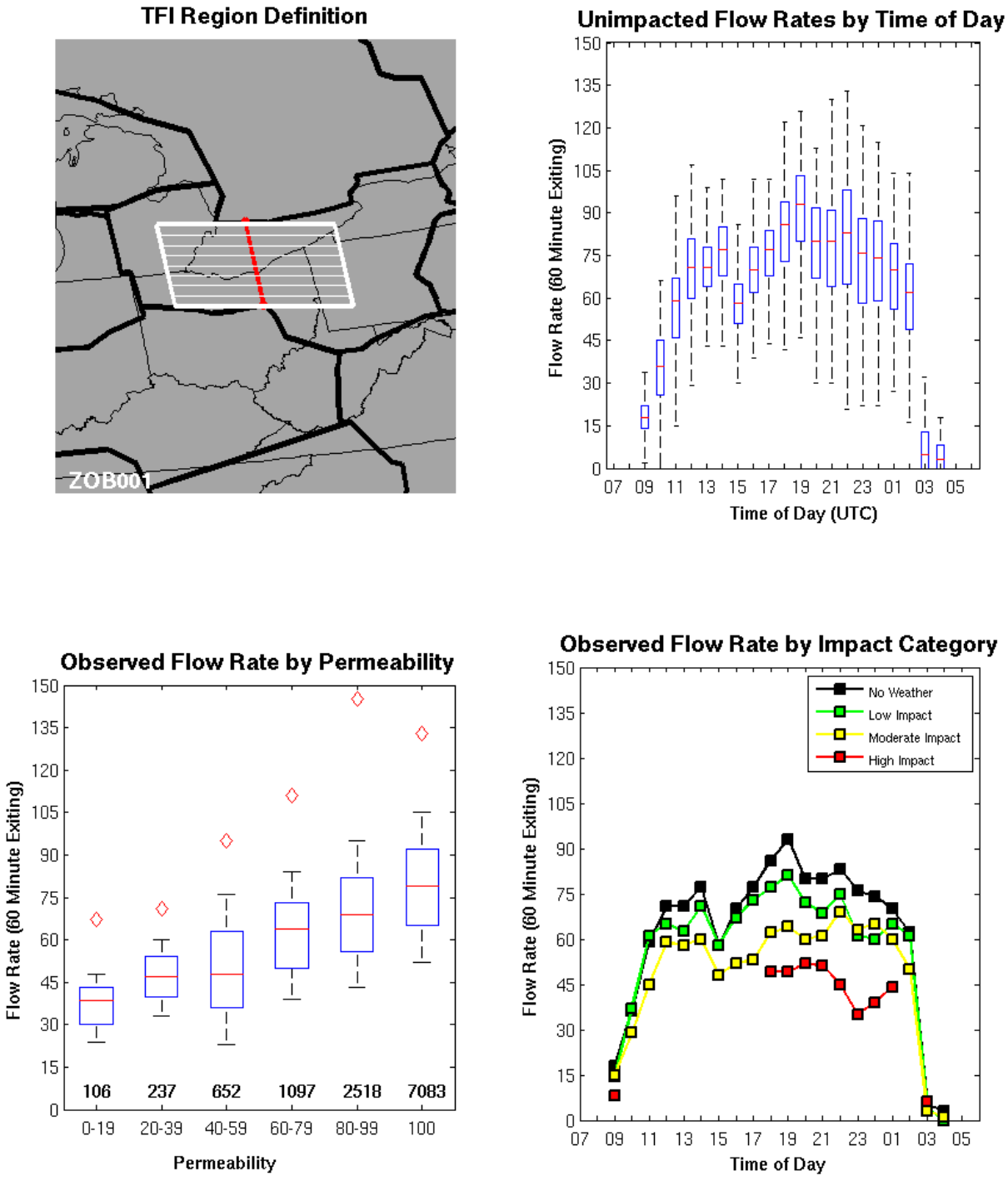

Figure A-13. Traffic Flow Impact region ZOB001: East-west traffic flow through the ZOB ARTCC over northern Ohio and Lake Ontario.

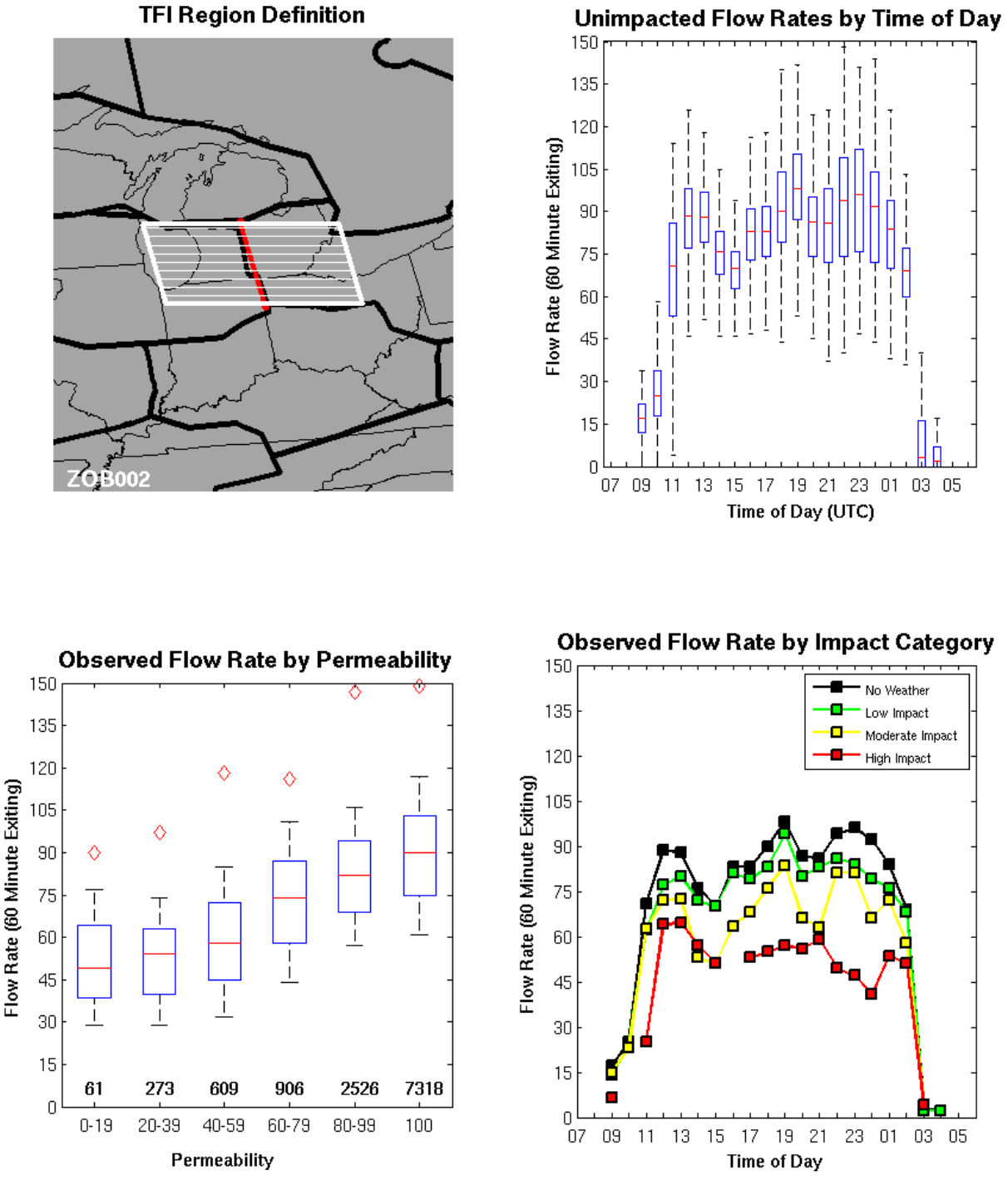

Figure A-14. Traffic Flow Impact region ZOB002: Air traffic transitioning between the ZAU and ZOB ARTCCs over southern Michigan and northern Indiana/Ohio border.

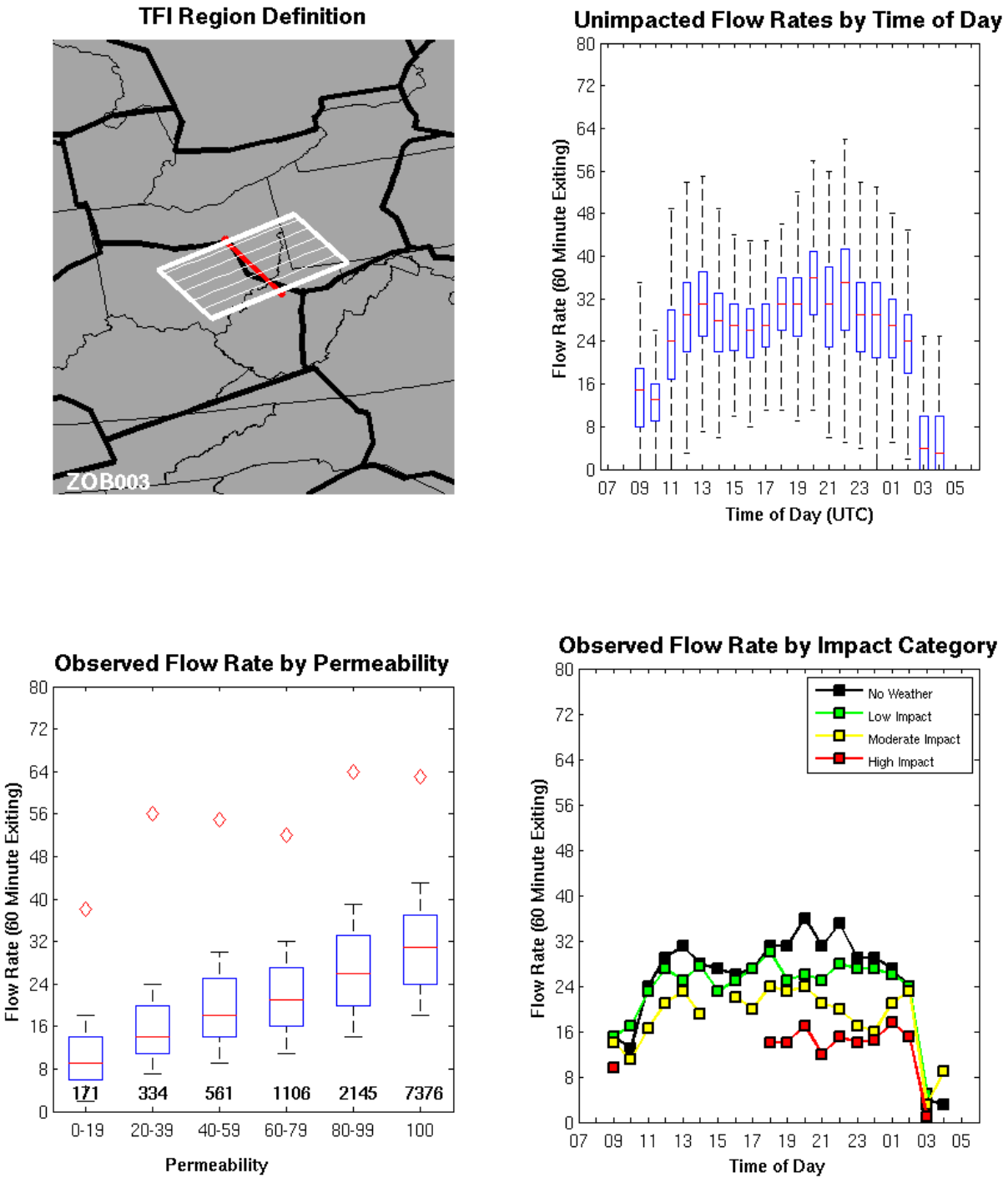

Figure A-15. Traffic Flow Impact region ZOB003: Air traffic transitioning between the ZID and ZOB ARTCCs over southeastern Ohio.

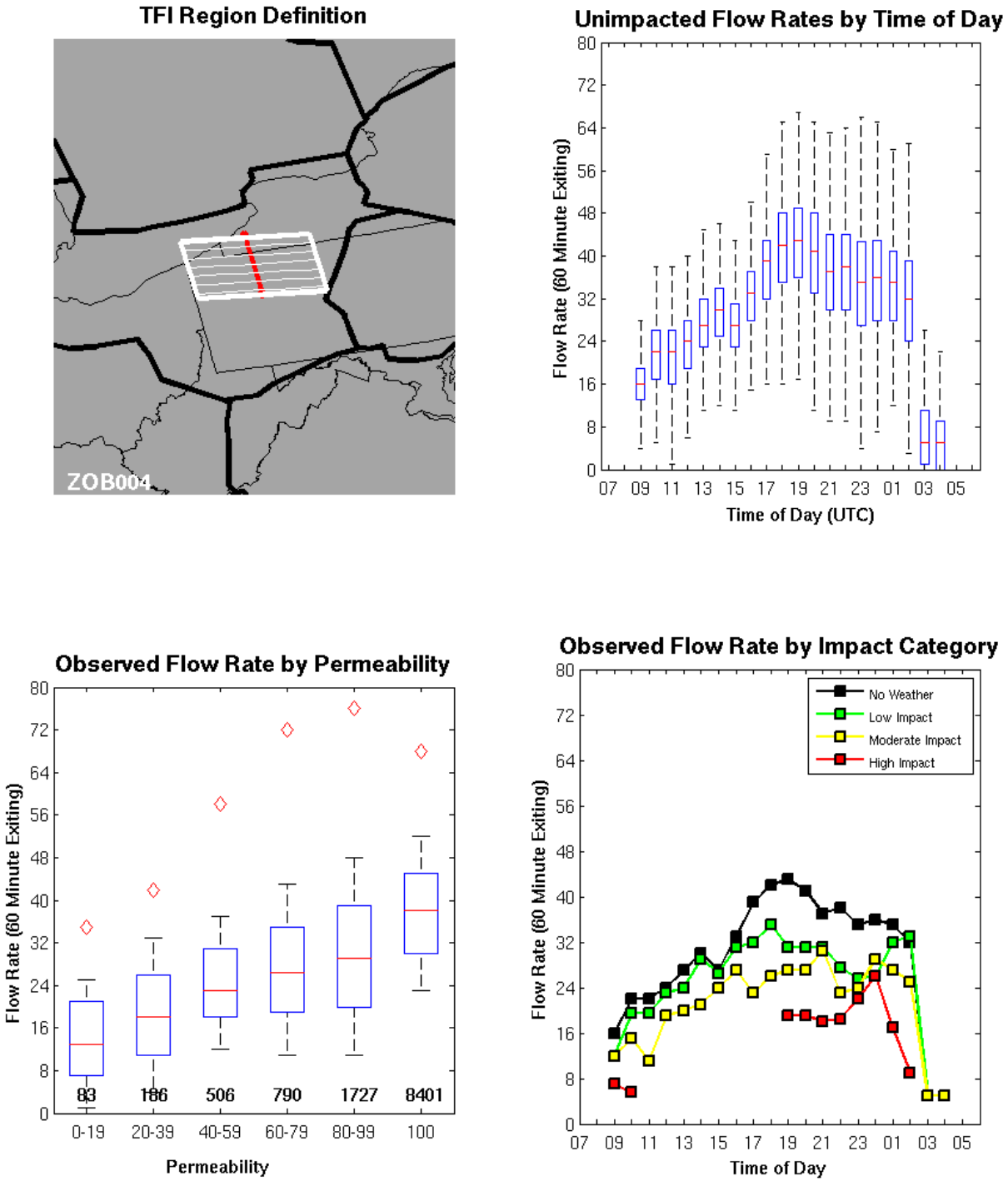

Figure A-16. Traffic Flow Impact region ZOB004: East-west flow on the eastern side of ZOB over northwest Pennsylvania. This flow is primarily destined for the NY metro airports.

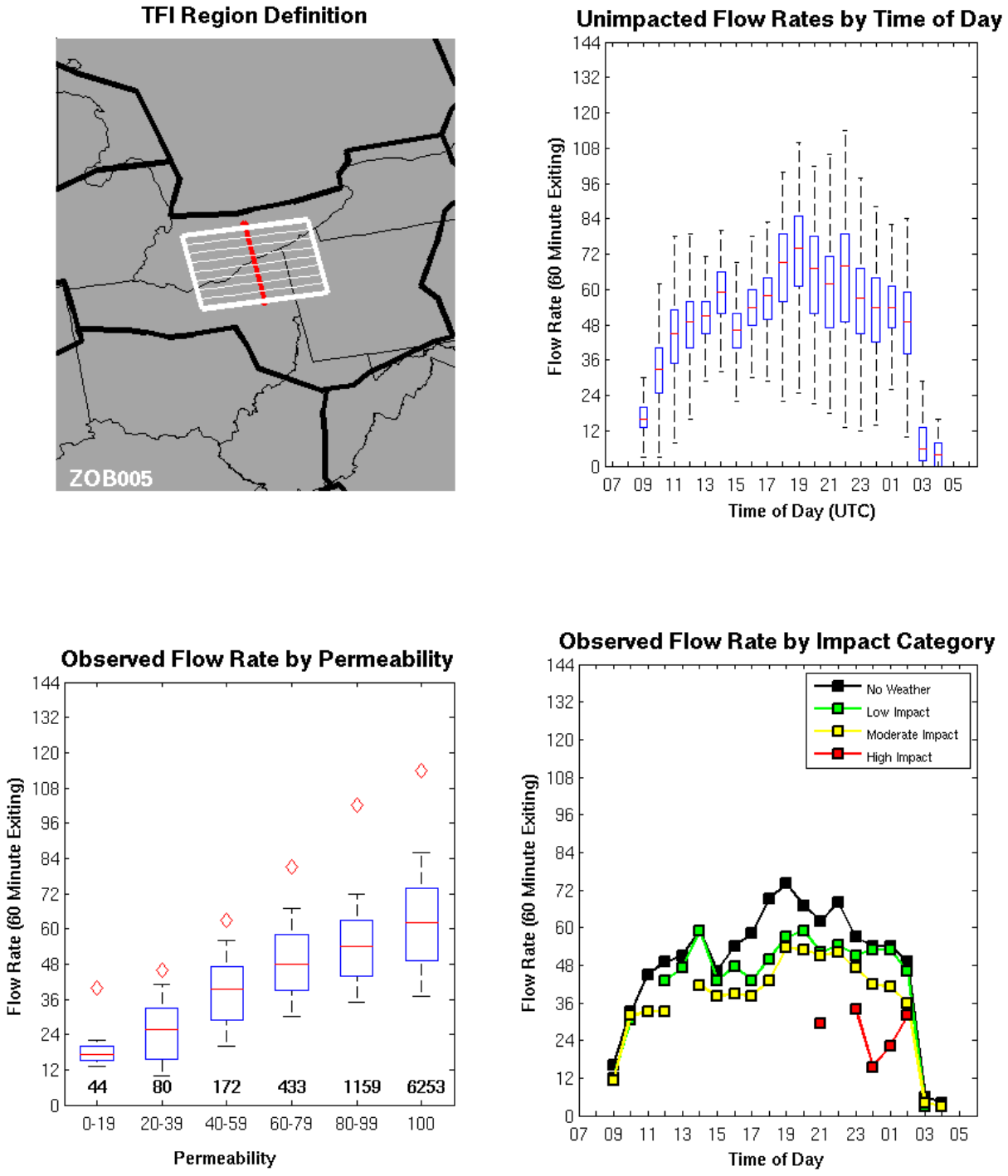

Figure A-17. Traffic Flow Impact region ZOB005: East-west flow on the eastern side of ZOB over northeast Ohio. This flow is primarily destined for the NY metro airports.

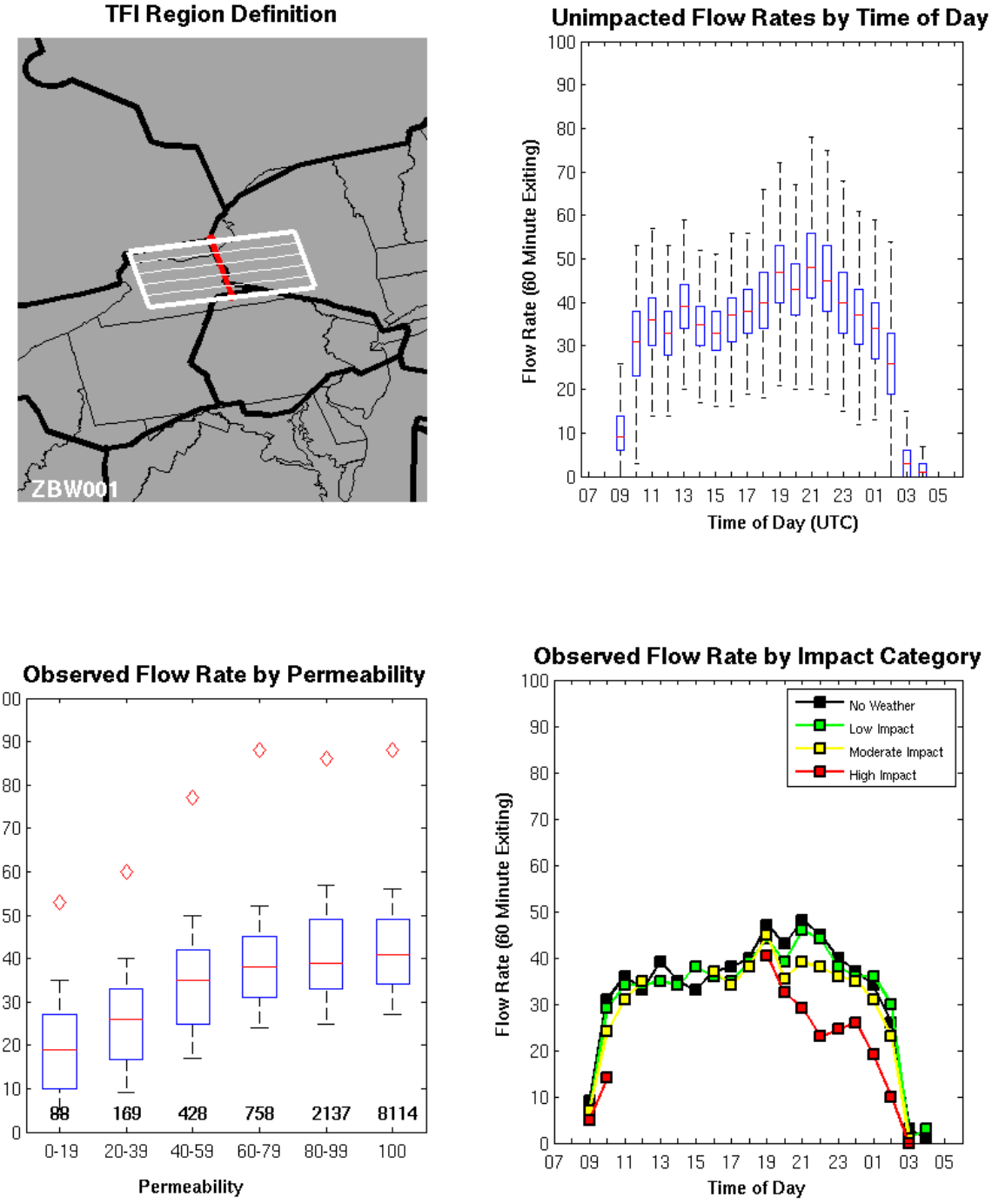

Figure A-18. Traffic Flow Impact region ZBW001: Air traffic transitioning between the ZOB and ZBW ARTCCs over western New York. This air traffic is primarily destined for New England, however, often serves as a weather avoiding alternative when ZNY is impacted.

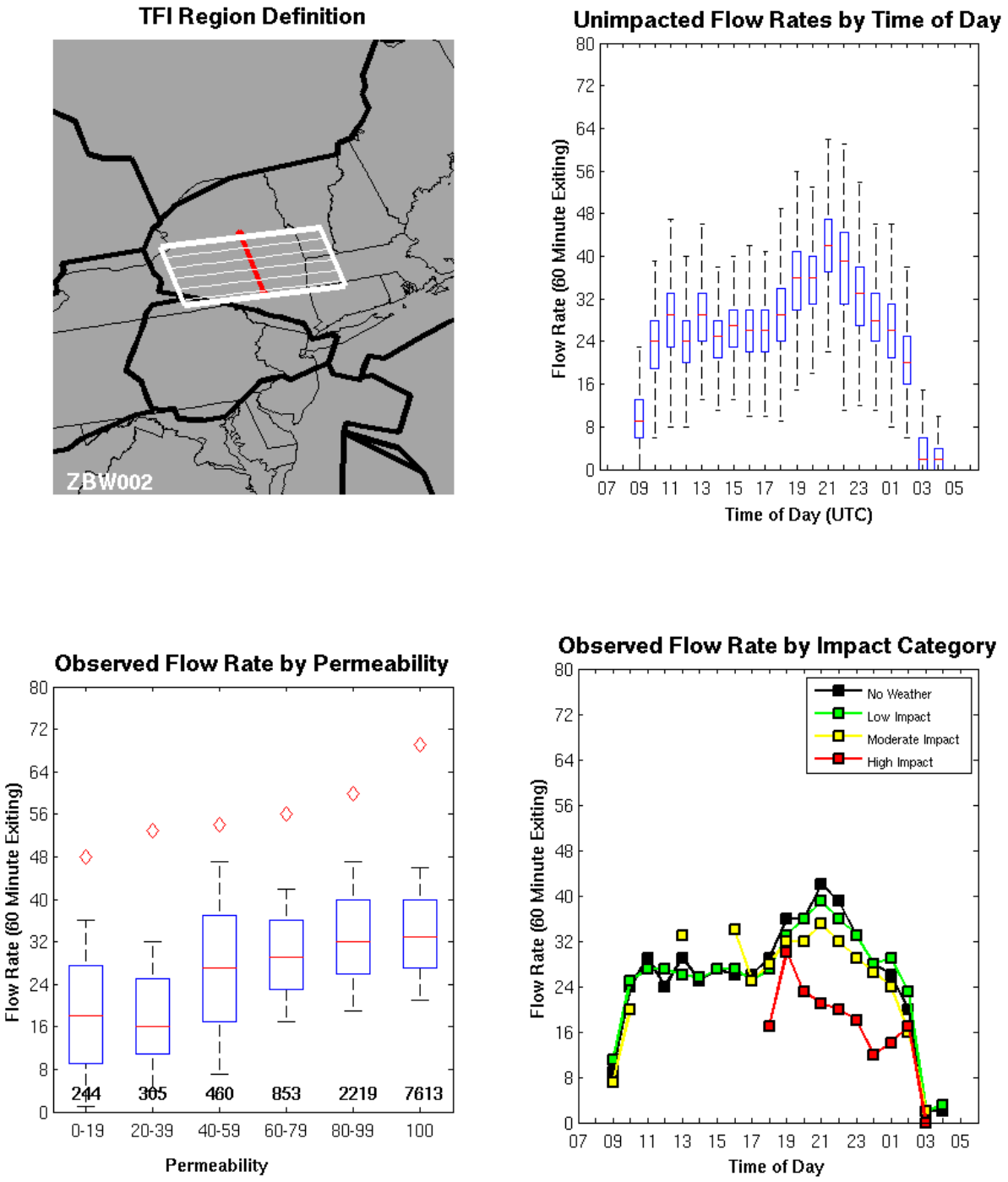

Figure A-19. Traffic Flow Impact region ZBW002: Air traffic flow in the ZBW ARTCC over eastern New York. This air traffic is primarily destined for New England, however, often serves as a weather avoiding alternative when ZNY is impacted.

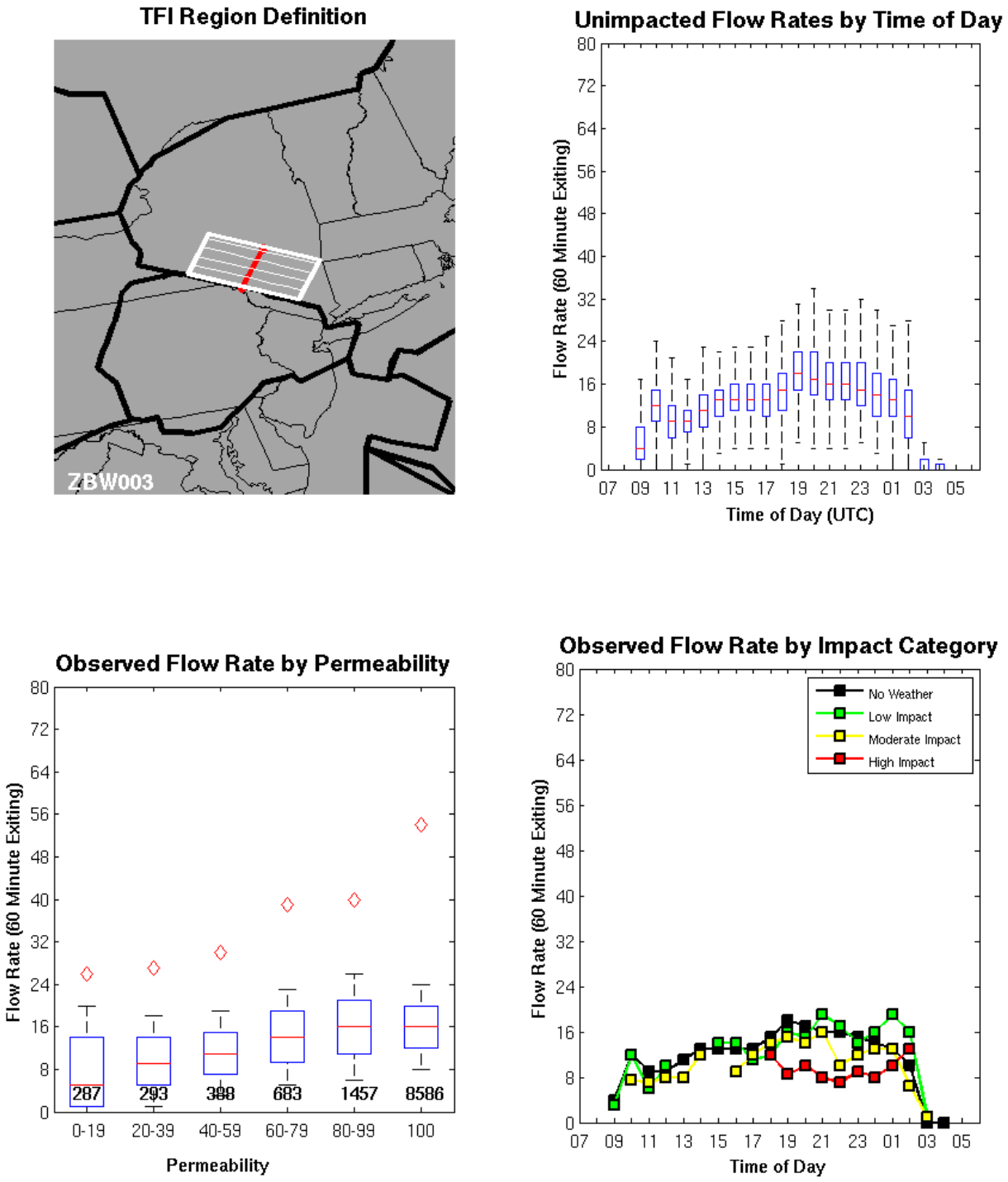

Figure A-20. Traffic Flow Impact region ZBW003: Air traffic flow in the ZBW ARTCC over southeastern New York. This air space often serves as a weather avoiding alternative when ZNY is impacted.

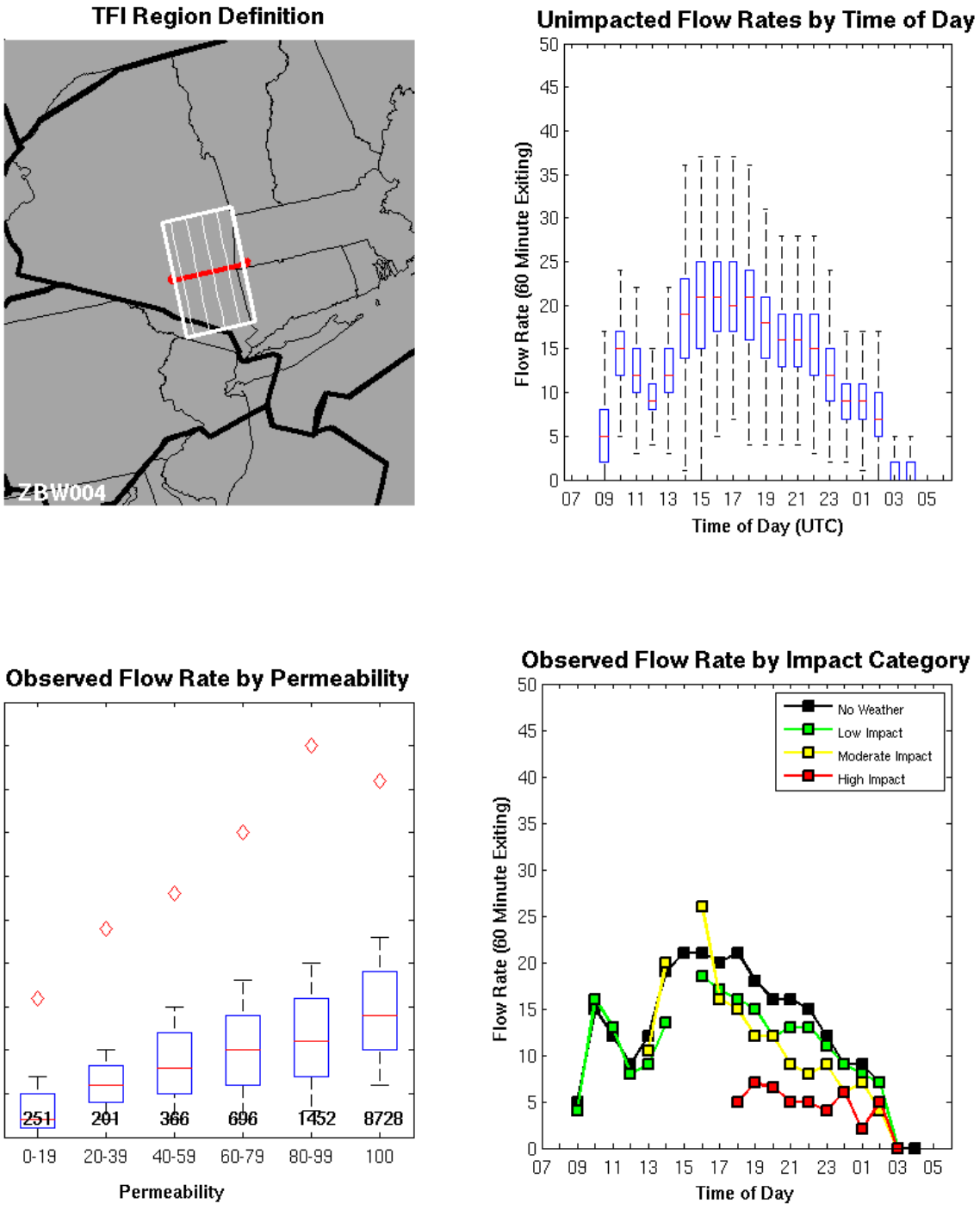

Figure A-21. Traffic Flow Impact region ZBW004: Air traffic flow in the ZBW ARTCC over southern New York. This air space serves as an arrival stream from the north for the metro NY airports and often serves as a weather avoiding alternative for the western arrival when ZNY is impacted.

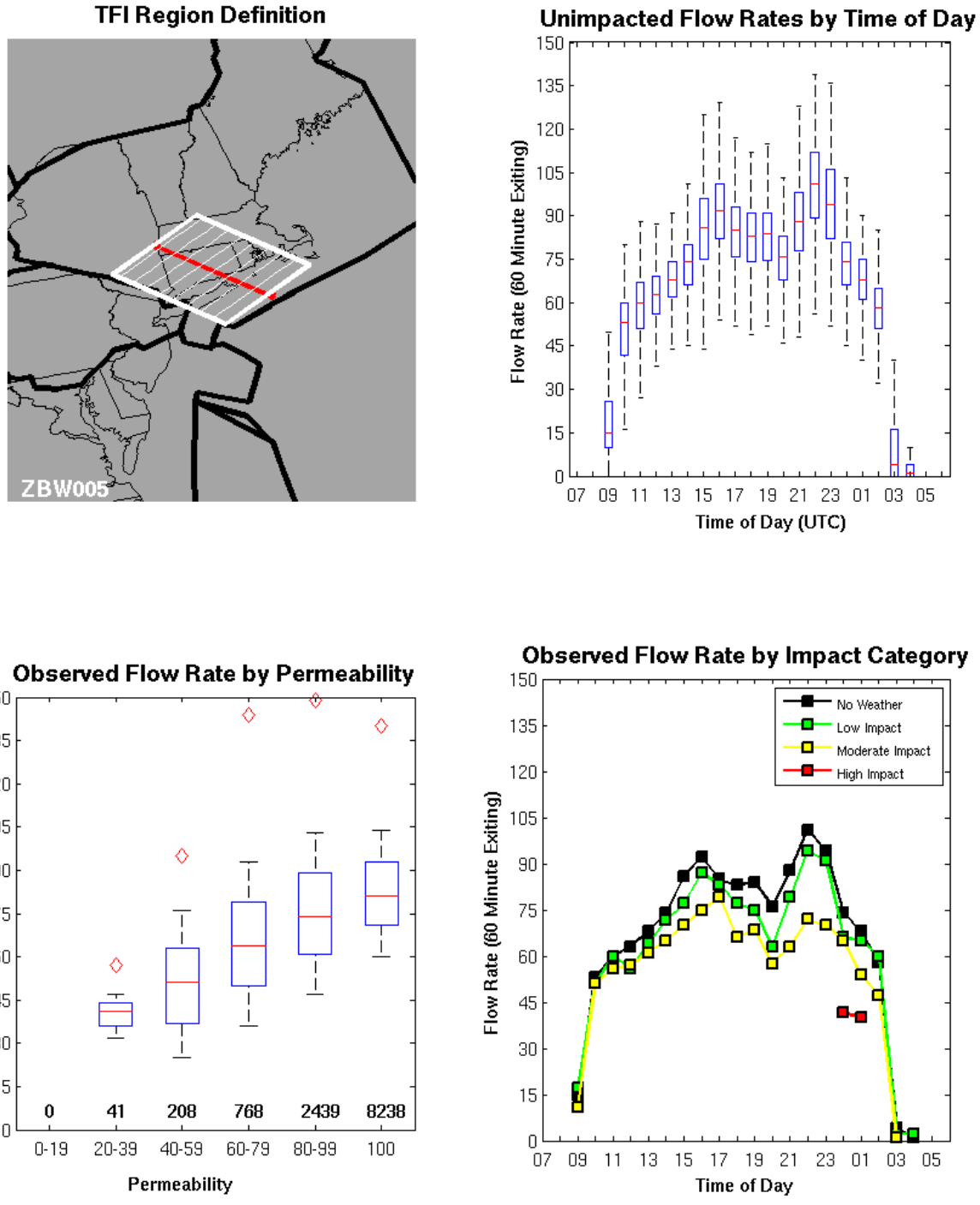

Figure A-22. Traffic Flow Impact region ZBW005: Air traffic flow over southern New England. This air space serves as an arrival stream from the northeast for the metro NY airports.

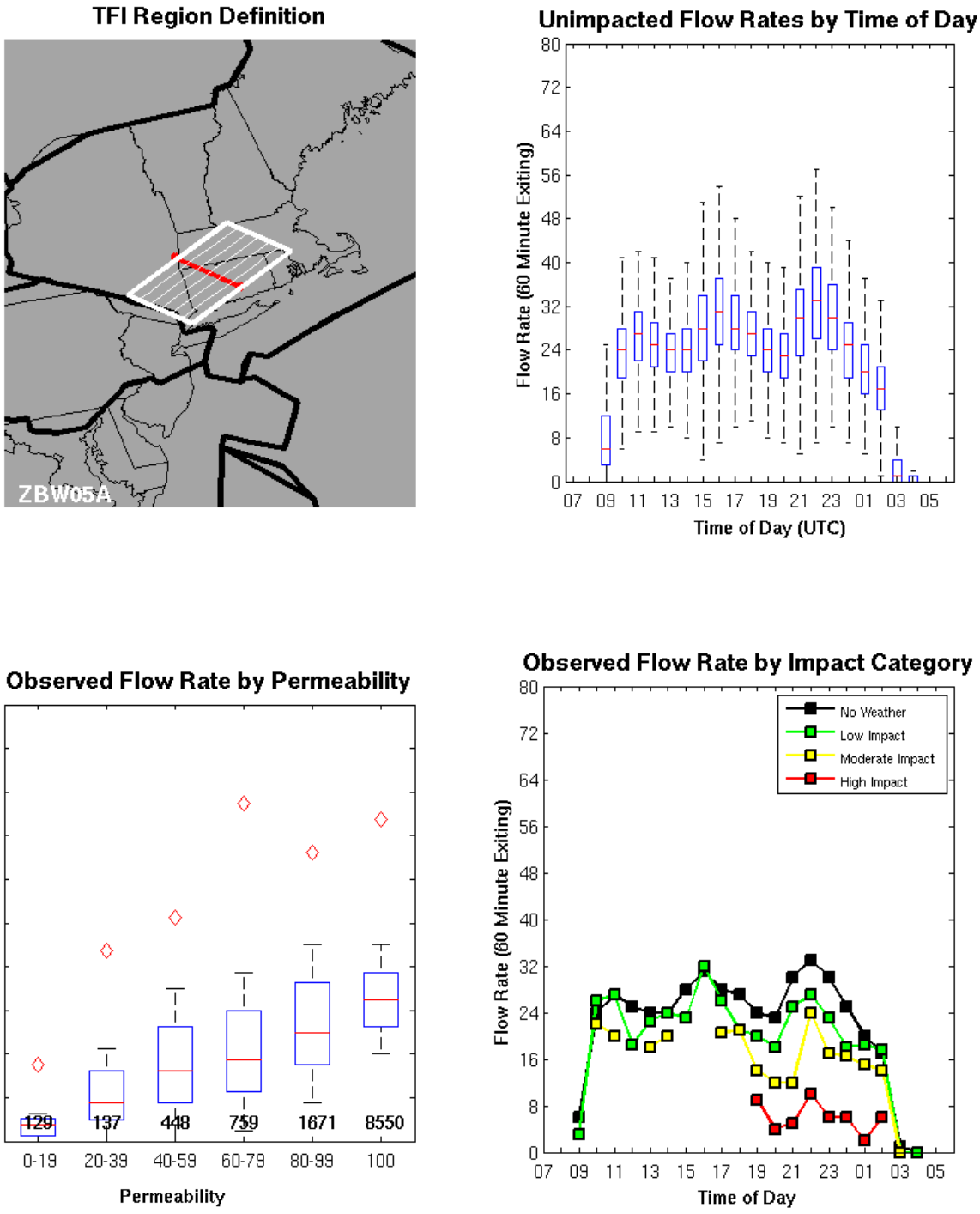

Figure A-23. Traffic Flow Impact region ZBW05A: Air traffic flow over southern New England. This air space serves as an arrival stream from the northeast for the metro NY airports.

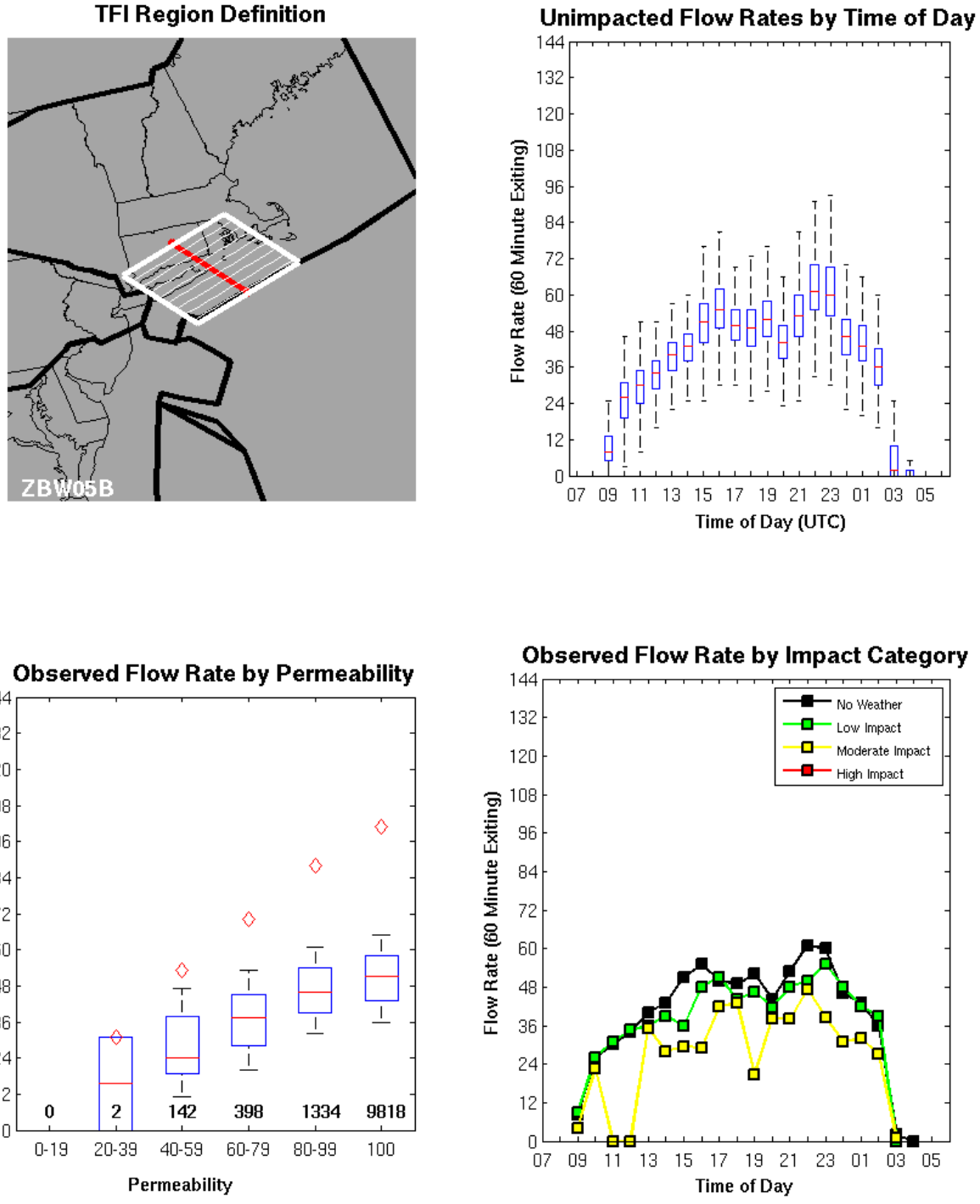

Figure A-24. Traffic Flow Impact region ZBW05B: Air traffic flow over southern New England. This air space serves as an arrival stream from the northeast for the metro NY airports.

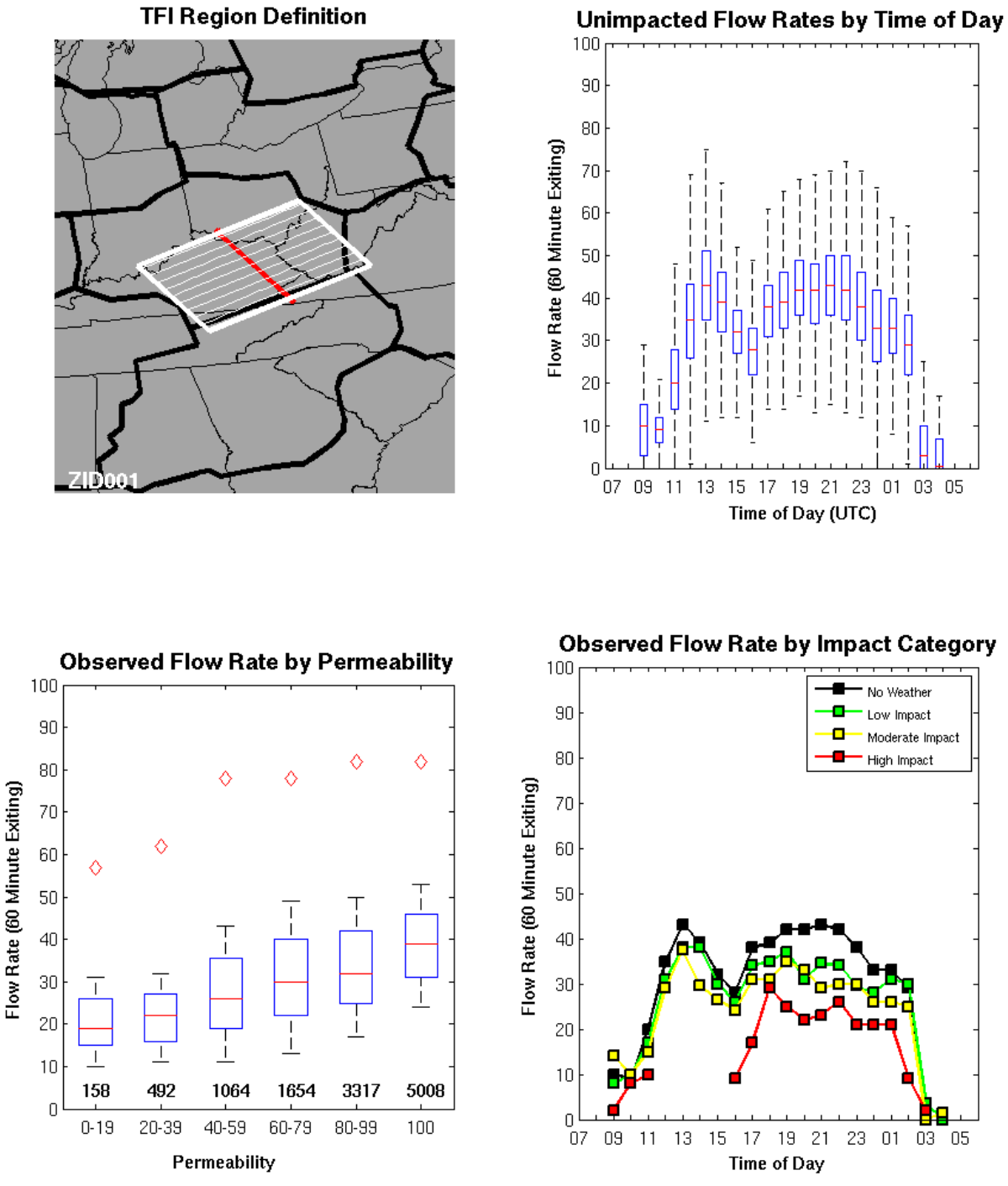

Figure A-25. Traffic Flow Impact region ZID001: Traffic flow through the ZID ARTCC primarily between the ZME and ZDC ARTCCs.

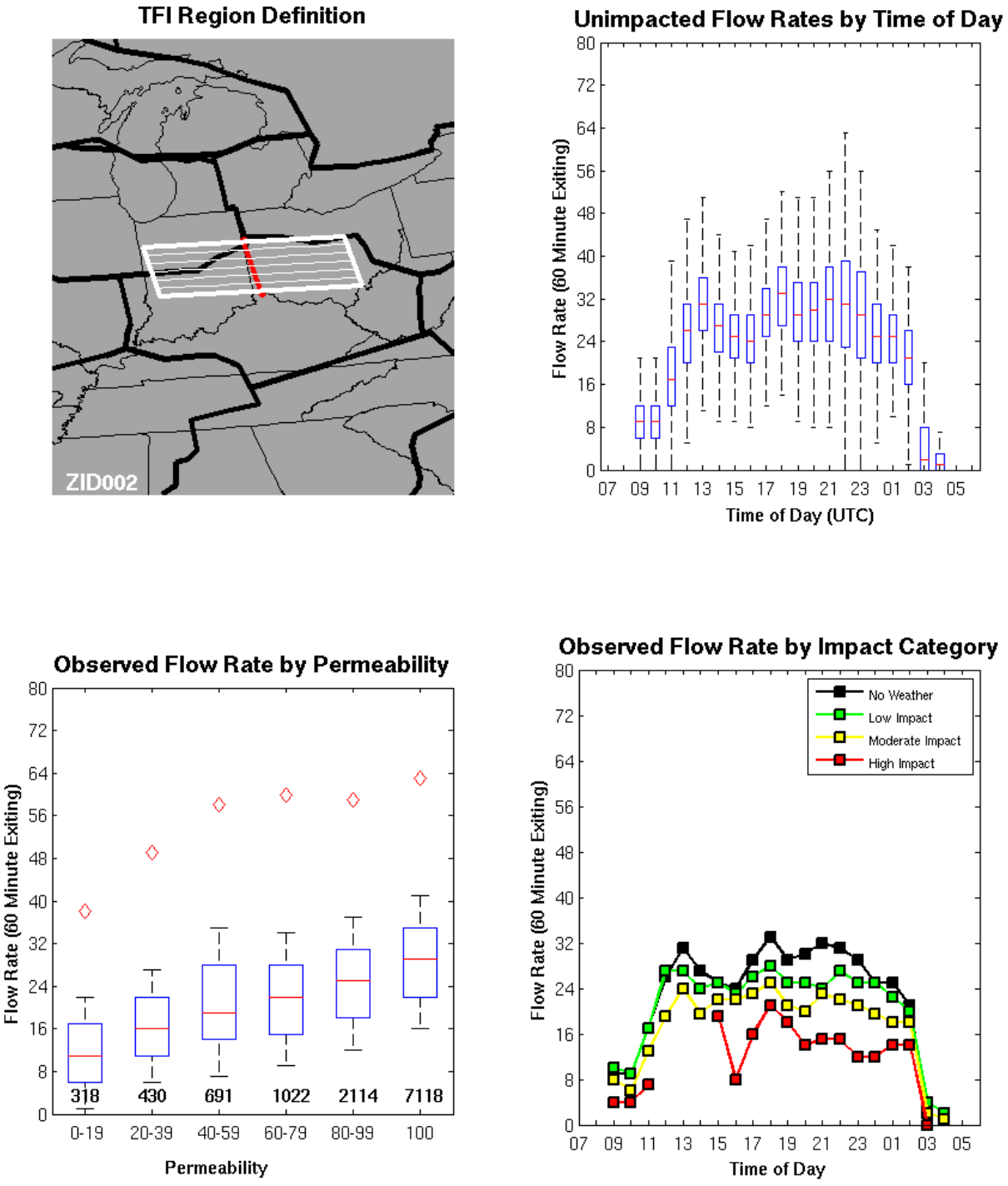

Figure A-26. Traffic Flow Impact region ZID002: Traffic flow through the northern half of ZID over the southern Indiana/Ohio border.

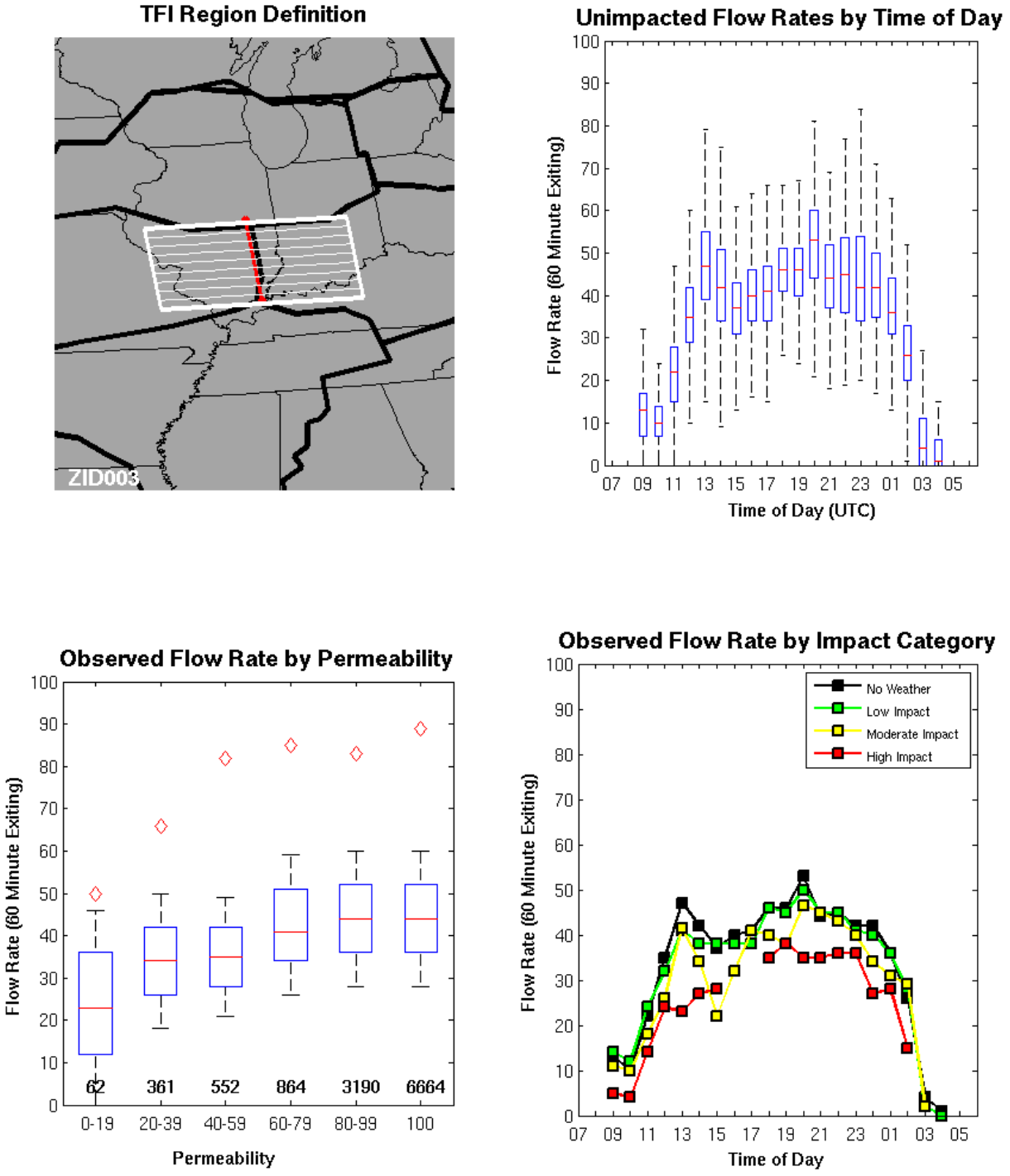

Figure A-27. Traffic Flow Impact region ZID003:Traffic flow transitioning between the ZKC and ZID ARTCCs over southern Illinois.

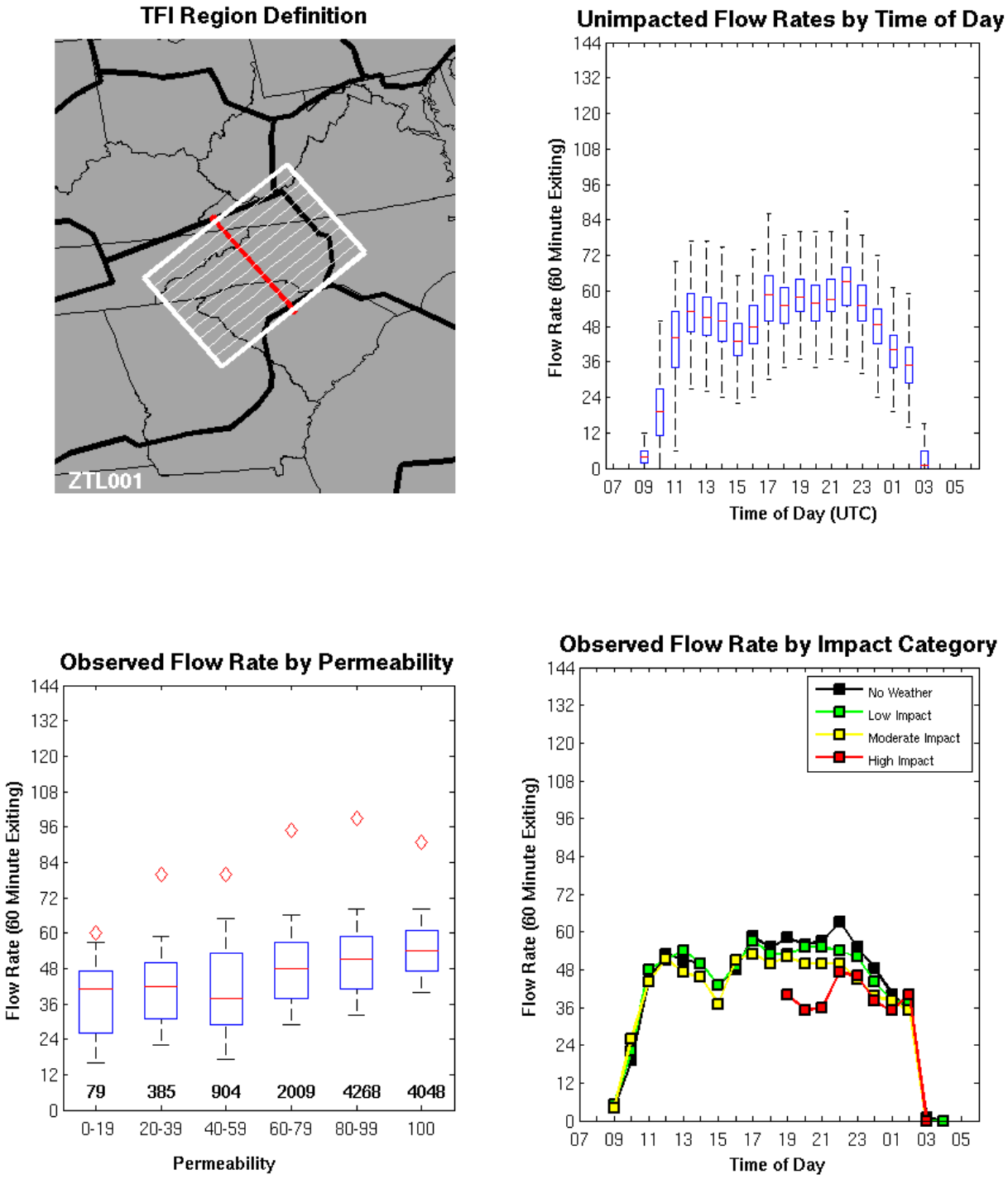

Figure A-28. Traffic Flow Impact region ZTL001: Traffic flow transitioning between ZTL and ZDC over western Virginia.

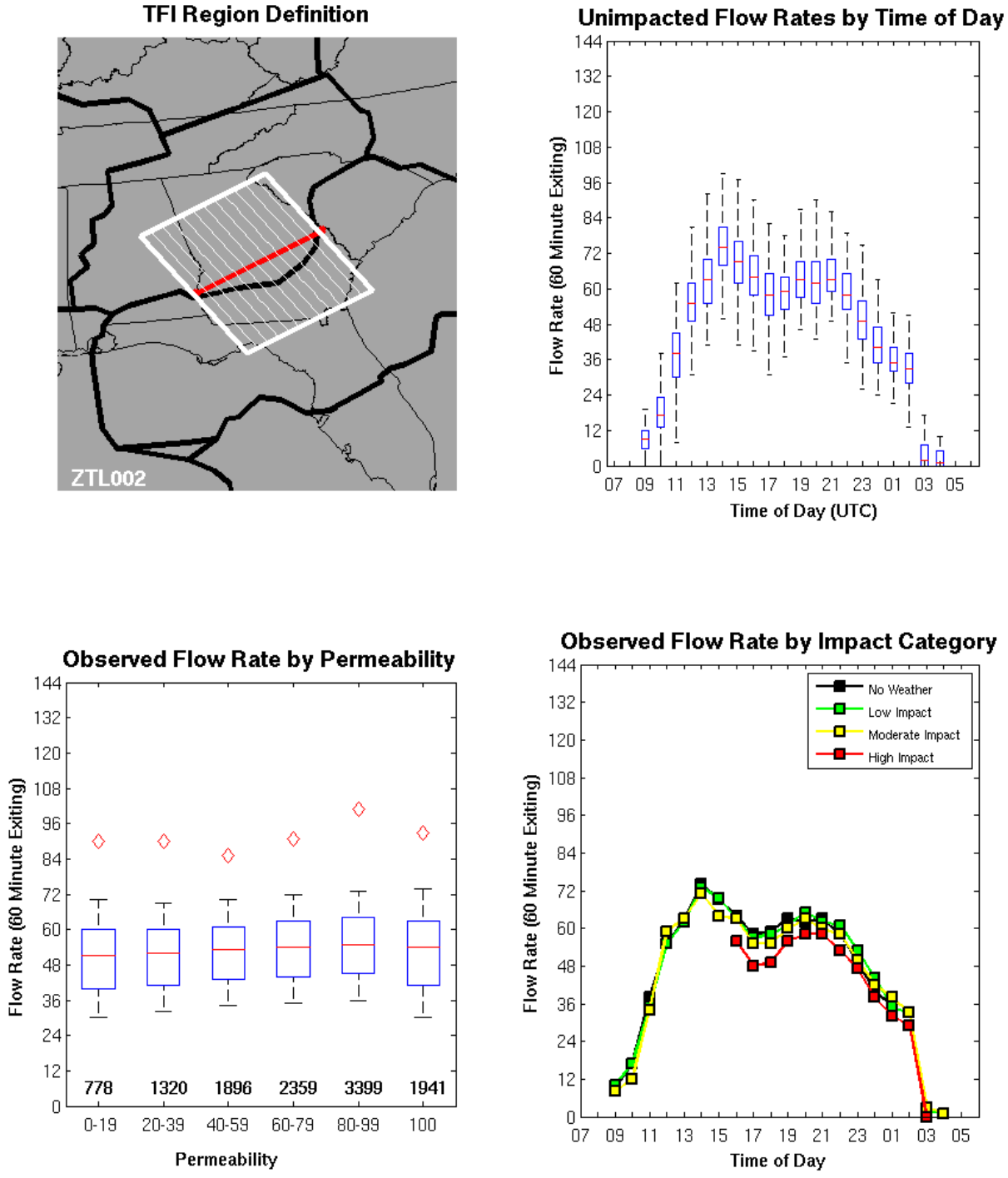

Figure A-29. Traffic Flow Impact region ZTL002: Traffic flow transitioning between the ZTL and ZJX ARTCCs. Traffic is primarily heading for Florida.

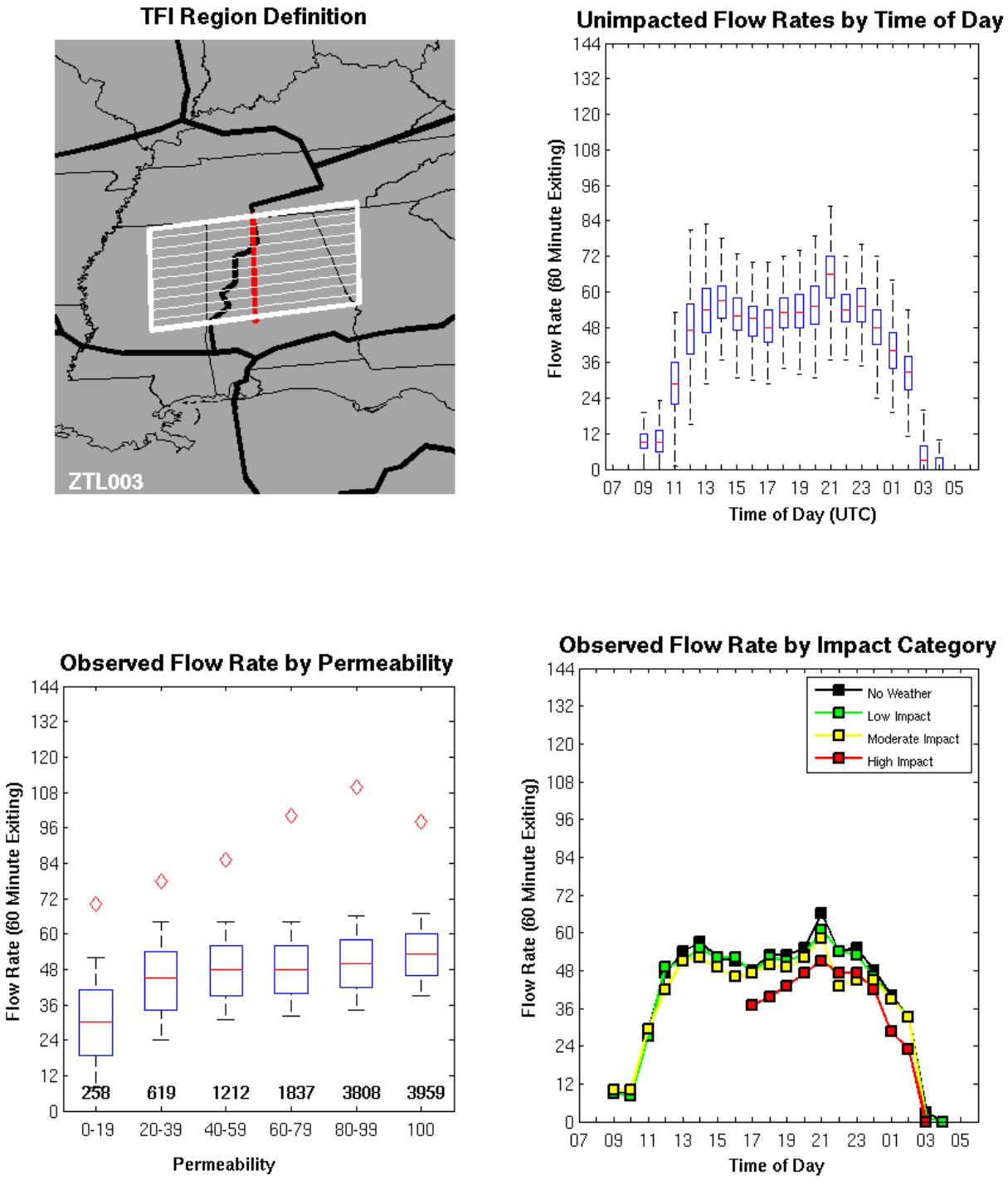

Figure A-30. Traffic Flow Impact region ZTL003: Traffic transitioning between the ZTL and ZME ARTCCs over Alabama.

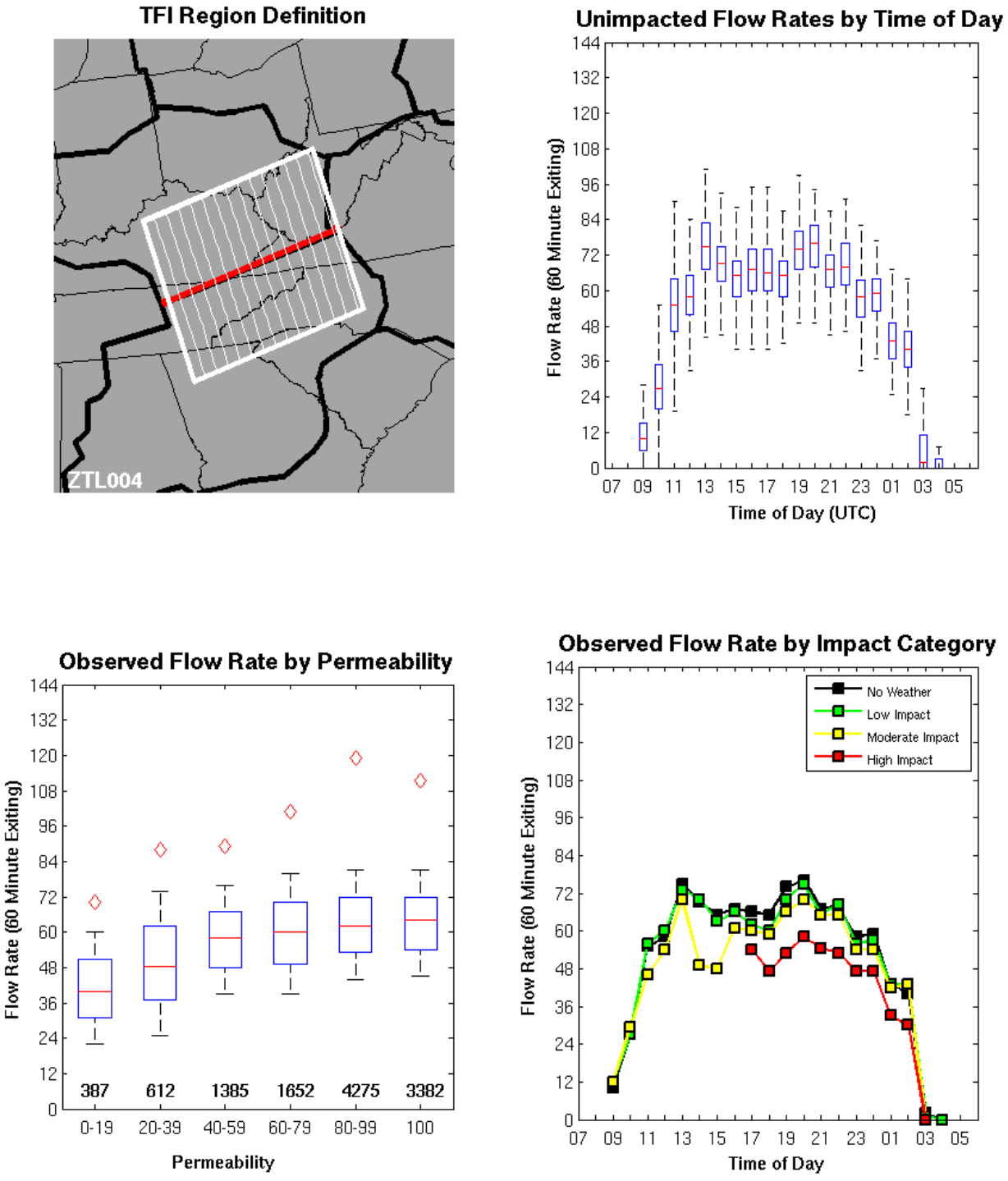

Figure A-31. Traffic Flow Impact region ZTL004: Traffic transitioning between the ZTL and ZID ARTCCs.

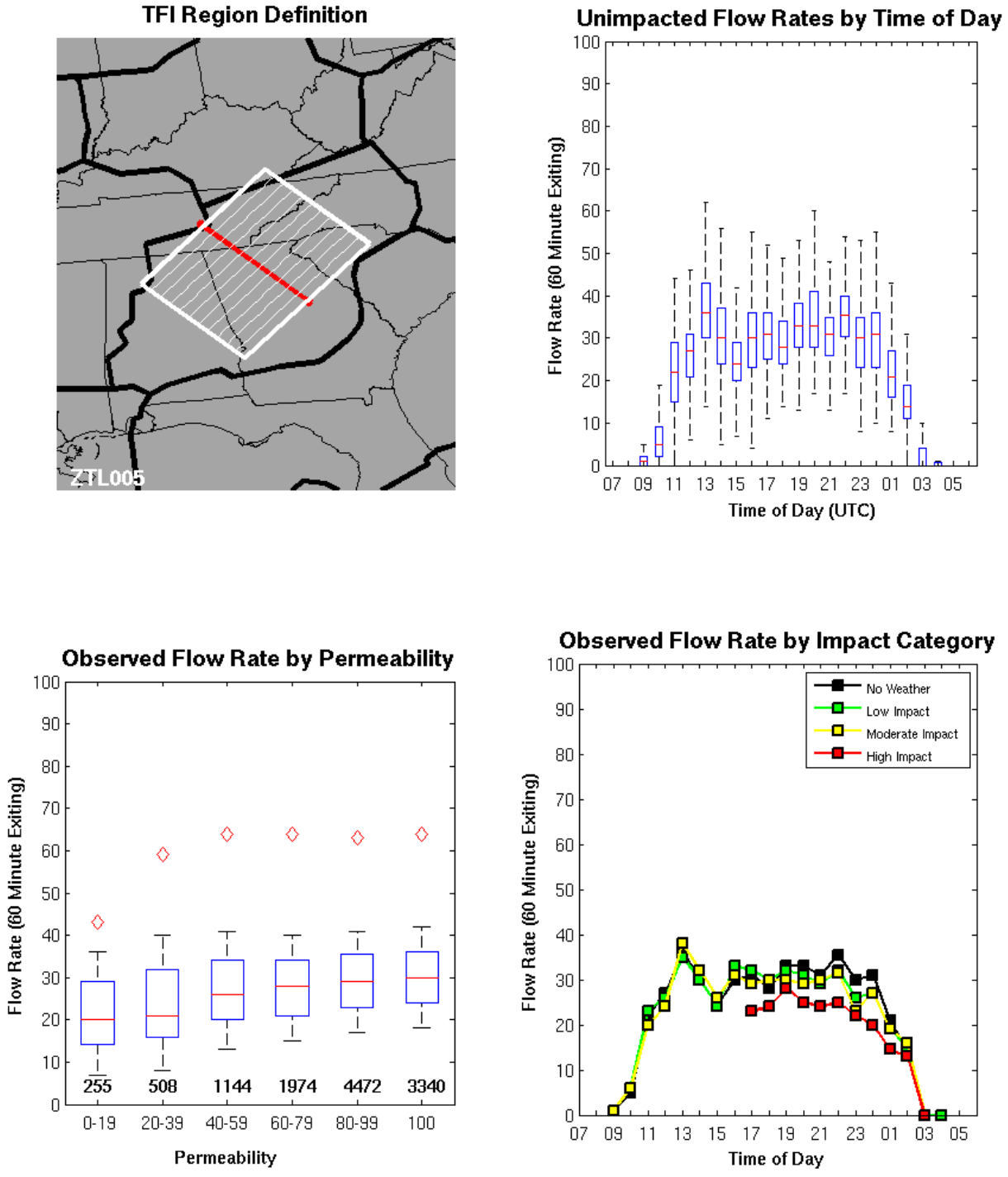

Figure A-32. Traffic Flow Impact region ZTL005: Traffic flowing through the Atlanta ARTCC in a northeast-southwest direction.

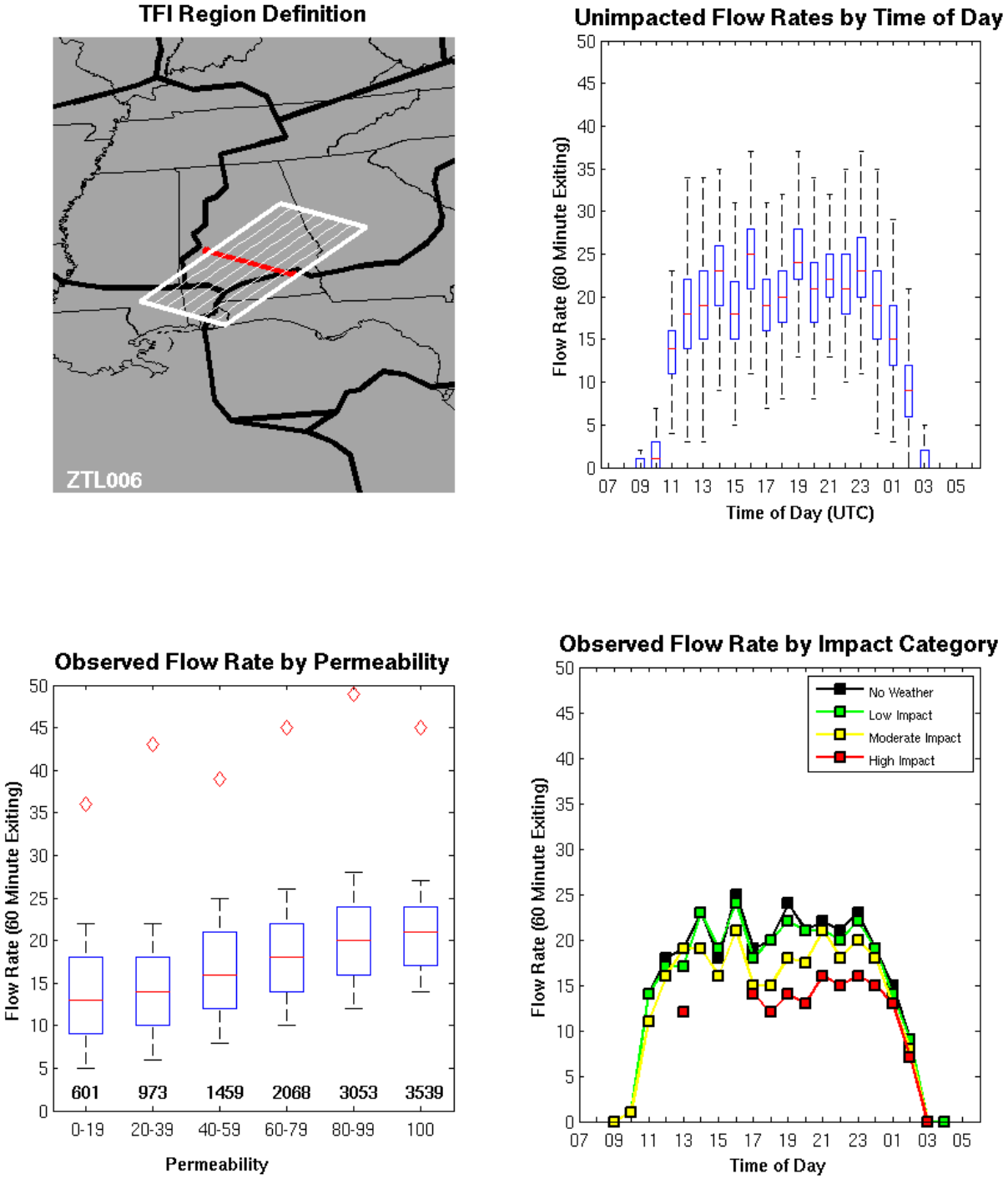

Figure A-33. Traffic Flow Impact region ZTL006: Traffic transitioning between the ZTL and ZHU ARTCCs over Alabama.

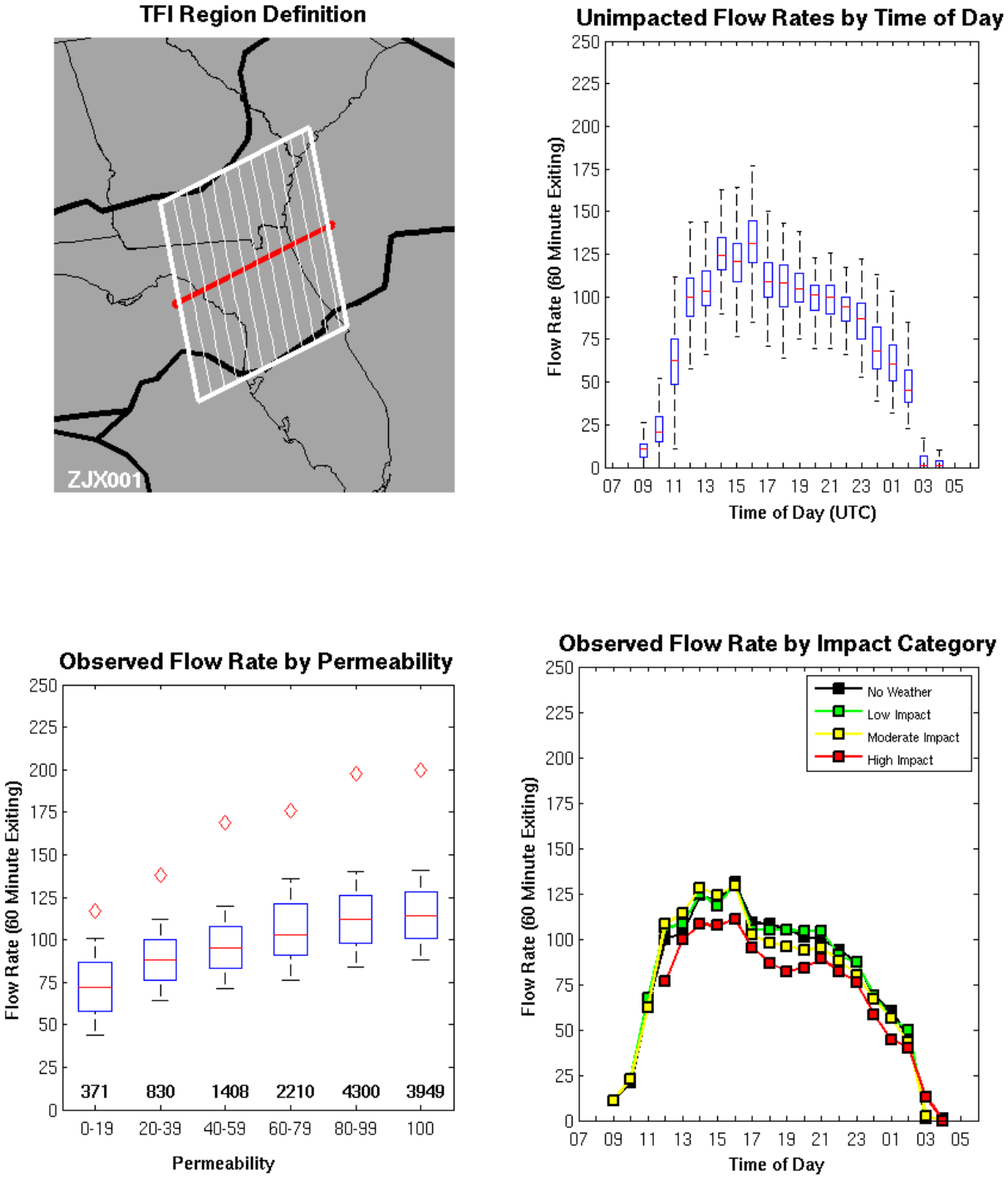

Figure A-34. Traffic Flow Impact region ZJX001: Traffic flowing through the Jacksonville ARTCC over the northern Florida peninsula.

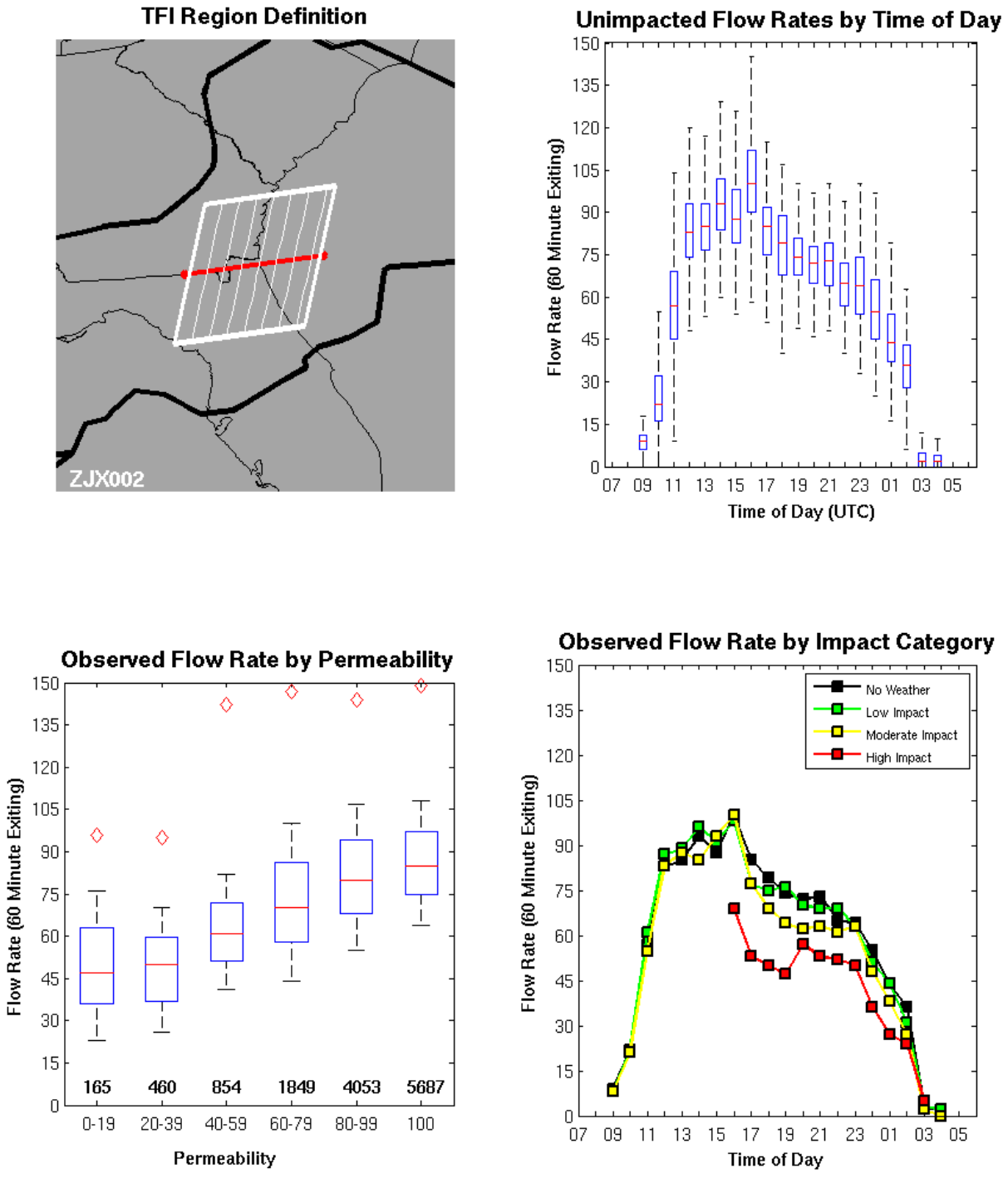

Figure A-35. Traffic Flow Impact region ZJX002: Traffic flowing through the Jacksonville ARTCC over the eastern Florida coast.

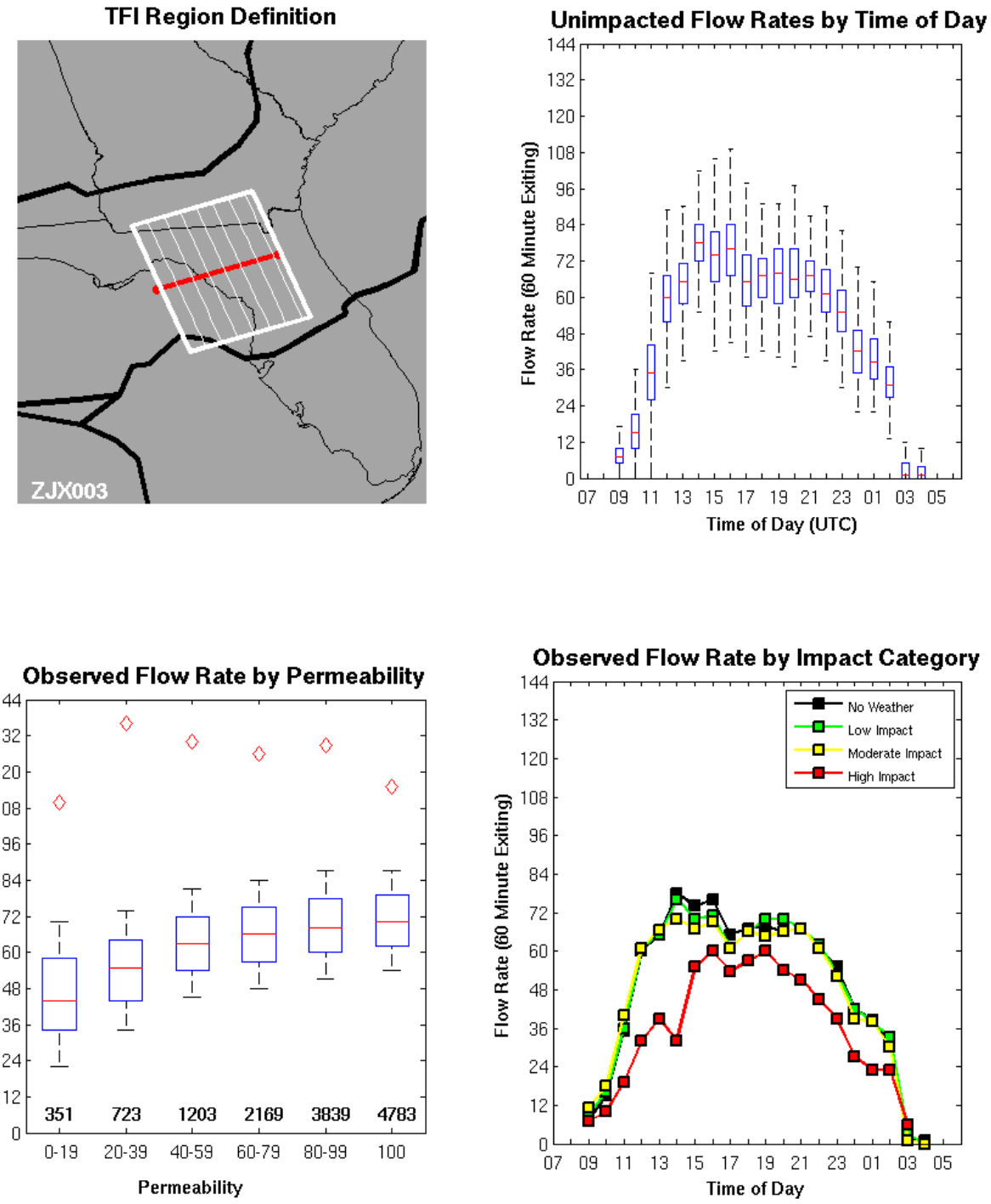

Figure A-36. Traffic Flow Impact region ZJX003: Traffic flowing through the Jacksonville ARTCC over the western Florida coast.

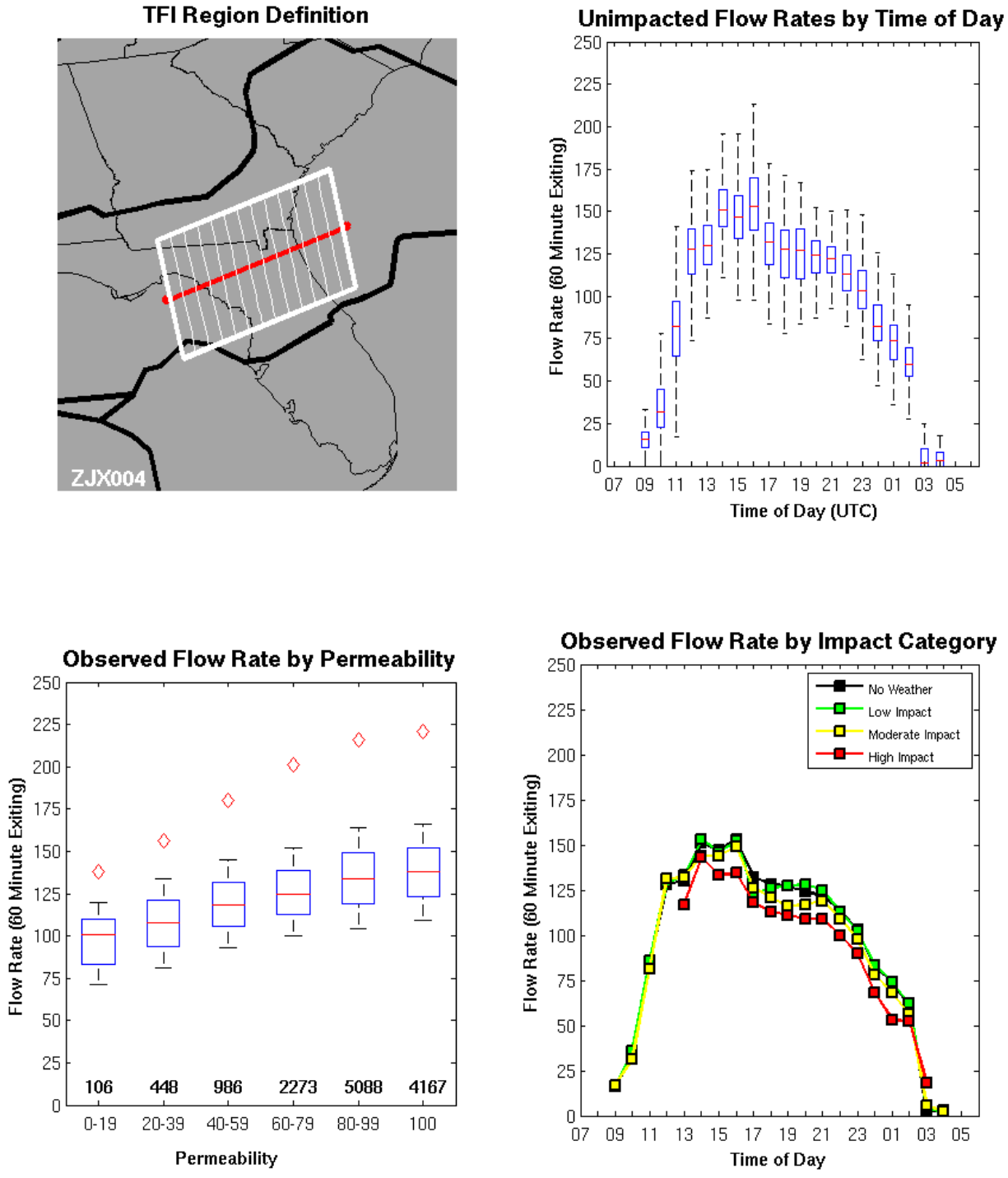

Figure A-37. Traffic Flow Impact region ZJX004: Traffic flowing through the Jacksonville ARTCC over the northern Florida peninsula.

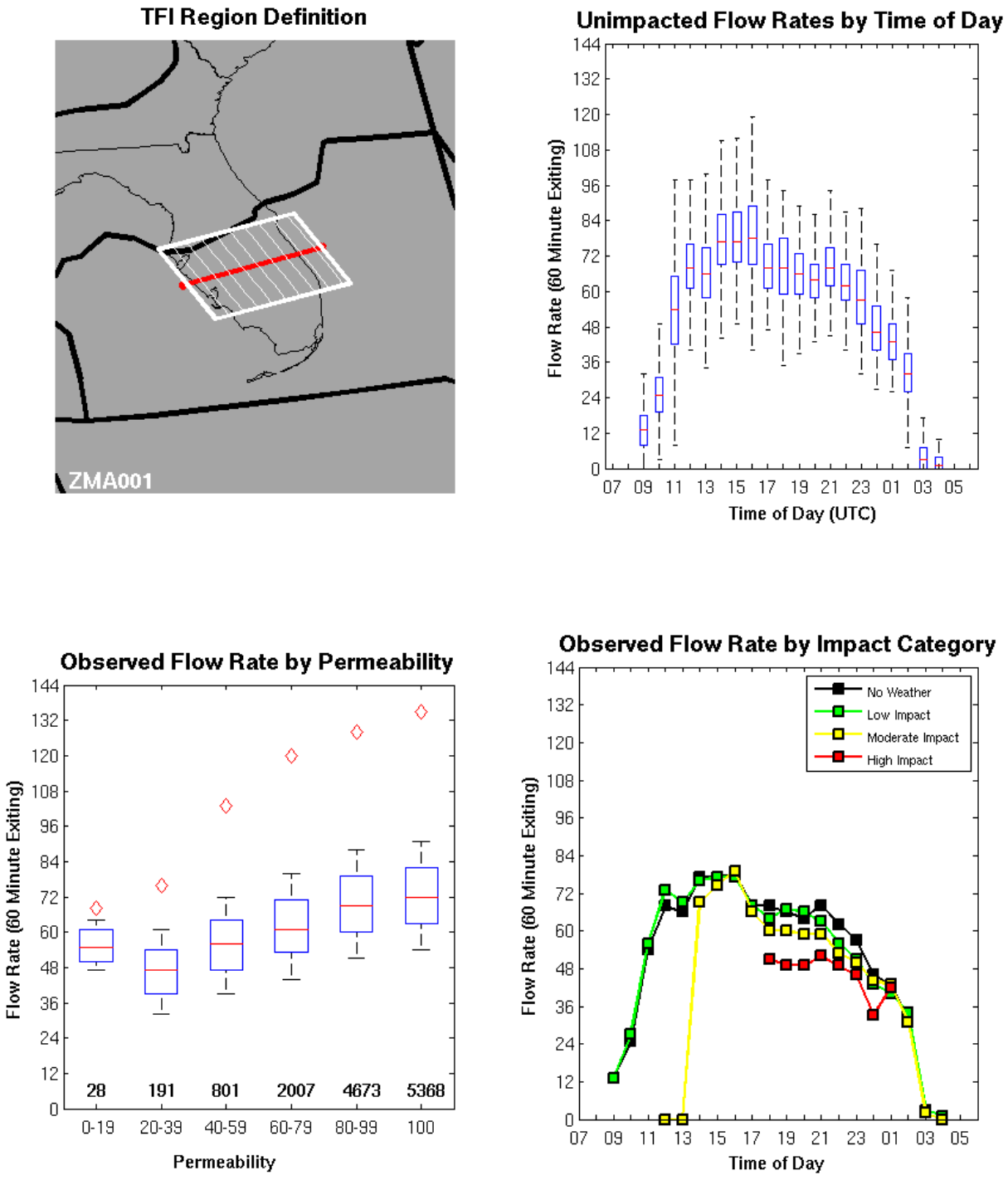

Figure A-38. Traffic Flow Impact region ZMA001: Traffic flowing through the Miami ARTCC over the southern Florida peninsula.

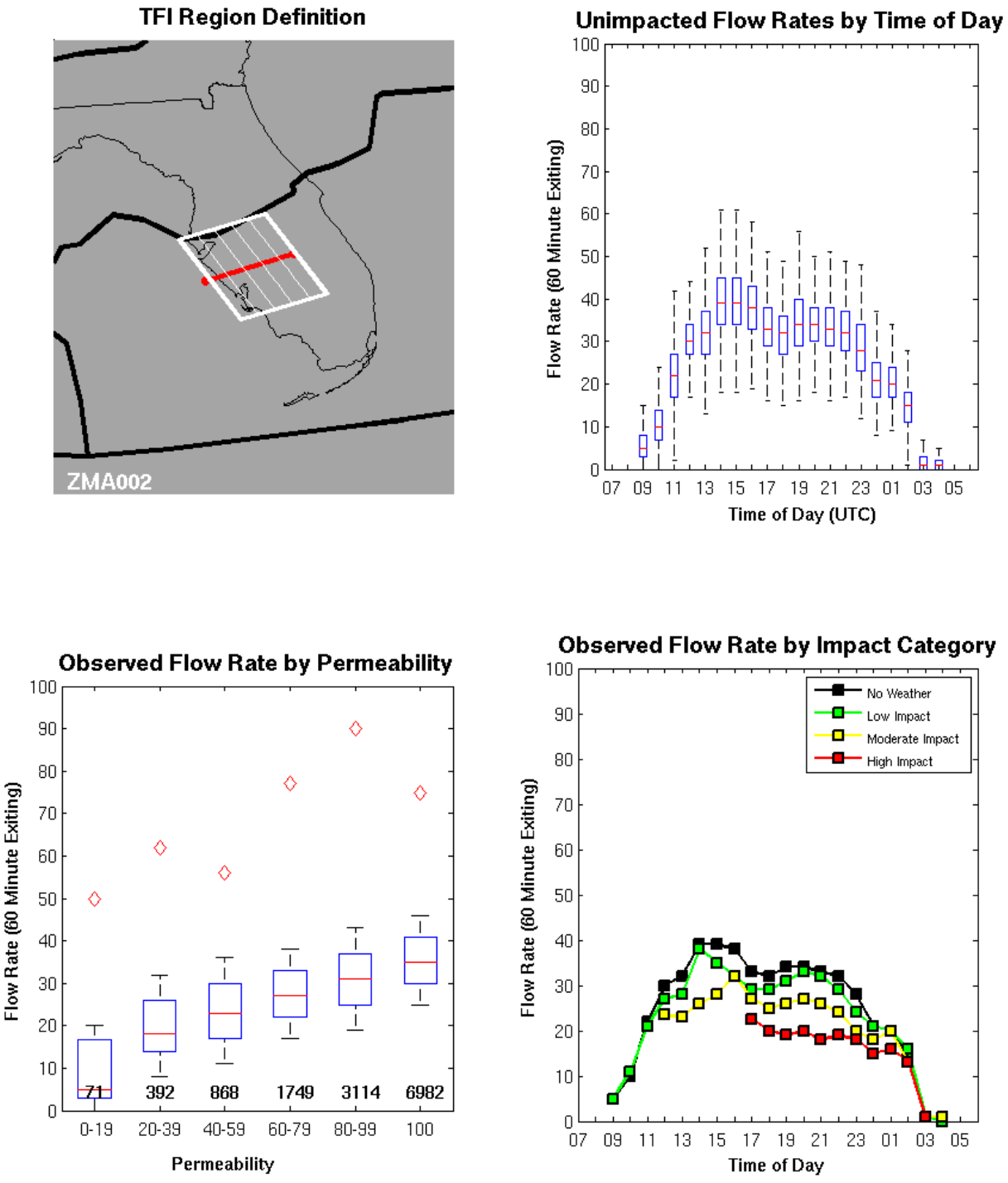

Figure A-39. Traffic Flow Impact region ZMA002: Traffic flowing through the Miami ARTCC over the western Florida coast.

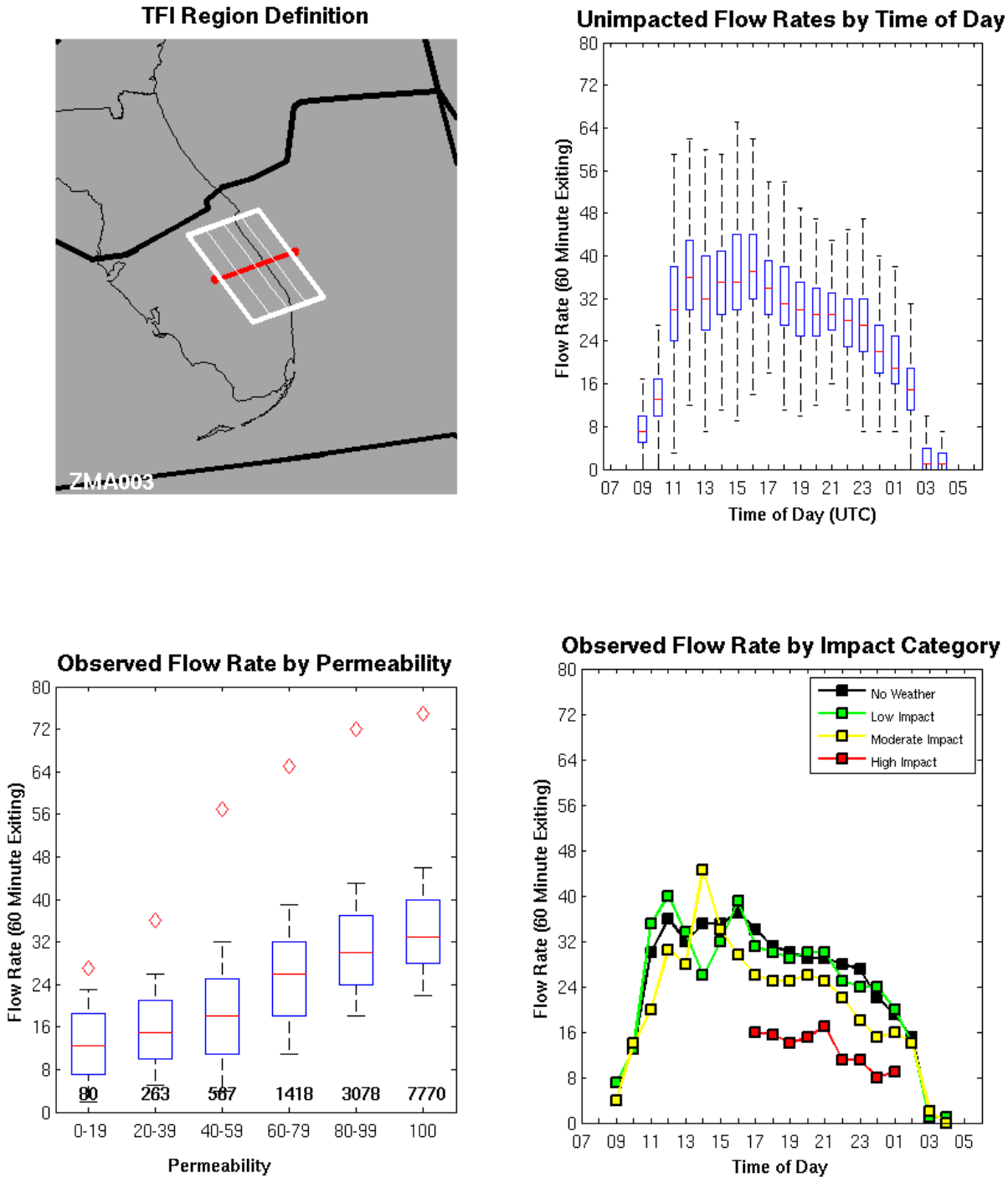

Figure A-40. Traffic Flow Impact region ZMA003: Traffic flowing through the Miami ARTCC over the eastern Florida coast.

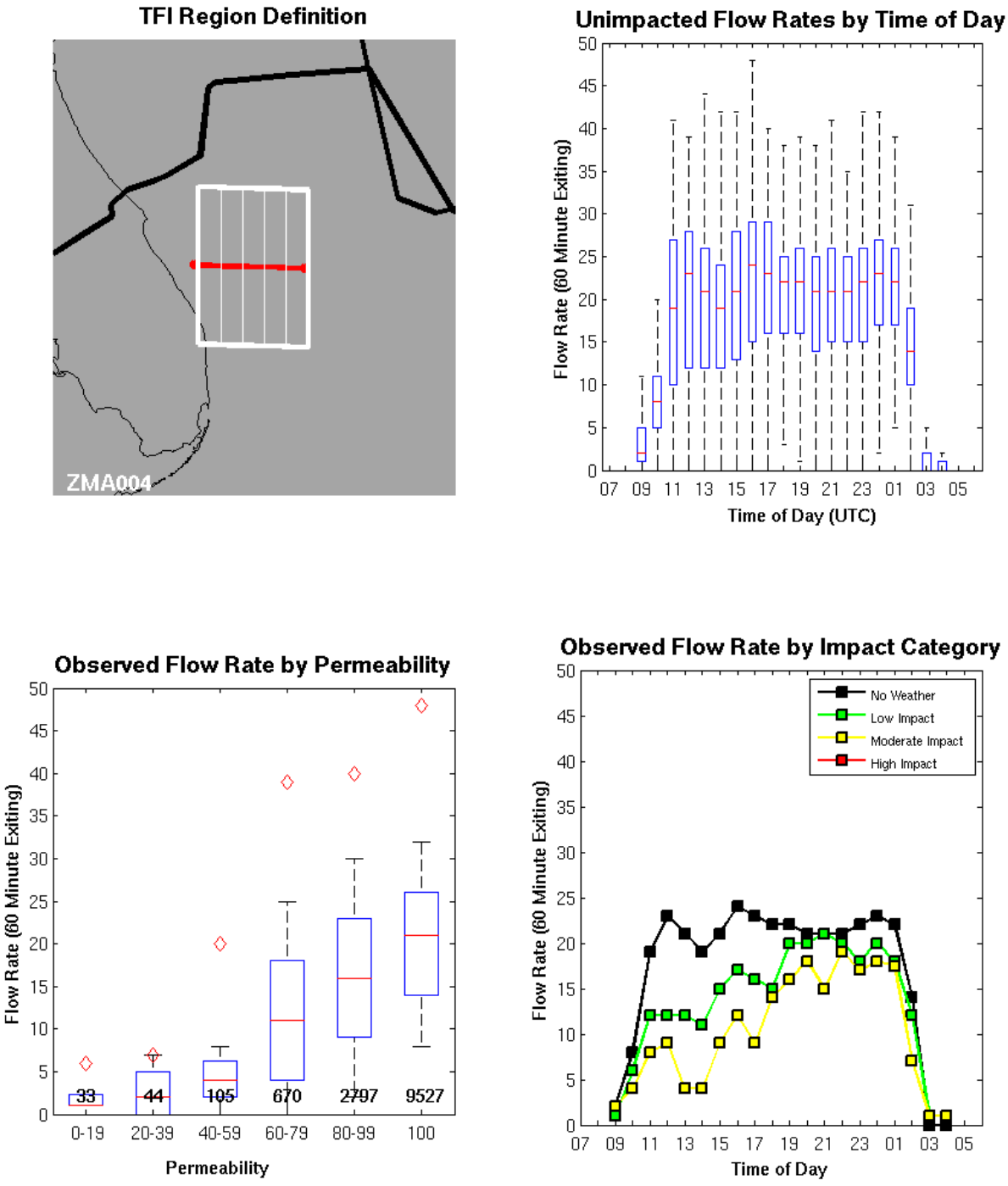

Figure A-41. Traffic Flow Impact region ZMA004: Traffic flowing over the Atlantic Ocean through the Miami ARTCC primarily heading to the east coast states. This route is a common weather avoiding route if there are no military restrictions.

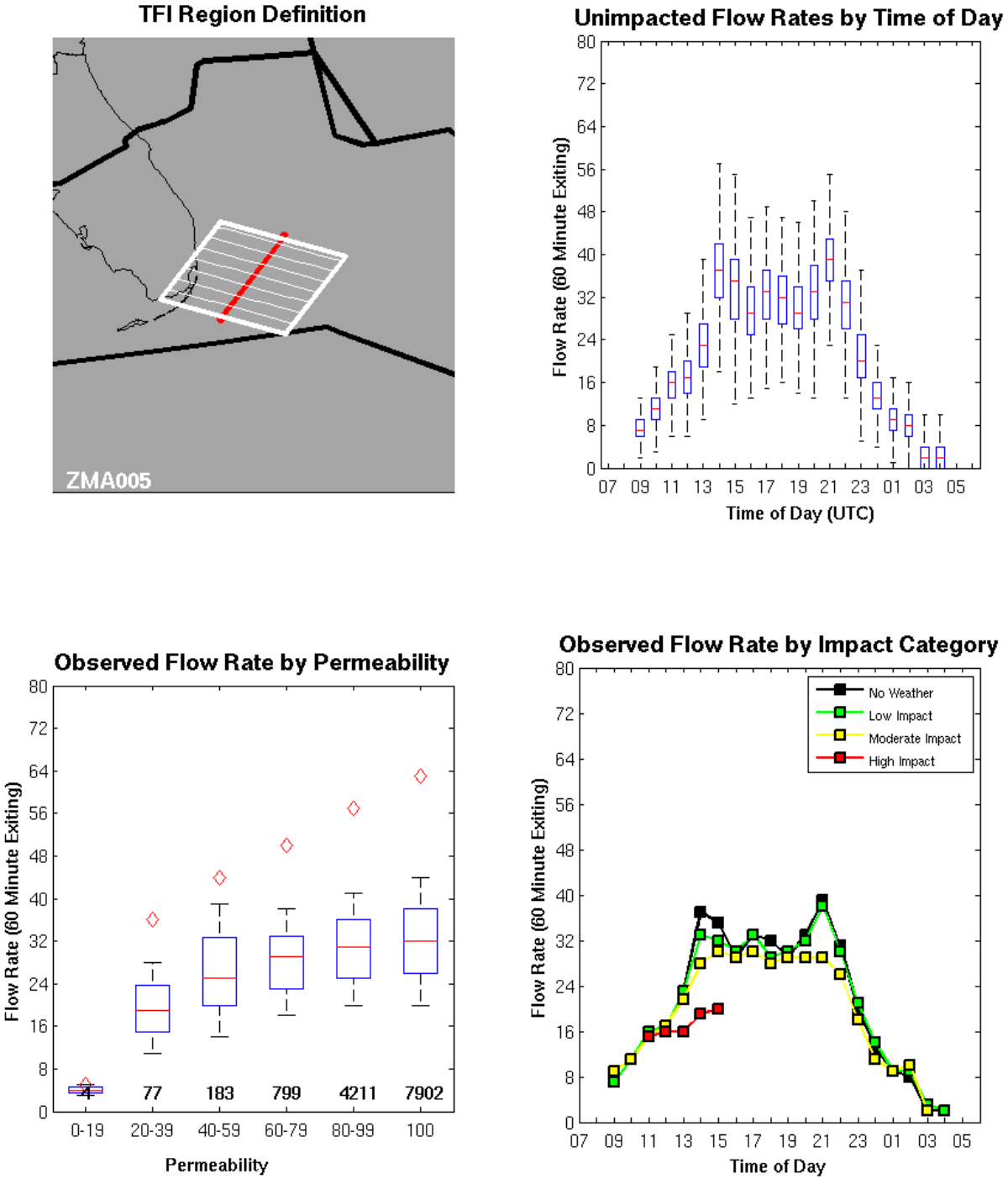

Figure A-42. Traffic Flow Impact region ZMA005: Traffic flowing over the Atlantic Ocean through the Miami ARTCC destined for the Caribbean and points south.

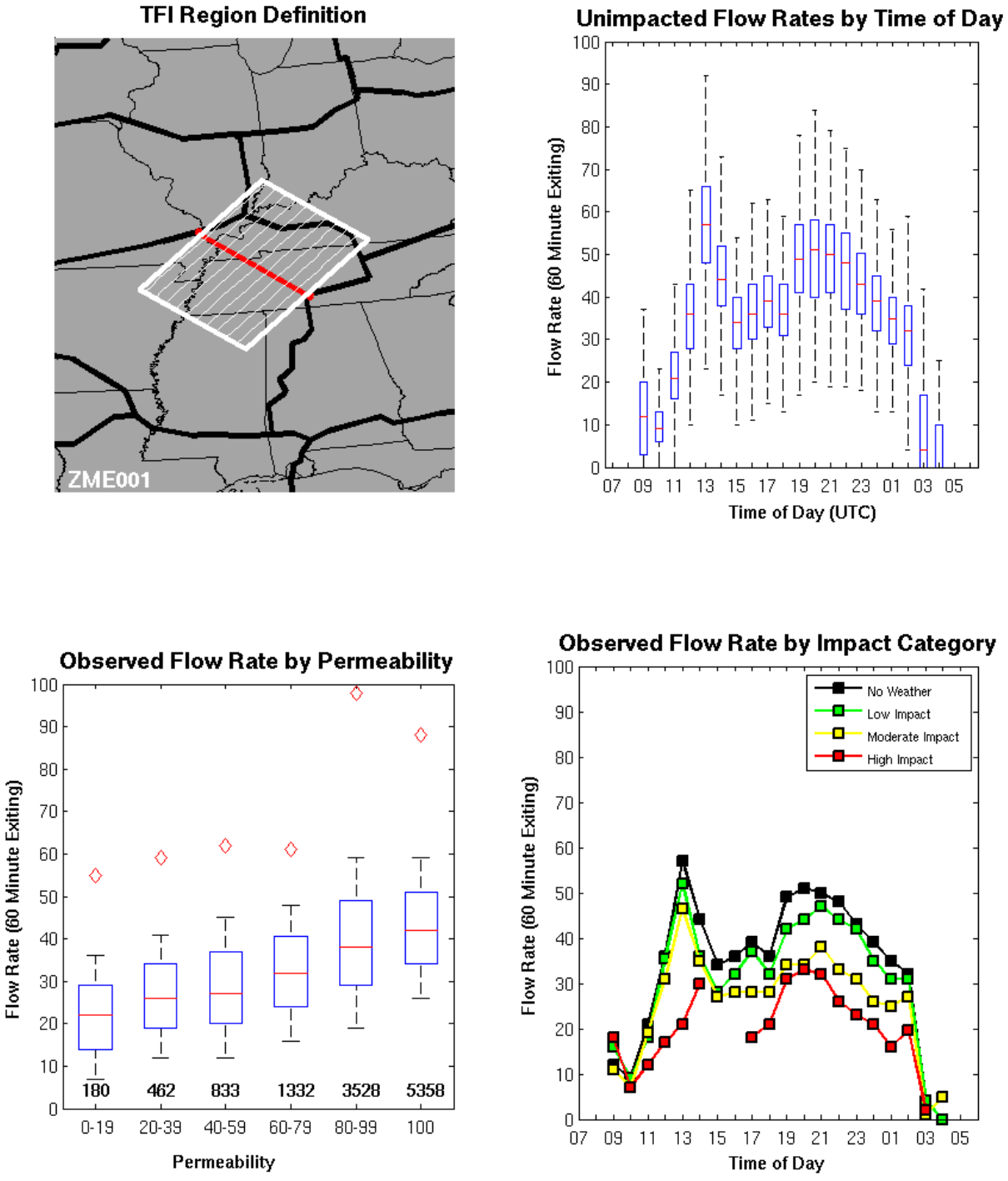

Figure A-43. Traffic Flow Impact region ZME001: Traffic transitioning between the ZME and ZID ARTCCs over western Kentucky.

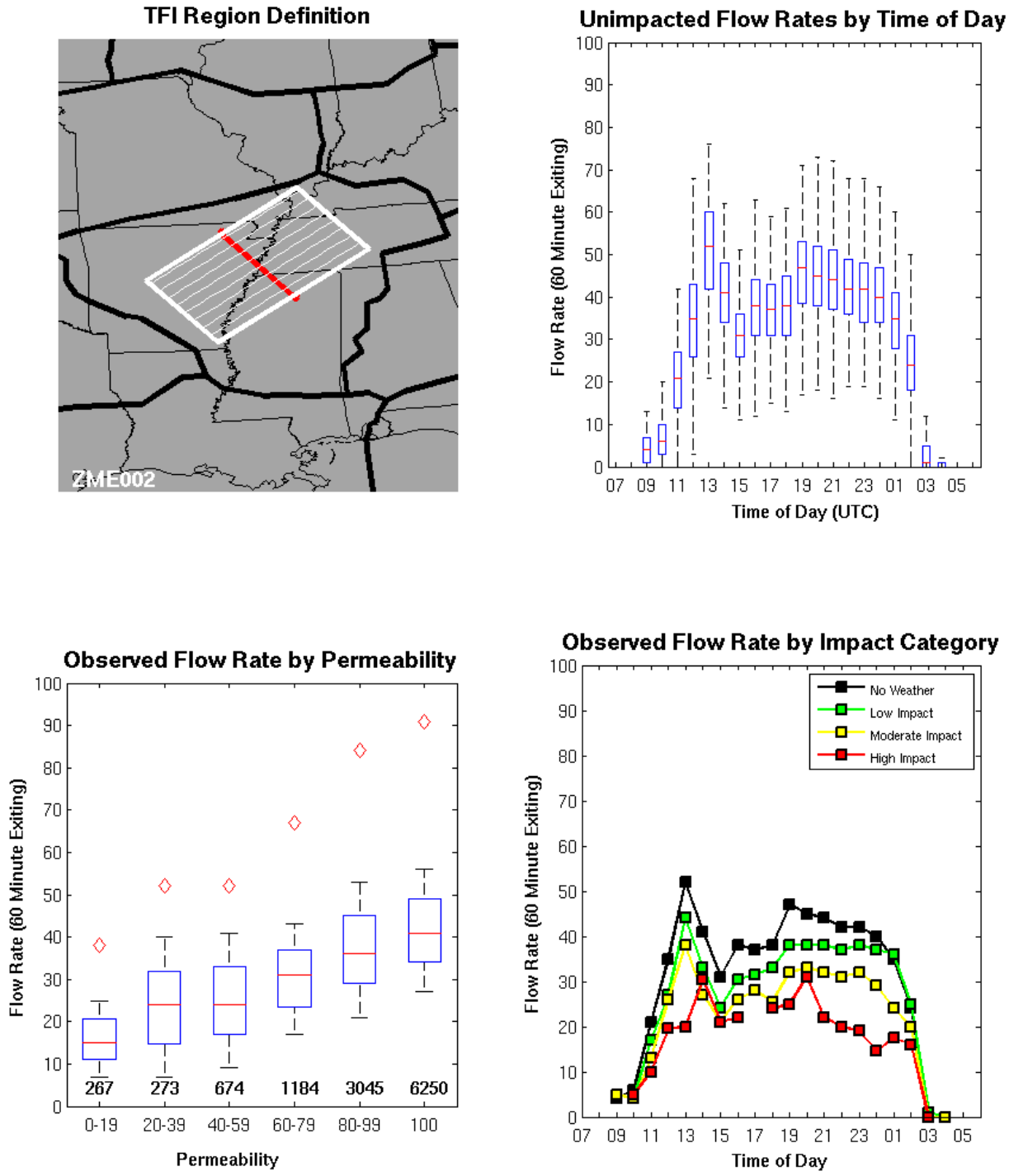

Figure A-44. Traffic Flow Impact region ZME002: Traffic flowing through the Memphis ARTCC in a northeast-southwest direction.

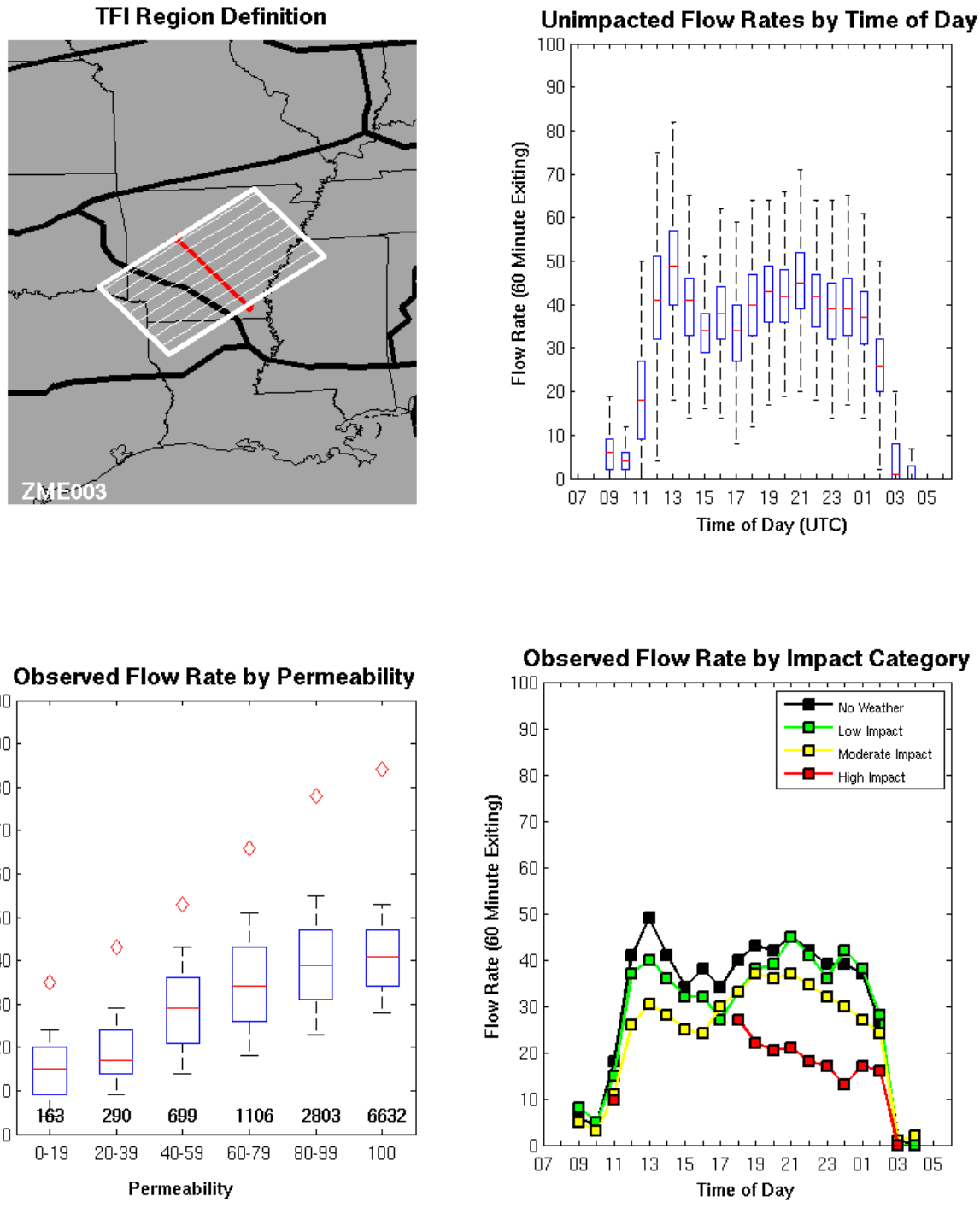

Figure A-45. Traffic Flow Impact region ZME003: Traffic transitioning between the ZFW and ZME ARTCCs over Arkansas.

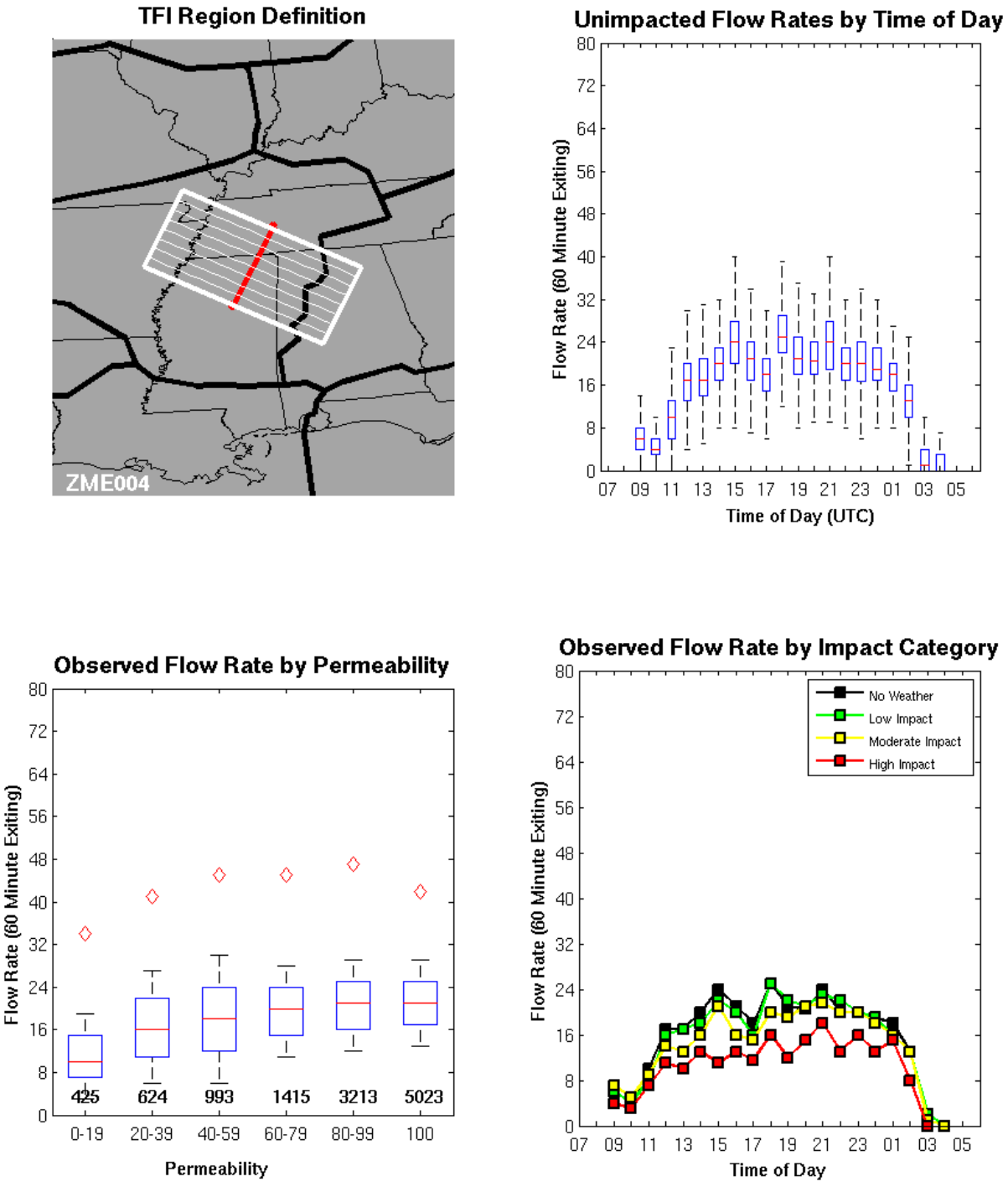

Figure A-46. Traffic Flow Impact region ZME004: Traffic flowing northwest-southeast through the Memphis ARTCC.

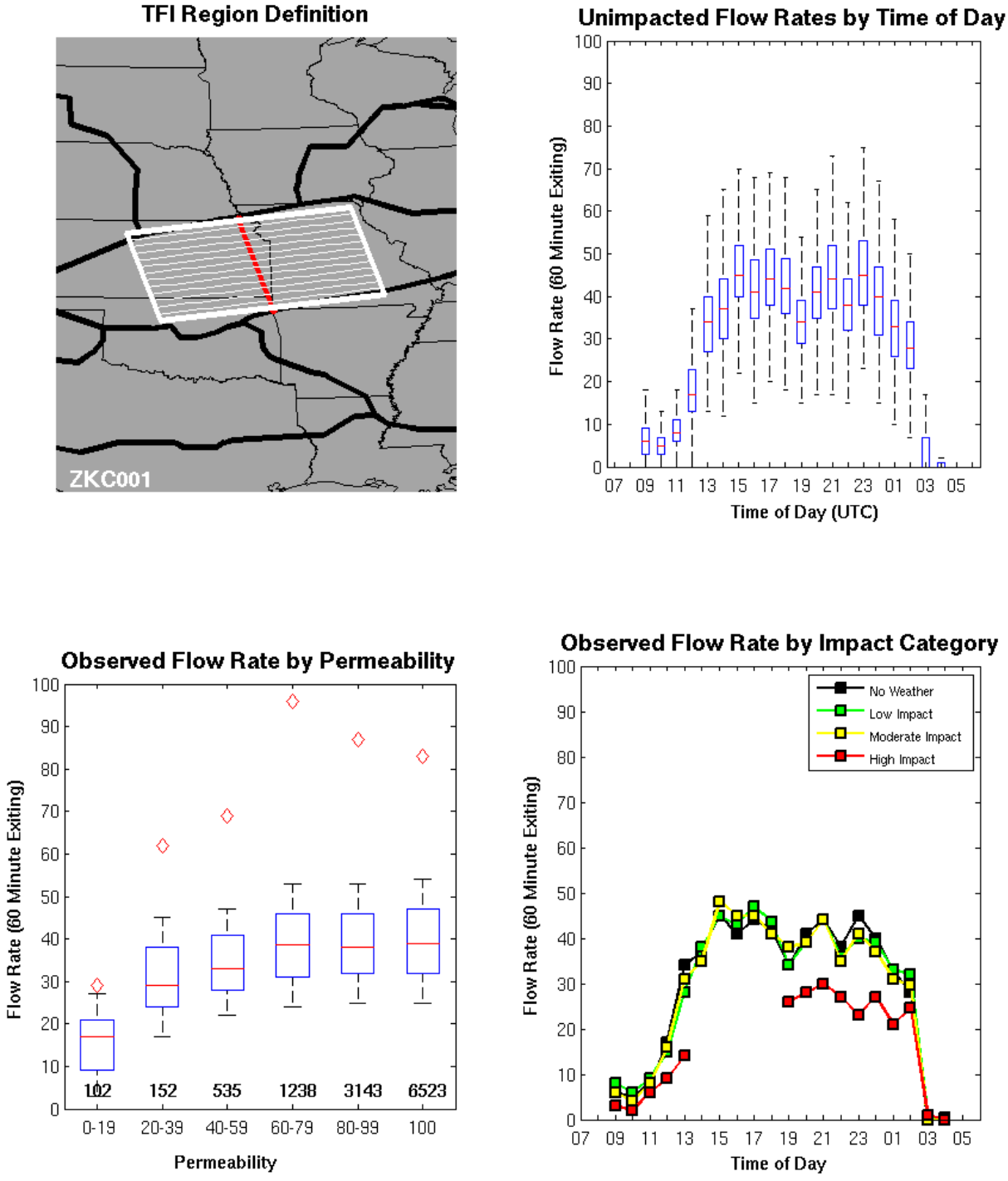

Figure A-47. Traffic Flow Impact region ZKC001: Traffic flowing through the Kansas City ARTCC in an east-west direction. This air space handles a large portion of the coast-to-coast traffic.

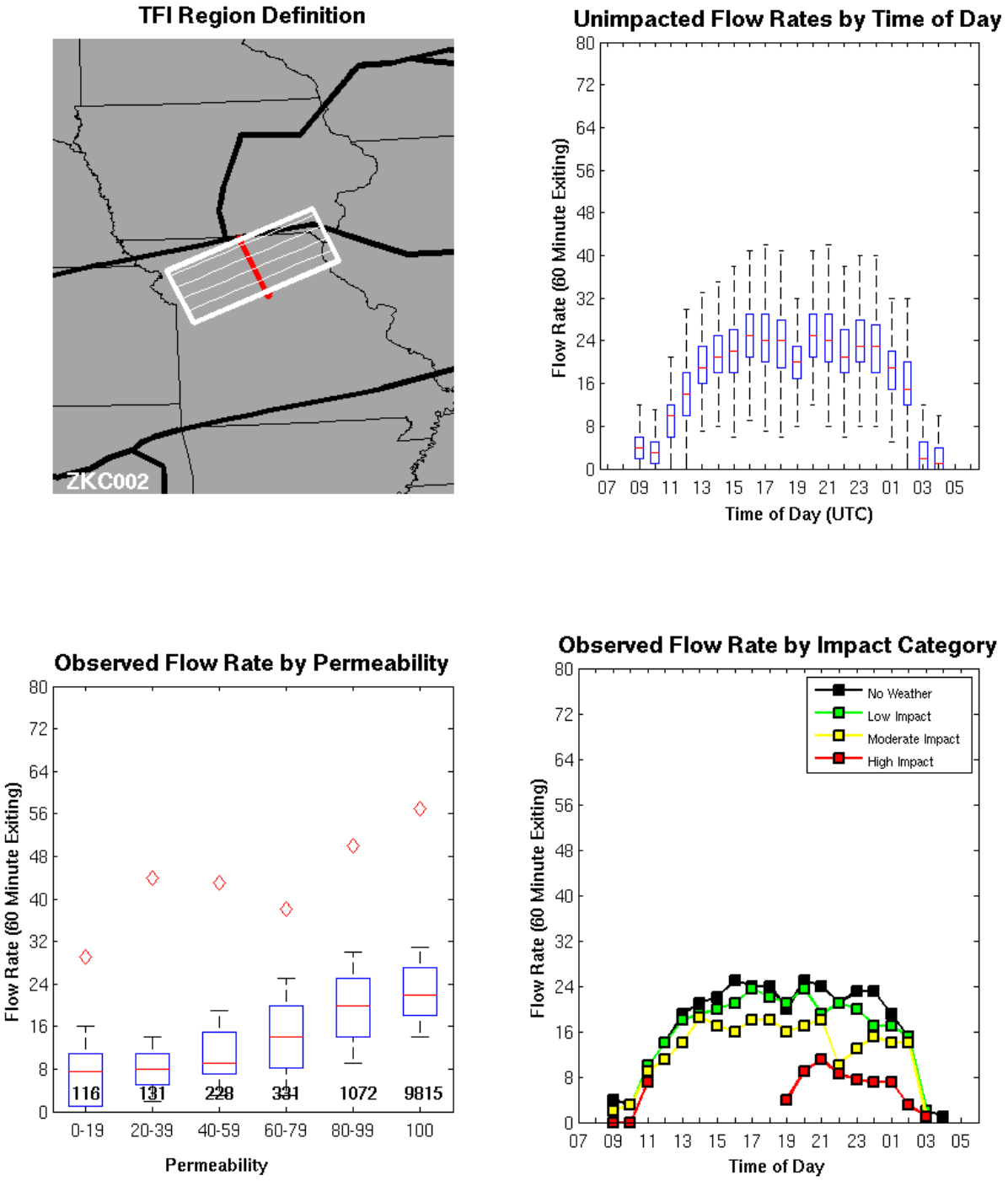

Figure A-48. Traffic Flow Impact region ZKC002: Air traffic flowing through the northern half of the Kansas City ARTCC over north Arkansas.

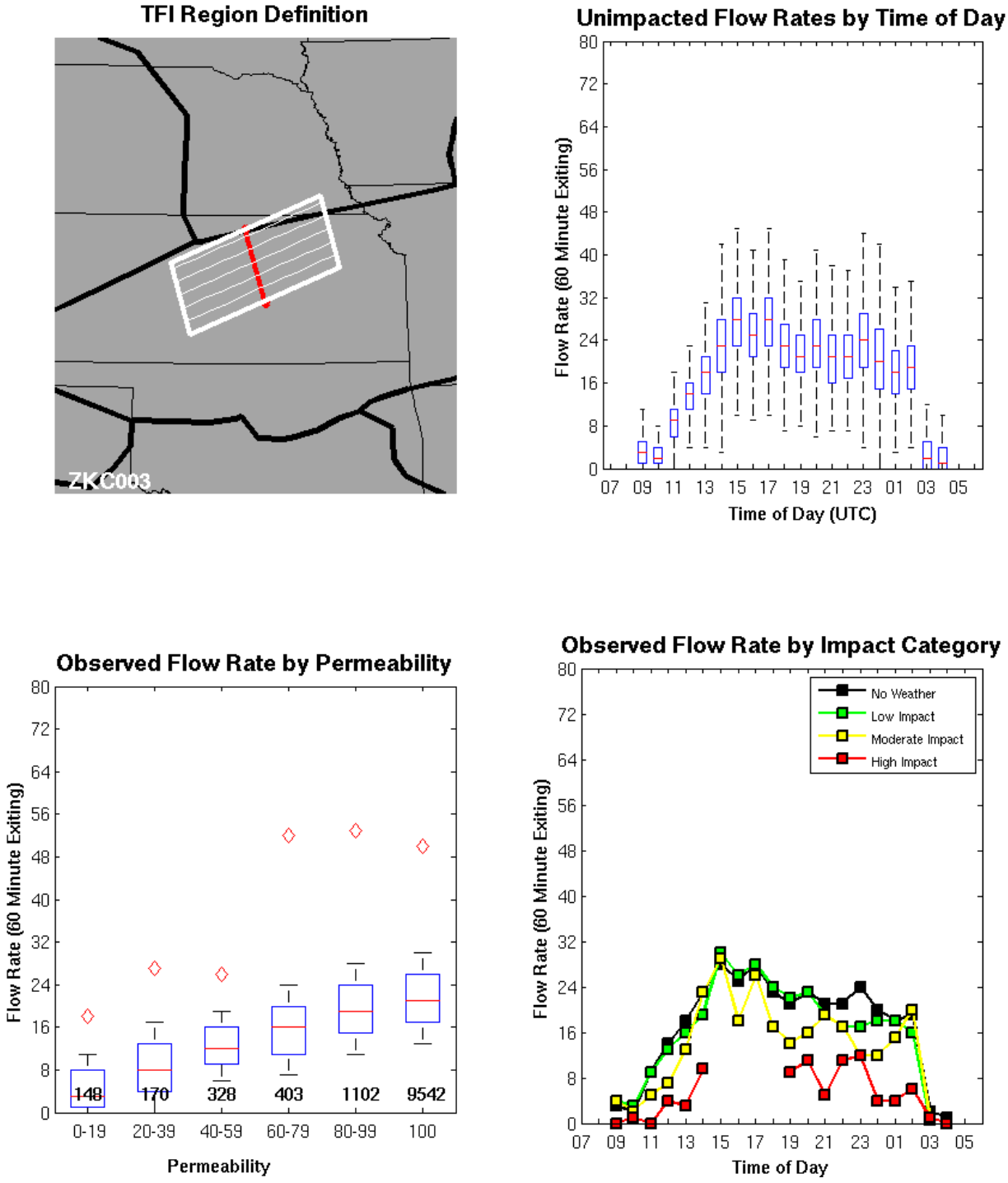

Figure A-49. Traffic Flow Impact region ZKC003: Air traffic flowing through the northern half of the Kansas City ARTCC over north Nebraska.

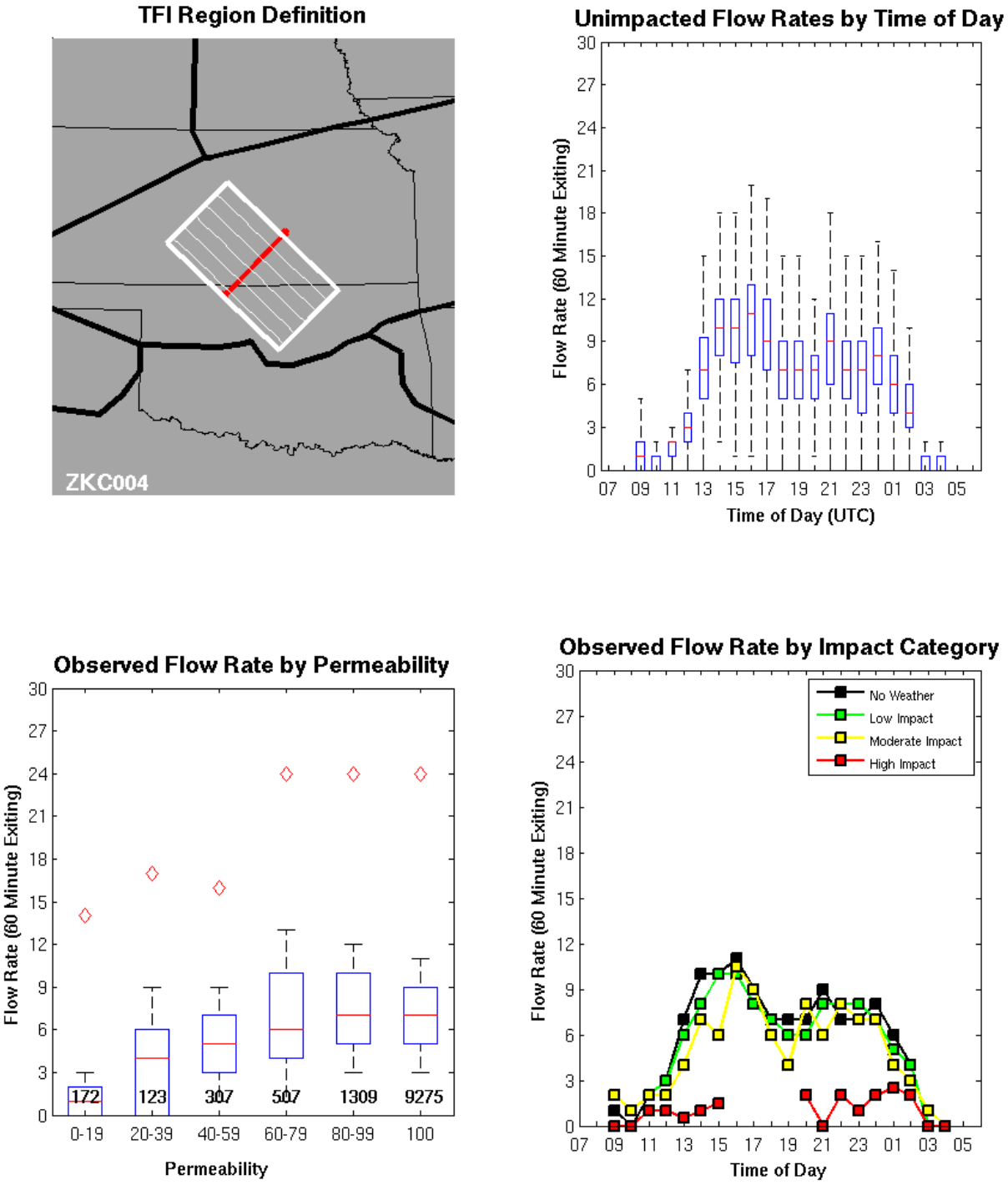

Figure A-50. Traffic Flow Impact region ZKC004: Air traffic flowing through the Kansas City ARTCC in a northwest-southeast direction.

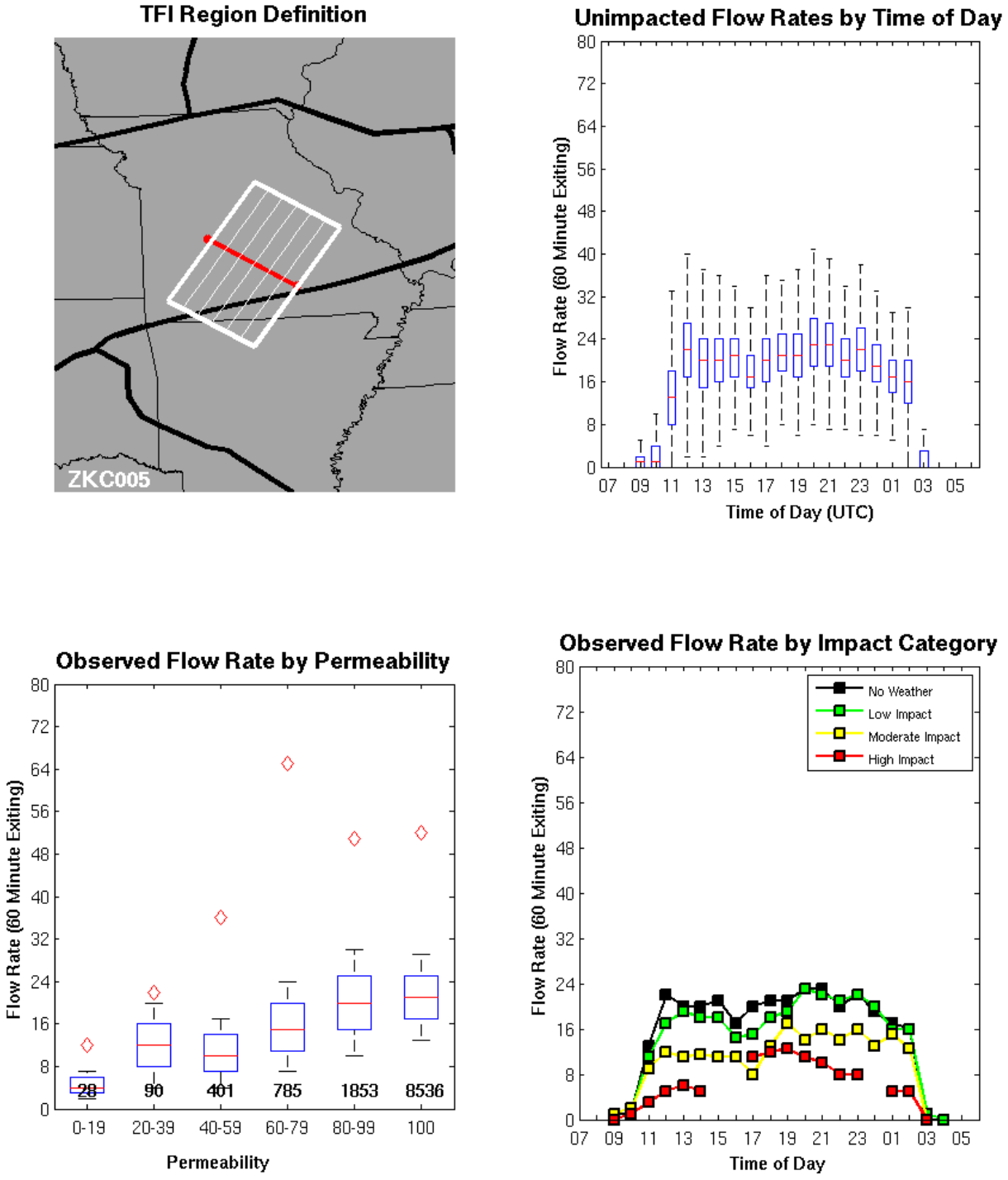

Figure A-51. Traffic Flow Impact region ZKC005: Air traffic flowing through the Kansas City ARTCC in a northeast-southwest direction over southern Arkansas.

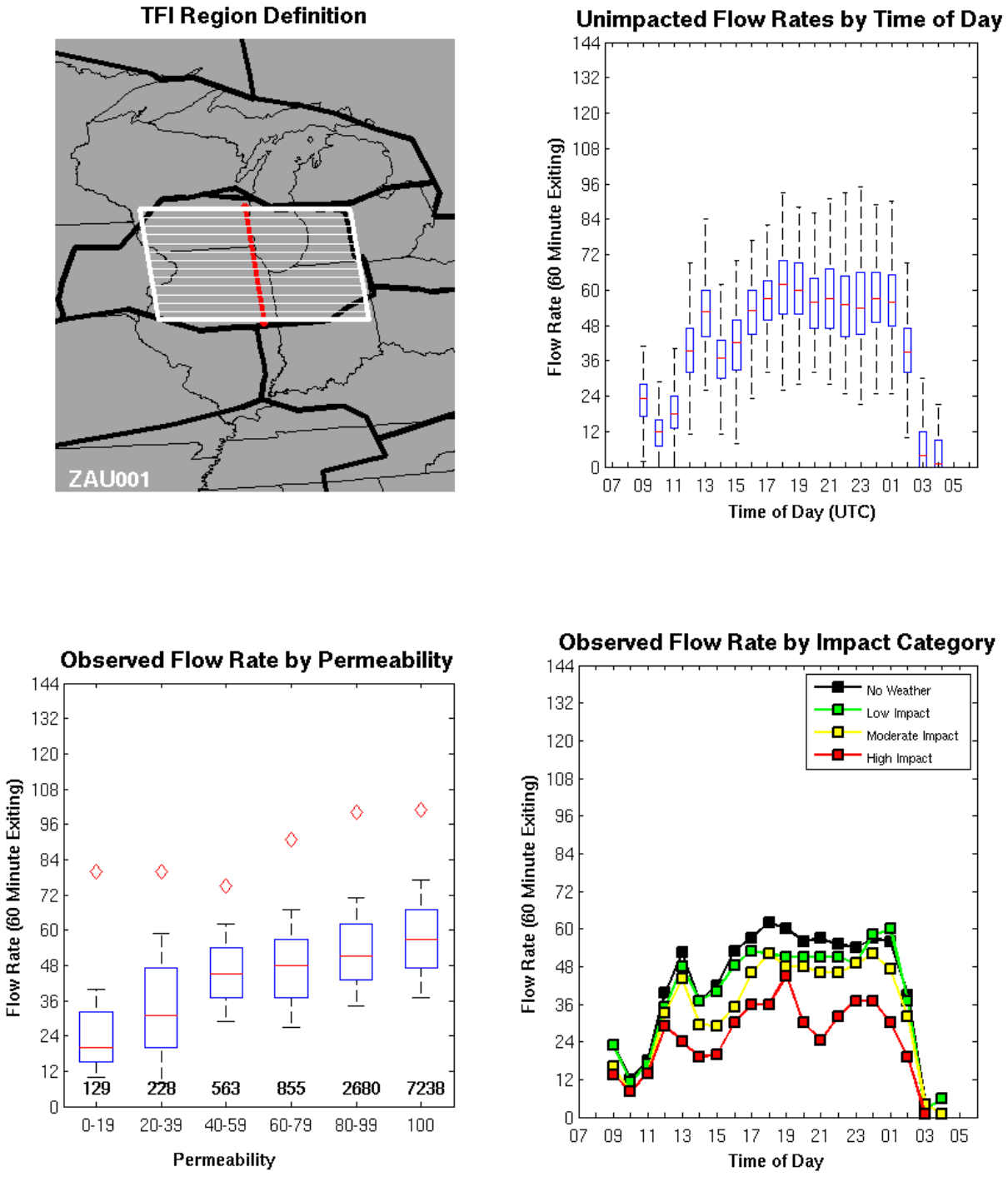

Figure A-52. Traffic Flow Impact region ZAU001: Air traffic flowing through the Chicago ARTCC in an east-west direction. This air space handles a large portion of the coast-to-coast traffic.

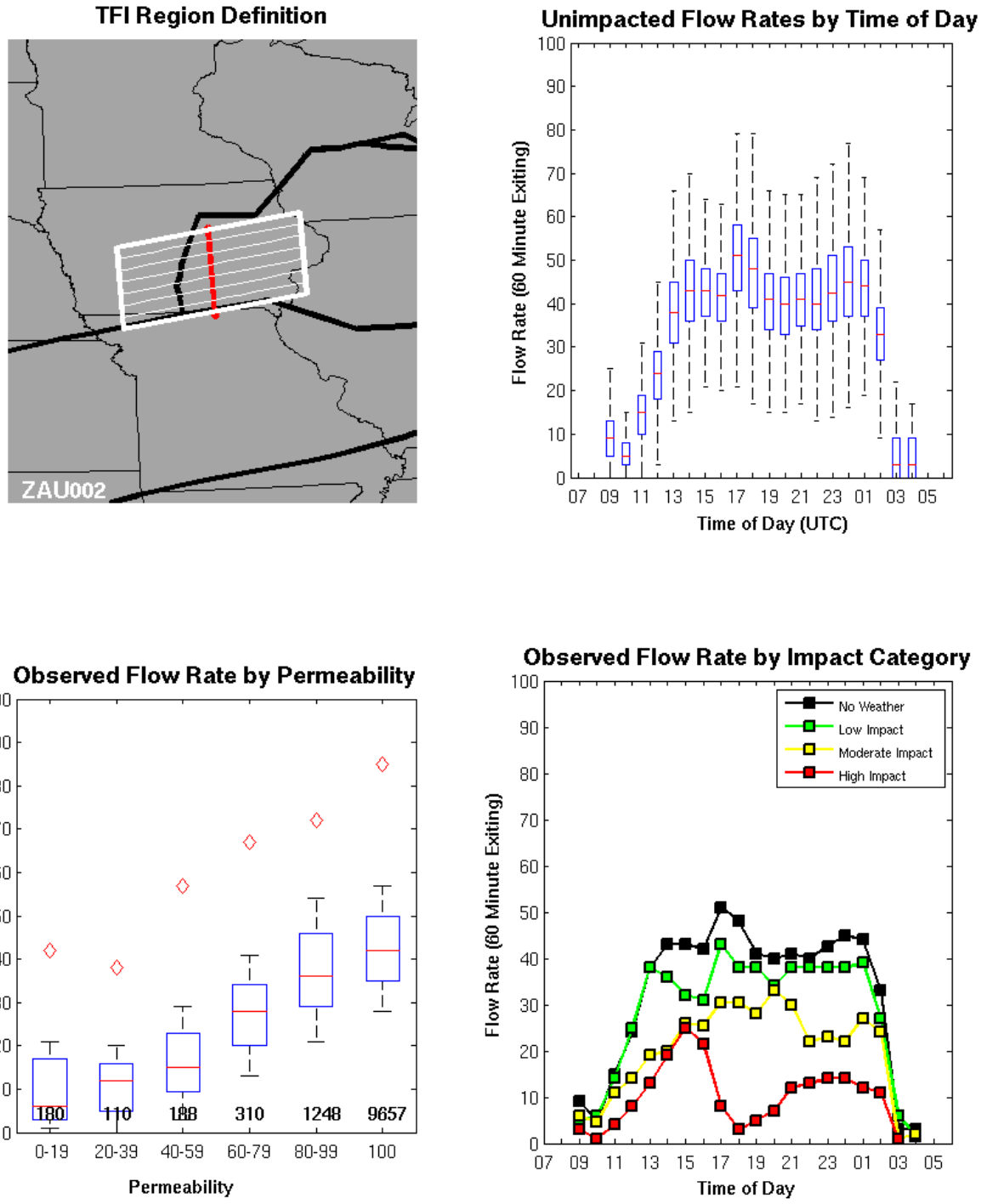

Figure A-53. Traffic Flow Impact region ZAU002: Traffic transitioning between the ZAU and ZMP ARTCCs in an east-west flow. This air space handles a large portion of the coast-to-coast traffic.

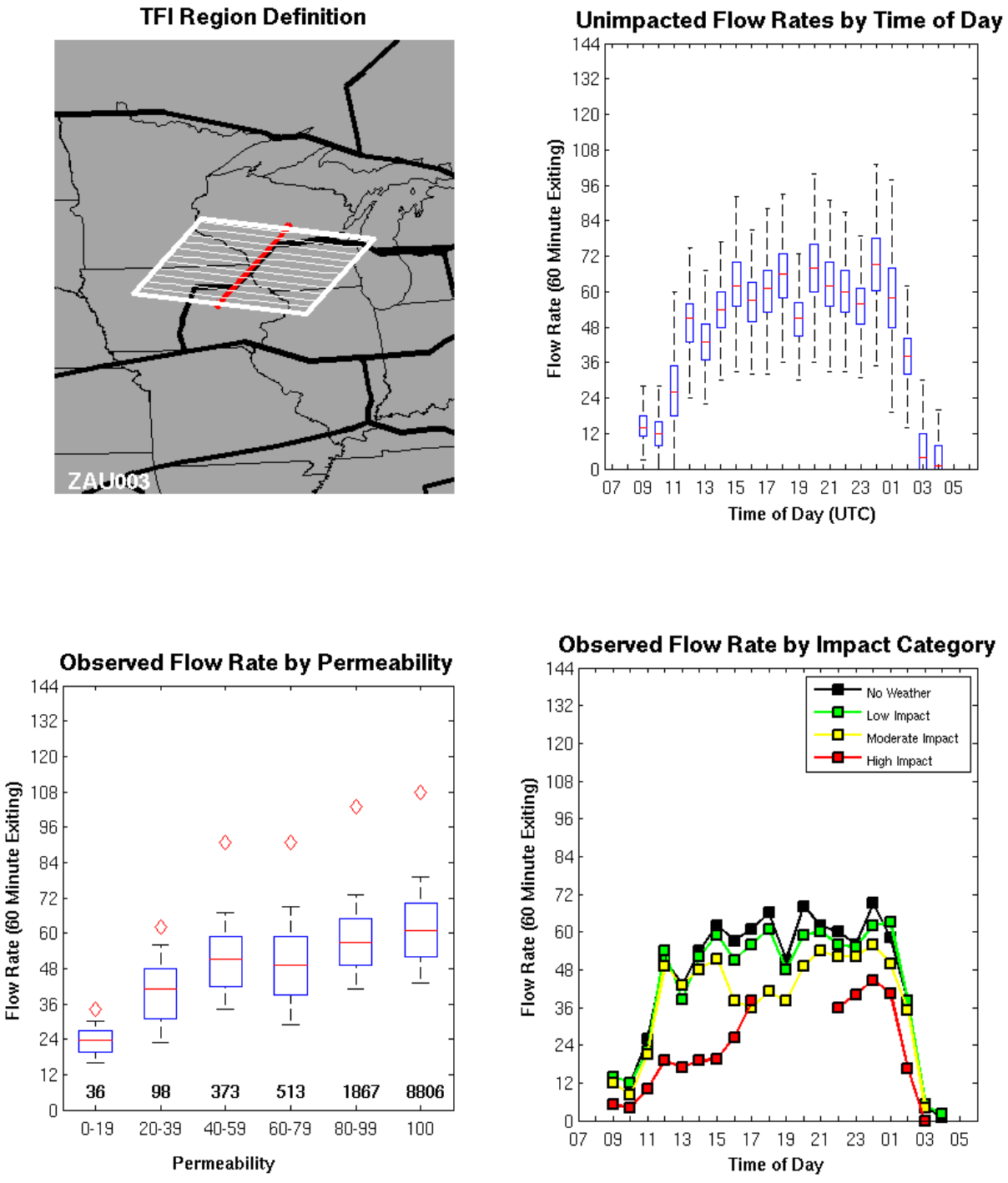

Figure A-54. Traffic Flow Impact region ZAU003: Traffic transitioning between the ZAU and ZMP ARTCCs in a north east-southwest flow.

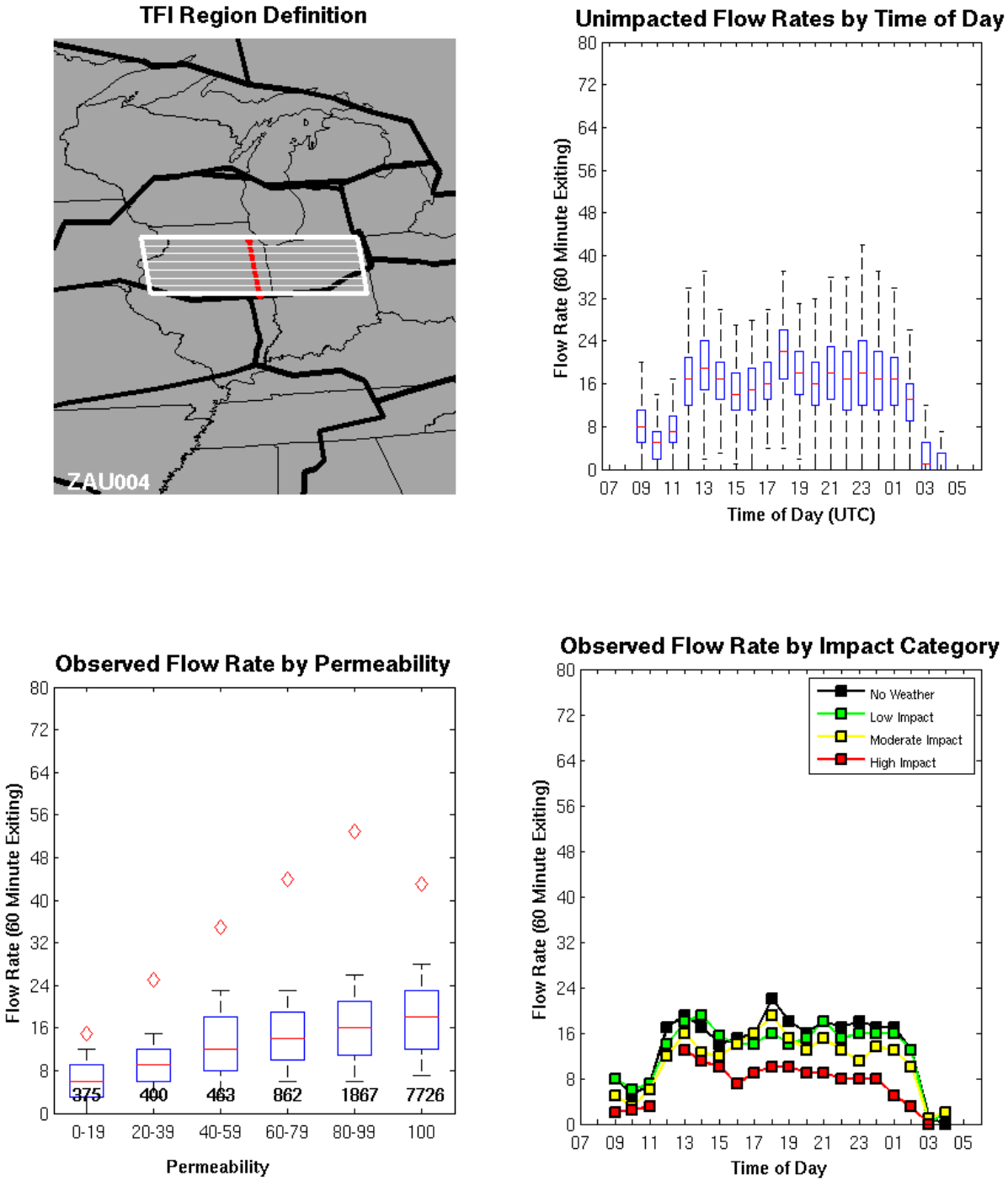

Figure A-55. Traffic Flow Impact region ZAU004: Traffic flowing through the southern half of the Chicago ARTCC in an east-west flow. This air space handles a large portion of the coast-to-coast traffic.

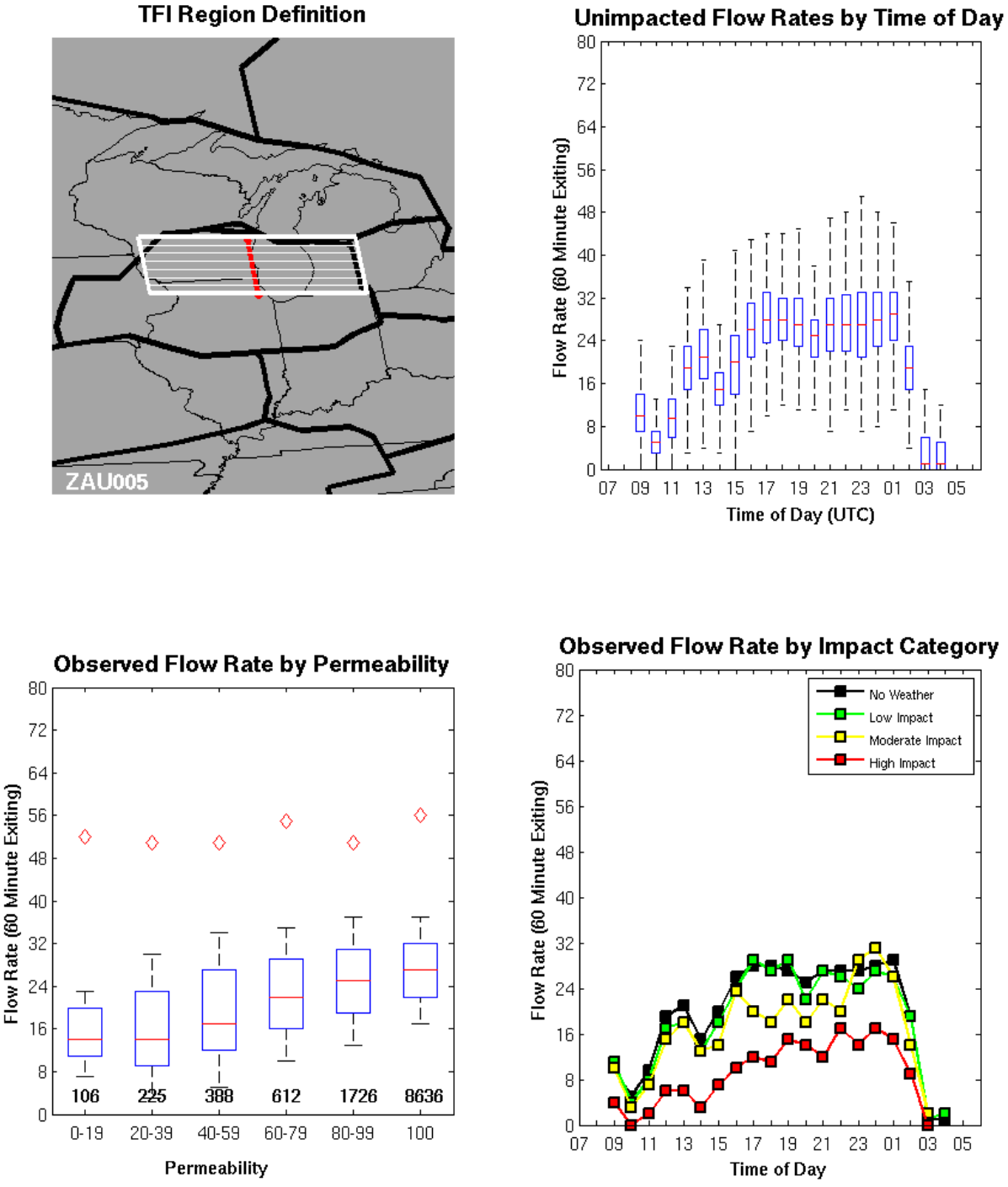

Figure A-56. Traffic Flow Impact region ZAU005: Traffic flowing through the northern half of the Chicago ARTCC in an east-west flow. This air space handles a large portion of the coast-to-coast traffic.

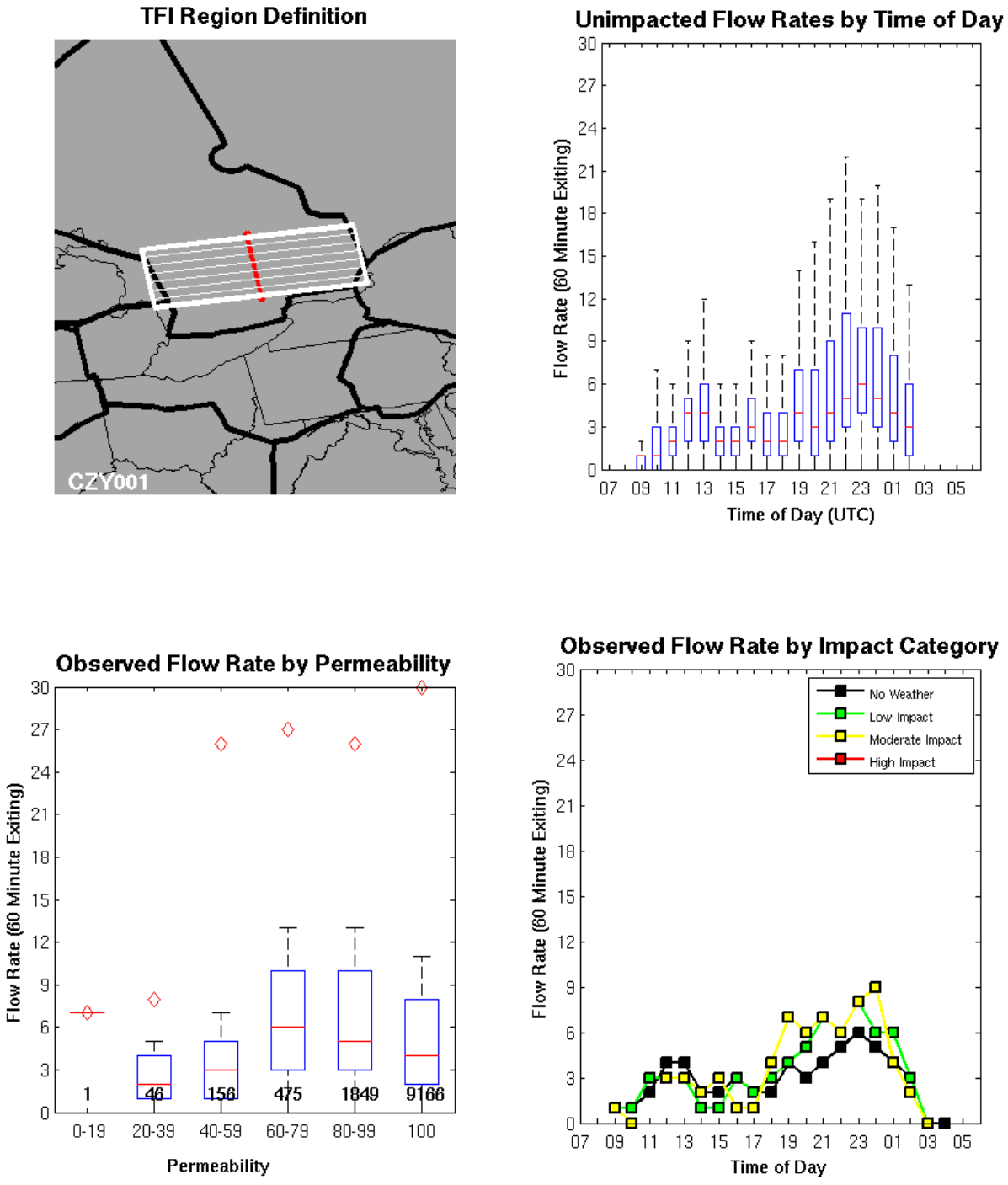

Figure A-57. Traffic Flow Impact region CZY001: Traffic flowing through the southern end of the Canadian ARTCC CZY. This air space serves as an weather avoiding alternative for the coast-to-coast flows when ZOB is impacted by weather.

GLOSSARY

AAL	American Airlines
AFP	Airspace Flow Programs
ARTCC	Air Route Traffic Control Center
ASDI	Aircraft Situation Display for Industry
ASPM	Aviation System Performance Metrics
ATC	Air Traffic Control
ATCSCC	Air Traffic Control System Command Center
ATFM	Air Traffic Flow Management
BOS	Boston Logan International Airport
CCFP	Collaborative Convective Forecast Product
CDF	Cumulative Distribution Function
CDM	Collaborative Decision-Making
CIWS	Corridor Integrated Weather System
CoSPA	Consolidated Storm Prediction for Aviation
CTOP	Collaborative Trajectory Options Program
CWAM	Convective Weather Avoidance Model
CWAP	Convective Weather Avoidance Polygons
CZW	Winnipeg Air Route Traffic Control Center
CZY	Toronto Air Route Traffic Control Center
EDCT	Estimated Departure Clearance Time
EWR	Newark Liberty International Airport
FAA	Federal Aviation Administration
FCA	Flow Constrained Area
FSA	Flight Schedule Analyzer
FSM	Flight Schedule Monitor
GDP	Ground Delay Programs
GFS	Global Forecasting System
HRRR	High Resolution Rapid Refresh
JFK	John F. Kennedy International Airport
LAMP	Local Aviation Model Output Statistics Program
LGA	LaGuardia Airport
LTE	Lateral Track Extension
MAE	Mean Absolute Error
METAR	Meteorological Terminal Aviation Routine Weather Report
MOS	Model Output Statistics
MSE	Mean Squared Error
N90	New York Terminal Radar Approach Control

NAM	National Aviation Meteorologist
NAS	National Airspace System
NOAA	National Oceanic and Atmospheric Administration
NOM	National Operations Manager
OPSNET	Operations Network
ORD	Operational Response Development
PIC	Prediction Interval Coverage
PIW	Prediction Interval Width
RAPT	Route Availability Planning Tool
SME	Subject Matter Expert
SPT	Strategic Planning Telecom
SREF	Short Range Ensemble Forecast
SWA	Southwest Airlines
SWAP	Severe Weather Avoidance Plan
TBFM	Time Based Flow Management
TFI	Traffic Flow Impact
TFM	Traffic Flow Management
TFMS	Traffic Flow Management System
TMI	Traffic Management Initiative
TMU	Traffic Management Unit
VIL	Vertically Integrated Liquid
WAF	Weather Avoidance Field
WRF-NAM	Weather Research and Forecasting – North American Model
ZAU	Chicago Air Route Traffic Control Center
ZBW	Boston Air Route Traffic Control Center
ZDC	Washington Air Route Traffic Control Center
ZDV	Denver Air Route Traffic Control Center
ZFW	Dallas Fort Worth Air Route Traffic Control Center
ZHU	Houston Air Route Traffic Control Center
ZID	Indianapolis Air Route Traffic Control Center
ZJX	Jacksonville Air Route Traffic Control Center
ZKC	Kansas City Air Route Traffic Control Center
ZLA	Los Angeles Air Route Traffic Control Center
ZLC	Salt Lake City Air Route Traffic Control Center
ZMA	Miami Air Route Traffic Control Center
ZME	Memphis Air Route Traffic Control Center
ZMP	Minneapolis Air Route Traffic Control Center
ZNY	New York Air Route Traffic Control Center
ZOB	Cleveland Air Route Traffic Control Center
ZSE	Seattle Air Route Traffic Control Center
ZTL	Atlanta Air Route Traffic Control Center

REFERENCES

1. Klingle-Wilson, D., Evans, J. E., "Description of the Corridor Integrated Weather System (CIWS) Weather Products"**,** Project Report ATC-317, MIT Lincoln Laboratory, Lexington, MA, 2005

2. Wolfson, M. M., Dupree, W. J., Rasmussen, R., Steiner, M., Benjamin, S., Weygandt, S., **"**Consolidated Storm Prediction for Aviation (CoSPA)," 13th Conference on Aviation, Range, and Aerospace Meteorology (ARAM), New Orleans, LA, *Amer. Meteor. Soc.*, 2008.

3. Du, J., S. L. Mullen, and F. Sanders. 2004. "The NOAA/NWS/NCEP Short Range Ensemble Forecast (SREF) system: Evaluation of an initial condition vs multiple model physics ensemble approach," 20th Conf. on Weather Analysis and Forecasting/16th Conf. on Numerical Weather Prediction, Seattle, WA, *Amer. Meteor. Soc*., vol. 21, 2006.

4. Huberdeau, Mark, and Gentry, J., "Use of the Collaborative Convective Forecast Product in the air traffic control strategic planning process," *Journal of Air Traffic Control* (2004).

5. Smith, T.L., Benjamin, S.G., Brown, J.M., Weygandt, S., Smirnova, T. , and Schwartz, B. NOAA Research – Earth System Research Laboratory, Global Systems Division Boulder, Colorado. "Convection Forecasts From The Hourly Updated, 3-km High Resolution Rapid Refresh Model (HRRR)". Preprints, 24th Conference on Severe Local Storms, Savannah, GA, *Amer. Meteor. Soc.*, October 2008.

6. Guyer, J.L., and Bright, D.R. NOAA/NWS Storm Prediction Center, Norman, Oklahoma, "Utility of Short-Range Ensemble Forecast (SREF) guidance for forecasting the development of severe convection". 24th Conference on Severe Local Storms, Savannah, GA, *Amer. Meteor. Soc.*, October 2008.

7. Glahn, B., and Ghirardelli, J.E. Meteorological Development Laboratory Office of Science and Technology, National Weather Service, NOAA, Silver Spring, Maryland**. "**The New and Improved Localized Aviation MOS Program Analysis and Prediction System." Joint Session, 17th Conf. on Probability and Statistics/20th Conference on Weather and Forecasting/16th Conf. on Numerical Weather Prediction, Seattle, WA, *Amer. Meteor. Soc.*, January 2004.

8. Cho, J. Y. N., Welch, J. D., Underhill, N. K.. "Analytical Workload Model for Estimating En Route Sector Capacity in Convective Weather," 9th USA/Europe Air Traffic Management R&D Seminar, Berlin, Germany, June 2011.

9. Song, L., Wanke, C., and Greenbaum, D. "Predicting Sector Capacity for TFM Decision Support." 6th AIAA Aviation, Integration, and Operations Conference. 2006.

10. DeLaura, R., and Evans, J., "An Exploratory Study of Modeling En route Pilot Convective Storm Flight Deviation Behavior." 12th Conference on Aviation, Range, and Aerospace Meteorology, Atlanta, GA, 2006.

11. Rubnich, M. and DeLaura, R. "An Algorithm to Identify Robust Convective Weather Avoidance Polygons in En Route Airspace," 10th AIAA Aviation Technology, Integration, and Operations (ATIO) Conference, Fort Worth, TX, 2010.

12. Robinson, M, DeLaura, R., Underhill, N., "The Route Availability Planning Tool (RAPT): Evaluation of Departure Management Decision Support in New York During the 2008 Convective Weather Season," Eighth USA/Europe Air Traffic Management Research and Development Seminar (ATM2009), Napa, CA, 2009.

13. Koenker, R. *Quantile Regression*. Cambridge University Press, 2005.

14. Portnoy, S., and Koenker, R., "The Gaussian Hare and the Laplacian Tortoise: Computability of Squared-Error Versus Absolute-Error Estimators." *Statistical Science* (1997): 279-300.

15. Wolpert, D. H. "Stacked Generalization." *Neural networks* 5.2 (1992): 241-259.

16. U.S. DOT FAA Order JO7210.3Z, Section 20, National Playbook.